WATER BALANCE MODELING WITH SWAT FOR INTEGRATED WATER RESOURCES ASSESSMENT IN RAYA VALLEY (TIGRAY, ETHIOPIA)

Assefa Gebregziabher

February, 2010

WATER BALANCE MODELING WITH SWAT FOR INTEGRATED WATER RESOURCES ASSESSMENT IN Raya Valley (Tigray, Ethiopia)

by

Assefa Gebregziabher Teklehaimanot

Thesis submitted to the International Institute for Geo-information Science and Earth Observation in partial fulfilment of the requirements for the degree of Master of Science in Geo-information Science and Earth Observation, Specialisation: (Groundwater resources assessment and modelling)

Thesis Assessment Board

Dr. Ir. M.W. (Maciek) Lubczynski	Chair man (WRS, ITC, Enschede)
Dr. W.W. Immerzeel	External examiner (Future water, Wageningen)
Dr. A.S.M. (Ambro) Gieske	First superviser (WRS, ITC, Enschede)
Dr. Ing. T.H.M. (Tom) Rientjes	Second supervisor (WRS, ITC, Enschede)

ITC

INTERNATIONAL INSTITUTE FOR GEO-INFORMATION SCIENCE AND EARTH OBSERVATION
ENSCHEDE, THE NETHERLANDS

Disclaimer

Abstract

The study focused on the water balance modelling of Raya Valley (Ethiopia). The modelling software package SWAT2005 with the Map Window interface was applied to the water balance modelling in the study area which is in the southern part of Tigray region, northern Ethiopia. Raya Valley lies at an altitude of about 1500 m between the lower Afar Depression in the east and the high mountain range in the west. Water availability in the study area is highly variable both in time and space and over-exploitation can cause depletion of the water resources. The demand of the water resources for irrigation and domestic use is increasing. Therefore the need for a better understanding of hydrological processes has become critical.

The hydrological and hydrometeorological data in the area are scarce and generally poor in quality. There are large data gaps. In this study, the SWAT daily weather generator algorithm used the monthly climate data for ten years (1996-2005) to generate the missing daily climatic data for the same period.

The Map Window SWAT 2005 (MWS) interface has built-in GIS data processing capabilities such as required for watershed delineation, input map characterization and processing, stream and outlet definition, the computation of the different geomorphologic characteristics and characterization of land cover and soil. Surface runoff was modelled based on the SCS- curve number approach. The SWAT-CUP2 package was used for calibration and uncertainty analysis of the SWAT model parameters.

Modelling of the area was carried out in two phases. An initial model simulation was made for the Golina catchment for the period from 1996 – 2005. This was followed by modelling of the Alamata catchment, just north of the Golina catchment, for the same period. It was necessary to first model the discharges of the Golina River, because no river gauge has ever been operational in the Alamata Basin. In the Golina River model two weather stations – with precipitation and temperature data - were used as a source for the weather generator package.

Calibration of the Golina River proved to be difficult because of the poor quality of the discharge data. It was only possible to construct an approximate monthly runoff curve after correcting for outliers and systematic errors. The calibration with SWAT-CUP therefore has to be considered strictly indicative. The conceptual model was then applied to the neighbouring Alamata Basin, using the same parameter values as determined for the Golina Basin.

The results of the conceptual SWAT model correspond with those reported previously. The indicative water balance is also in good agreement with groundwater studies of the area. The daily runoff curves show very fast daily and possibly sub-daily runoff after heavy rains, suggesting a reason why hydrometric analysis of these catchments has proved to be difficult.

Abbreviations and Acronyms

AEC	Agro Ecological Zone
AMC	Antecedent Soil moisture Condition
ASTER	Advanced Space borne Thermal Emission and Reflection Radiometer
CECE	Concert Engineering and Consulting Enterprises
CN	Curve Number
DEM	Digital Elevation Model
ET	Evapotranspiration
EGS	Ethiopian geological survey
FAO	Food and Agricultural Organization
GIS	Geographic Information System
GML	Gauss-Marquardt-Levenberg
GPS	Global positioning System
GUI	Graphic User Interface
HRU	Hydrologic Response units
INTC	Evaporation of Intercepted Canopy water
ISRIC	International Soil Reference and Information Centre
ITCZ	Inter Tropical Convergence Zone
IWMI	International Water Management Institute
MWR	Ministry of Water Resources
MWSWAT	Map Window SWAT
NMA	National Meteorological Agency
NS	Nash and Sutcliff
PET	Potential Evapotranspiration
RMSE	Root Mean Square Error
REST	Relief society of Tigray
SCS	Soil Conservation Service
SUFI	Sequential Uncertainty Fitting
SEBAL	Surface Energy Balance Algorithm for Land
SWAT	Soil and Water Assessment Tool
SWAT-CUP	Soil and Water Assessment Tool-Calibration and Uncertainty Programs
USGS	United States Geological Survey
WWDSE	Water works Design and Specification Enterprise

Acknowledgements

First, I would like to use the opportunity to express my appreciation to NUFFIC (Netherlands organization for international cooperation in higher education) who enabled me to attend my MSc study in ITC (International Institute for Geo-information Science and Earth observation). Next, I would also like to express my appreciation to my organization, Water Resources, Mines and Energy Bureau and Adwa Woreda Water Resources, Mines and Energy Office.

I am very happy to express my gratefulness to my first supervisor Dr. Ambro S.M. Gieske whose intellectual advice, guidance and encouragement were very valuable and inspiring in the process of the proposal writing, research undertaking and thesis writing. His visit to Ethiopia during my fieldwork also gave me the opportunity to improve my data collection. His continued willingness to listen and discuss helped me to produce this dissertation in an appropriate way. I would like to thank my second supervisor Dr. Ing.Tom H.M Rientjes for his constructive advice during proposal writing and base map preparation. I would also like to express my appreciation for his critical comments and suggestions on the draft of this thesis and other related papers. I extend my deepest gratitude to ITC staff and WREM 2008-2009 students.

I express my appreciation to Ato Dejen Berhe, Woreda Adwa Administrator, for the financial and moral support he has given me. I also appreciate his decision to select me for this enterprise.

I would also like to acknowledge my field assistants, Miss Hiwot Gidey, Mr Gebrehawaria Gebrekristos and Mr Assefa (driver).

Last but not least, I would like to express my deepest appreciation to my father (Haleka Gebregziabher Teklehaimanot) and Brother (Tekleweini Gebregziabher) for their care and love, and for remembering me in all their prayers.

Table of contents

List of figures

List of tables

1. Introduction

1.1. Background

Water balance modelling techniques are extensively used to make quantitative estimates of water resources and the impact of human activities on the hydrologic cycle. They are often in the form of predesigned tools which are best suited in a decision support or policy evaluation role at strategic or functional planning stages. On the basis of the water balance modelling approach, it is possible to make quantitative evaluations of water resources and their dynamic behaviour under a varying range of driving conditions. It is possible to evaluate individual contribution of sources of water in the system over different time periods, and to establish the degree of variation in water regime due to changes in components of the system. The complexity of the computation of the water balance tends to increase with increase in area. This is due to a related increase in the technical difficulty of accurately computing the numerous important water balance components. A prerequisite for successful application of the techniques is the availability of extensive and accurate hydrological and meteorological data (REST, 1997)

The objective of this study is to apply such a model (SWAT) to an area in Ethiopia (Raya Valley) where large water resources developments are taking place. SWAT is currently applied worldwide and it is considered a versatile model that can be used to integrate multiple environmental processes, which support more effective watershed management and the development of better informed policy decision. But little has been published on the application of the SWAT model in tropical catchments particularly in East Africa and Nile basin (Bärlund et al., 2007).

Raya Valley (see Figure 1) is found in the southern part of Tigray region along the main road from Addis Abeba to Mekele, about 150 km south of Mekelle near the town of Alamata. Raya Valley lies at an altitude of about 1500 m between the low Afar Depression in the east and the high mountain range in the west. The total land in the study area is estimated to be about 2580 km^2. No perennial rivers and streams are known in the Raya Valley plain. There are springs at the contact between the western escarpment and the lower plain. Runoff is generated from the mountains during the July-August rainy season and flows as sheet flow in the plain area. Groundwater is the primary source of water for urban and rural inhabitants of the valley. Irrigation projects are being developed at present using all available surface and groundwater resources. However the sustainable amount of water resources in the catchment is not well known. An additional difficulty lies in the lack of comprehensive data sets. The climate, soil conditions as well as the plant characteristics of the study area determine the water balance of the catchment. Quantification of the amount of water present in the catchment is a prerequisite for efficient water resource management. It is particularly important in regions with large demands for groundwater supplies, where such resources are the key to economic development.

For these reasons I have decided to study the water resources in the Raya Valley using SWAT model and GIS-Remote sensing techniques.

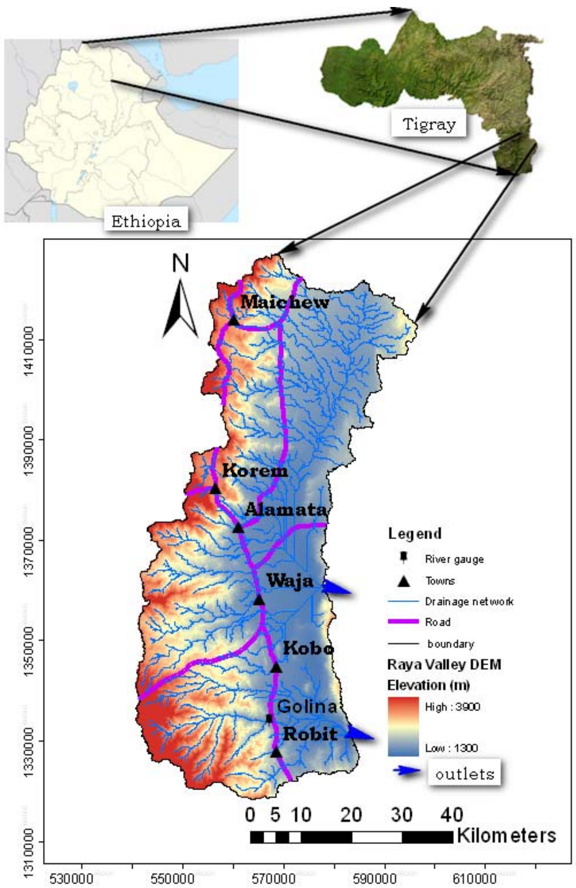

Figure 1.1 Location map of the study area

1.2. Problem statement

The Raya Valley catchment receives recharge by the water coming from the hills as sheet flow and direct rainfall. In the study area there are many boreholes for agricultural purposes. However, the amount of water present within the catchment has not been assessed properly so far. Modelling of the hydrological processes with the SWAT model would yield important information with regard to the sustainability of the resources. Without this knowledge no efficient management decisions can be taken.

1.3. Objectives

The main objective of the study is to quantify the water balance components of the Raya Valley catchment on monthly basis. The specific objectives of the research project are as follows:-

- To estimate the various water balance components of the catchment (evapotranspiration, surface runoff, precipitation, net groundwater flow and abstraction)
- To study drainage characteristics
- To calibrate the water balance model using stream discharge
- To give recommendations for the use of surface and groundwater resources

1.4. Research questions

- What are the main components controlling the catchment's hydrological abstractions?

- Can the water balance model improve the understanding of future abstractions?
- What is the model's sensitivity to changes in the parameters?
- What inputs are required to estimate the water balance components?

1.5. Research hypothesis

- The amount of water in the catchment can be predicted through the water balance modelling.
- The extraction of water for consumption can affect the level of water table.
- The predicted mean daily stream flow will be found similar to observed during the water balance simulation.

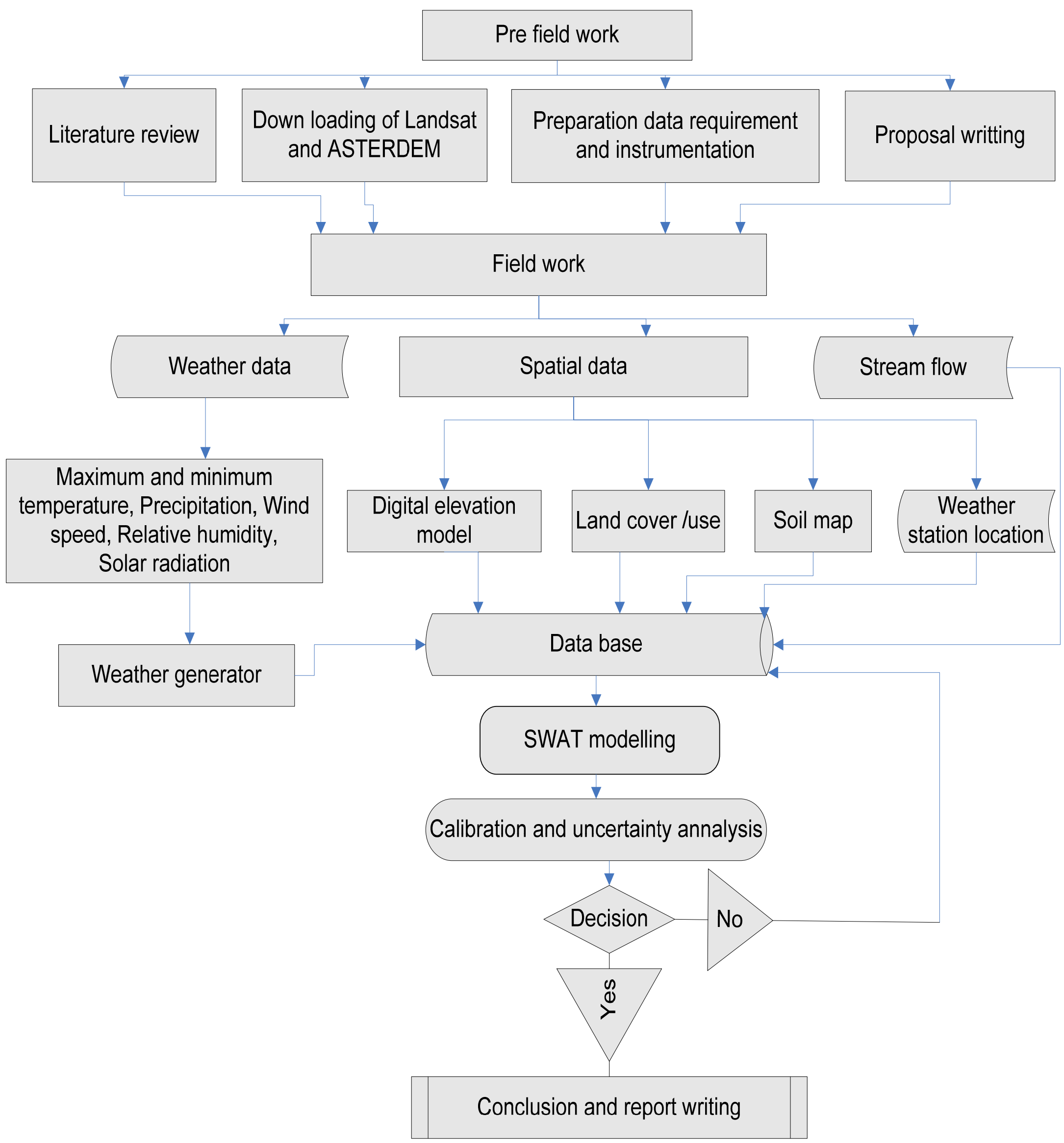

Figure1.2. Flow chart

1.6. Methods and materials (Methodology)

The methodology used in the study processes are based on the objectives. The details are explained in the flow chart above. It consists mainly three phases which are pre-field work, field work and post field work.

1.6.1. Pre-field work

This phase includes reviewing of previous works and literature related works using SWAT model for water balance and other applications. Additionally in this phase images were downloaded and processed to use as input for the model. The images were ASTERDEM and LANDSAT. ASTERDEM images were used to process the digital elevation model using Ilwis software and the landsat images were used for landcover classification using ERDAS Imagin software. The acquisition time for the landsat is the same as the simulation period for the discharge data. In this phase preparation of the base map and collection of field materials were done.

1.6.2. Fieldwork

We used three weeks to carry out the field work in September, 2009. It was at the beginning of September 2009. It was organized to collect all the data which are necessary for the model. During the field visit primary and secondary data were collected such as the typical land cover and boundary of the catchment Meteorological data (Rainfall, Relative humidity, sunshine hour, temperature and wind speed) were collected from Ethiopian National Meteorology Agency (NMA). Daily discharge of Golina and Alwuha Rivers were also collected from Ministry of Water Resources (MWR). Mostly the data runs from 1985 to 2005. The groundwater data were taken from the Ministry of water resources. Soil and Land cover map were obtained from the Geological Survey of Ethiopia.

1.6.3. Post fieldwork

In this phase the data collected during the pre-field and field work were processed according to the model input format. The SWAT model requires a special data format. This was a large task in this phase. During data processing GIS software and Excel were used to prepare the input data. Weather generators were prepared to fill the missed rainfall and temperature data and to generate climate data (relative humidity, wind speed, solar radiation). Among the spatial data Digital Elevation Model (DEM) was prepared from ASTERDEM as it is required by SWAT. From this the boundary of the study area is produced. The Land cover and soil map were converted from feature class to raster tiff format as MWSWAT requires the format. Then the model was run for the Golina catchment using the prepared data. Based on the soil, land cover and slope maps the HRU's were produced. These are helpful to subdivide the catchment into areas with different hydrologic properties. In this phase the final work includes calibration, validation, sensitivity, discussion of results and thesis writing.

1.7. Materials

The materials and equipments used to collect the required data were topographic maps of the Alamata and Kobo sub-basins, ASTER DEM and ASTER images. These were used to delineate the boundary of the study area. Equipment, such as the Garmin GPS and compass, was used to collect the ground control point data for the validation of the land cover classification.

1.8. Thesis outline

This chapter has given a brief outline of the background of the thesis with the main research objectives. Chapter two summarizes the findings of previous work in the area, while the study area is introduced in chapter three. The available data with regard to precipitation, climate and river discharge is described in chapter four. The chapter also deals with the aspects of filling the gaps in the data with the built-in SWAT procedures. Moreover, the chapter also describes the DEM hydroprocessing leading to the watershed configuration. The SWAT2005 model and the MapWindows GUI are described in Chapter 5. The modelling results and discussions for the Golina and the Alamata basins are given in Chapters 6. Finally, conclusion and recommendations are given in Chapter 7.

2. Literature review

Hydrological work in the area was carried out in the area in the framework of the Raya Pressurized Irrigation Project (Michael and Seleshi, 2007; WWDSE and CECE, 1999; WWDSE and CECE, 2008) and the Giranna Kobo Pressurized Irrigation Project (Metaferia, 2008). Groundwater studies of the Alamata Basin are available from (Dessie, 2003; Halefom, 2006). According to Michael and Seleshi (2007) the Raya Valley is part of the Denakil River basin which has a total catchment area of 74000 km^2 and lies inside the Tigray, Amhara and Afar regional states. This river basin has a total mean annual flow of about 0.86 Billion m^3 per year.

According to REST (1997) moisture stress is the major limiting factor for crop production in the Raya Valley. Rain fall is inadequate and erratic in distribution. In the lowland areas of the valley it is difficult to produce crops such as the local long season sorghum variety, with the limited amount of rainfall. As a result farmers in the lowland areas of the Raya Valley are used to traditionally harvest flood water that comes from the neighbouring highland areas with relatively better rainfall to supplement their crops.

According to the Kidane (2009) spate irrigation in the Raya Valley results from the rainfall on the Maichew and Ofla highlands west of the Mekoni and North of Alamata. When there is insufficient rainfall in the valley, rainfall from the surrounding mountains becomes the main source of supplementary irrigation which enables farmers to harvest a reasonable crop. The farmers in the Fokisa, Boboteya and Hara spate irrigation systems manage the water that comes from the neighbouring highlands in an organized way to irrigate their plots.

According to REST (1996) report, depending on the depth of the ground water and yields there can be a possibility of exploiting some for irrigation. This may be achieved by hand dug wells if found at shallow depth and hand pumps and other powered pumps depending on the depth of water table and their economy. According to Dagnew (2007) the Hashenge and its surroundings have different sowing time of various crops which is depending on the onset and continuity of the rainfall. There are two known and traditionally used cropping seasons. Short cropping season is the one, which starts at the end of the harvesting time of the previous crop. Successful short rainy season crops are meant to leave the land for the second crop season and hence will be harvested around May, allowing enough time for land preparation and sowing of the long rainy season crops. The second cropping season is the long rainy season as it is practiced in most parts of the country. The catchment is characterized by two soil types namely vertisols and cambisols.

The present study focuses only on the hydrological component of the model. What distinguishes SWAT from common techniques used to estimate runoff is that it is a physical model. The model takes into account such data as climate, soil properties, topography, land cover and management, and produces outputs with the use of common hydrological equations. Apart from the ability to take into account land use and soil data, SWAT differs from other physical models in its ability to separate the watershed into sub-basins and Hydrologic Response Units (HRUs). The main basin is divided into smaller ones, by selecting points on the stream network that act as outlets. In this way, the model can provide output data, such as discharge, at specific points of the river network. The partitioning of the basin or the sub-basins in HRUs has the meaning of dividing the watershed into no more than 100 different areas, which have the same properties regarding land use and soil. The equations are applied in each HRU separately and surface runoff and groundwater flow are routed to neighbouring HRUs, up to the outlet of the basin (Arnold et al., 1998; Pikounis et al., 2003). If the total water harvested by the HRU exceeds the field capacity of the soil profile, it will become percolation. This is different from the SWAT irrigation operation, which limits the water application to what can be stored in the soil profile.

The SWAT model is a widely known tool that has been used in several cases world-wide. SWAT has the ability to predict the impact of land management practices on water, sediment yield and agricultural chemical yield in large complex watersheds (Neitsch, 2005). In this study use is made of the SWAT graphical user interface (GUI) Map Windows (Leon, 2009).

There are only a few applications of the SWAT model in African. For example:

A GIS based hydrologic model, SWAT (Soil and Water Assessment Tool) was applied by Birhanu et al. (2007) and Birhanu (2009) for modelling the Weru Weru catchment at the foot slopes of Mt. Kilimanjaro in Northern Tanzania. This study demonstrated that prediction efficiencies can be determined through the SWAT model of physically-based distributed and lumped hydrological systems. A second study (Govender and Everson, 2005) tried to determine if the SWAT model could reasonably simulate hydrological processes in two small South African catchments using daily time steps. A third paper presents advances in hydrologic modelling of the Simiyu River catchment using SWAT in Tanzania (Mulungu and Munishi, 2007). Tunizian authors (Ouessar et al., 2008) studied how main hydrologic processes in arid environments can be simulated with SWAT. The model was applied to the 270 km^2 watershed of Wadi Koutine in southeast Tunisia, which receives about 200 mm annual rainfall. Most hydrologic models require daily weather data to run. While this information may be abundant in some parts of the world, in most parts such data is not available on daily basis. Distributed hydrologic models are particularly adversely affected by the lack of daily data or the existence of very inaccurate data as they impart large uncertainties to the model prediction. The weather generator was used weather statistics to generate daily data from monthly data in a SWAT model application to West Africa (Schuol and Abbaspour, 2007). Finally, Shimelis et al (2009) assessed the performance and applicability of the soil water assessment tool (SWAT) model for prediction of stream flow in the Lake Tana Basin, Ethiopia.

3. Study area

3.1. Topography

The study area is located in the Alamata sub basin in the Raya Valley (see Figure 1). It extends over an area of 2586 km^2. The valley is situated in the southern part of Tigray region between latitudes $12^0$16' and $12^0$55' N and longitudes $39^0$22' and $39^0$53'E. The study area is about 150 km south of the Tigray Province Capital City Mekelle. It is bordered by Afar region to the East, Amhara region to the South, Ofla and Enda mekoni woredas to the West and Alaje and Hintalo woredas to the North.

The topography of Raya Valley is characterized by a lower plain surrounded by mountains and small plateaus. The mountain part ranges from 1600 to 3900m.a.s.l while the lower plain falls between altitudes of 1311 to 2000m.a.s.l. The slope of the irrigable area generally decreases from west to east. (See Figure 3.1 and 3.2)

Generally, the physiography of the Raya Valley can be classified into three land classes as follows. The hills and mountain ranges in the western and eastern parts of the study area are mostly covered by natural vegetation. The plateaus found around Korem, Maichew, Chercher and Bala towns are mainly under highland crop cultivation. Highly suitable agricultural fields of the lowland flat plains extend from Waja to Mekoni. Presently the major part of this flat plain is used for lowland crop cultivation of sorghum, maize and teff and the rest is under natural vegetation cover used as an improved pasture for livestock and wood supply for different domestic uses.

3.2. Climate

The area has a semiarid to sub-humid climate. The mean annual rainfall of the highland, midland and lowland areas are 700 mm to 1000 mm, 400 mm to 900 and 650 mm to 750 mm respectively and the main rainy season is from June to September.

The rainfall pattern is determined by moist air associated with the Inter-Tropical Convergence Zone (ITCZ), with air moving into the area initially from the south east (March-May) to south west during monsoon (July to September). Therefore, the Raya Valley has a bi-modal type of rainfall with April as a peak for Belg rains and July for the Kremt rains. In the valley the mean annual rainfall varies from less than a 400mm in the north-eastern part around Chercher to above 1000mm in the western part of the study area around Hashenge Lake.

The seasonal distribution of rainfall in the area is associated with the annual progression of the Inter Tropical Convergence Zone (ITCZ) (REST, 2007). Mean daily temperature is highest in the months of July and August and lowest in the months of December and January. In the Raya Valley the mean temperature correlates with altitude. In the upper part of the catchments mean annual temperature varies from 16.2^0C to 22^0C in Korem, in Alamata and Chercher 28^0C and 20.9^0C in Mekoni. In general, the climate in the Raya Valley varies from warm temperate to hot semi-arid type in the lower Raya plains. In the study area frost hazard is expected to occur during the months of November to January, mainly occurring at altitudes above 2300m.a.s.l.

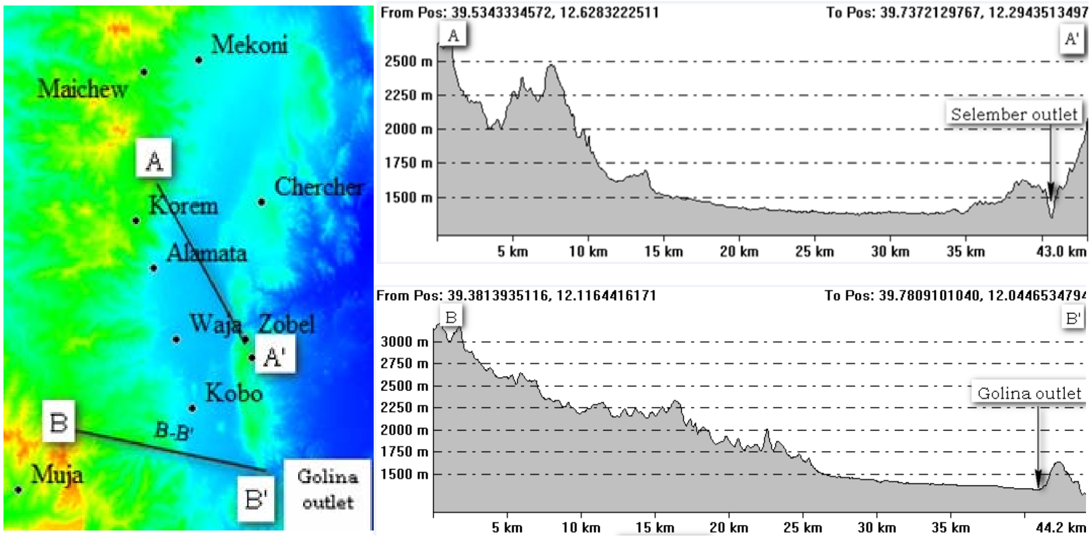

Figure 3.1 A-A' Cross section of Golina catchment
Figure 3.2 B-B' cross section of Alamata –Selember

As we can see in Figure 3.1 and 3.2 the only outlets are the Selember and Lower Golina which are the lowest elevation in the study area.

As mentioned above, in the Raya Valley three broad Agro-Ecological Zones (AEZs) can be identified mainly based on altitude, moisture and physiography. These are as follows:

Dry Kolla Flat plains

This is located in the Alamata-Mekoni flat plain, specifically in the south central part of the study area from Waja to around Kukuftu. The altitude of this AEZ is below 1500m.a.s.l and the mean annual rainfall varies from 500 mm in the east to 700 mm in the west. The highest temperatures and Potential Evapotranspiration (PET) are recorded in this AEZ because of its low altitude.

Dry to Moist Woyna Dega Flat plains, Hills and Mountains

According to Raya Valley pressurized project report WWDS and CECE (2008) this large AEZ is located in the eastern, northern and western parts of the study area. The altitudinal range of this AEZ is from 1500m to 2300m.a.s.l and the mean annual rainfall varies from 450mm in the east and north to 1000 mm in the western part. The general character of this AEZ is flat plain in the north and hills and mountains in the east and west part. The temperatures and PET in this AEZ are lower than those in the Dry Kolla flat plain. However, within this AEZ, the elements vary with altitude. In the Raya Valley the extent of this AEZ is 164,000 ha of land which is about 67 % of the total study area.

Moist Dega Mountains

In the Raya Valley the altitude of this AEZ is above 2300m.a.s.l and it is found located in the western mountains of the study area. Here rainfall is higher and more evenly distributed than in the other two AEZs. However, the best agricultural lands are located where rainfall is low and variable. Because of high altitude, the temperatures and the potential evapotranspiration in this AEZ are much lower and therefore the LGP is high ranging from 120 to 150 days.

3.3. Geology

According to Dessie (2003) the geological units in Ethiopia fall roughly into three main categories : the Precambrian Basement, Late Palaeozoic to early tertiary sediments and Cenozoic Volcanics with associated sediments. These sequences reflect a complex history of periodic uplifts, marine transgressions, volcanism and rifting. The Cenozoic Volcanism is associated with the Great East African Rift System which started to develop during the Miocene. Following the initial subsidence of the Afar Depression, high volcanic activity developed along the rift axis. Meanwhile sedimentary processes have continued in this era forming valleys filled with colluvial and alluvial material along the edges of the rift. Raya Valley (see Fig. 3) is found at the westernmost range of a downthrown block in the vicinity of the great scarp of the Ethiopian plateau. The boundaries of the trough are formed in the west by the rift escarpment, while low hills in the east constitute the boundary between Raya Valley and the Afar Depression. Outflow from the basin may take place through the gaps in this eastern range of hills: i.e. through Selember, the Golina and the Alwuha Rivers further south.

Figure 3.3 Outcrop near Selember (basaltic rock)

The dominant geological formations found in the valley floor are poorly compacted sedimentary basin fill deposits. The frame is mainly composed of Tertiary volcanic rocks. Both the geophysical survey and the existing water wells did not penetrate the entire thickness of the sediments, hence the information on the distribution, thickness and composition of the basin fills is limited.

Generally the lower geological unit of the basin fill is believed to be a lake deposit while the upper one is a river deposit. Its sediments consist of many lithologically different strata which are poorly compacted, the material, obviously, originated from weathering debris of the adjacent mountain areas.
Commonly a subdivision is made in three layers: old, middle and young:

- The old basin fill has been preserved at greater depth with a thickness ranging between a few meters and 240m. Clayey rocks predominate and they probably are lacustrine fresh water clays.
- The sediments of the middle basis fill are characterized by having been re-worked more strongly; their total thickness is generally between 20 and 50 ms.
- The sediments of the young basin fill, too, show a great variation in nature of origin, grain size distribution and regional structure. Their total thickness is between 20 and 30m. Generally fluvial sediments predominate in the western part of the sub-basin, their grain sizes rapidly decreasing towards the east.

The upper most part of the sediments of the basin fill is further sub-divided into three major groups:

- Colluvial and river deposits
- Inter-fluvial fan foot plains and valley bottom deposits
- Central valley flood plain deposits.

3.4. Soils and Landuse

3.4.1. Soils

The soils data used by SWAT can be divided into two groups, physical characteristics and chemical characteristics. The physical properties of the soil govern the movement of water and air through the profile and have a major impact on the cycling of water with in the HRU (Neitsch, 2005). The soil data was obtained from Ethiopian Geological Survey which is developed based on FAO and the International Soils Reference and Information centre (ISRIC) (Mulungu and Munishi, 2007). The major soil types exhibit a general relationship with altitude. It is clear that the soils of the valley have developed on recent alluvial-colluvial sediments derived from parent material on the adjacent mountain ranges.

In general in the study area and in particular in the lowland plains there are two types of dominant soils: verti-cambisols/lithosols and chromic vertisols (see figure 3.4 below) (black heavy clay soils). Fluvisols (medium textured soils) occur in the plains along the rivers. Texturally these two types of soils are clayey and loamy. The clay soils usually occur in flat plains and the loamy soils on the foot slopes of hills and mountains. Shallow Leptosols are the dominant type of soil found in the mountains and hills surrounding Raya Valley.

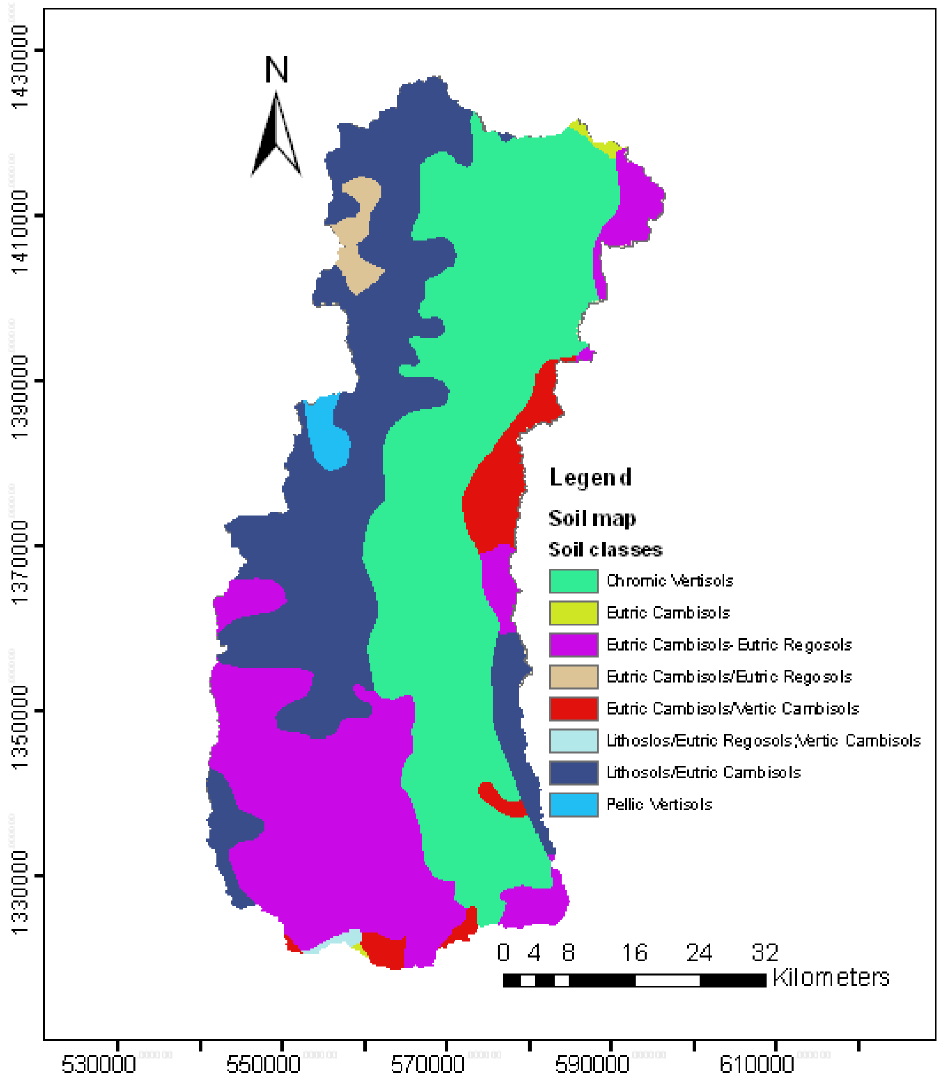

Figure 3.4 Soil map of the study area (after EGS, 2002)

3.4.2. Land use

The cropping intensity, which can be determined by the fertility of soil and moisture availability, indicates the rate of cropping of a farmland during a given year. In the case of the existing situation of Raya Valley, it could be possible to crop two or three times a year if water is adequately available (WWDSE and CECE, 2008).

Variable and low rainfall is the major crop production constraint in general in the Raya Valley and in particular in the low lands and eastern part of the study area. In the study area the rainfall is bimodal that is small rains in February to April and big rains in the July to September. On the high lands there were evergreen trees and is the area with high dense forest. The major of the areal coverage is with sparsely vegetated forest. The cereal crops are largely found in the valley flat plain area but there are also small areas used for the cultivation in the mountainous area.

Wheat and barley are the major crops in the highland areas of Tigray. In the lowlands, sorghum and maize are most commonly grown. Teff is grown in all of the altitudinal zones, but is most common in lowlands (Kjell et al., 2002).

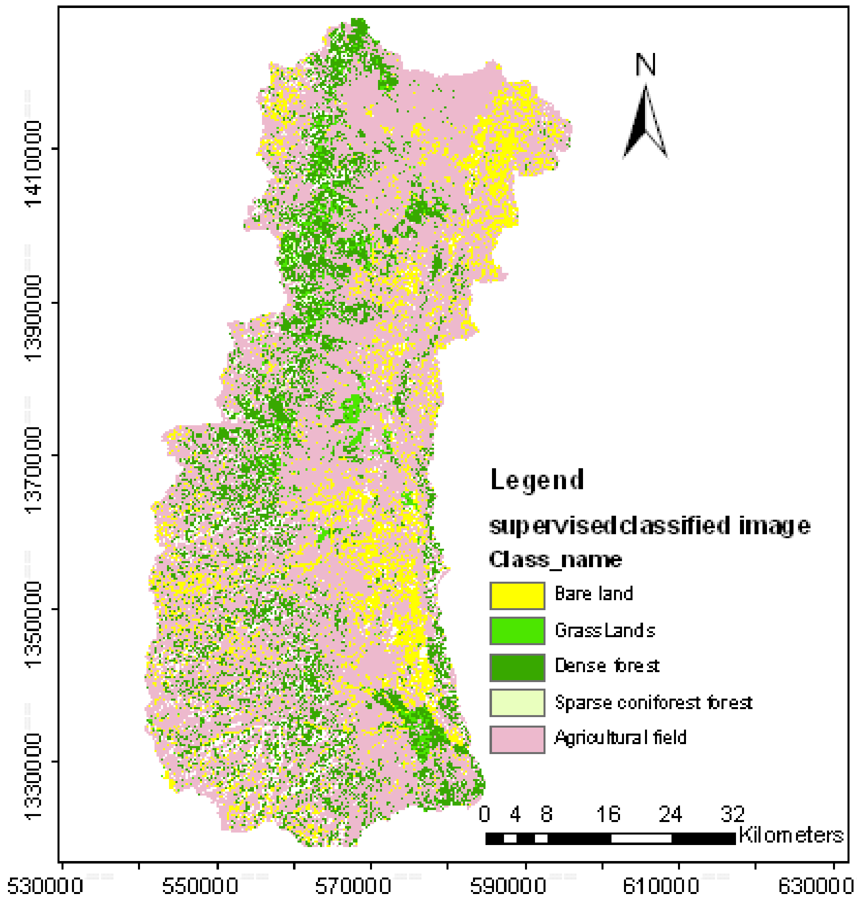

Figure 3.5 Land cover classification of Raya Valley

The type of land use and cover of Raya Valley catchment is determined from a classification of the Landsat images. This classification is validated using ground control points. The images were free from cloud cover and coincided with the flow simulation period. The images were imported into GIS software (ERDAS Imagin). The images were enhanced after geometric correction using some control points which were taken during field work and finally the study area is extracted using the basin boundary prepared from the ASTER Digital Elevation Model (DEM). For the purpose of classification, the false colour composites of the bands that carry most of the information, Bands 3, 4 and 5 were created and used for better interpretation of land use and land cover of the catchment (Mulungu and Munishi, 2007). Prior to the classification process, the sites were developed by on-screen digitization of the different areas. The software then produces the signatures using 'makesig' command. Then, the reclassified land cover/use data is prepared for the SWAT simulations. But for the simplification I am going to use the land cover obtained from the Ethiopian Geological Survey (EGS) (Figure 3.6).

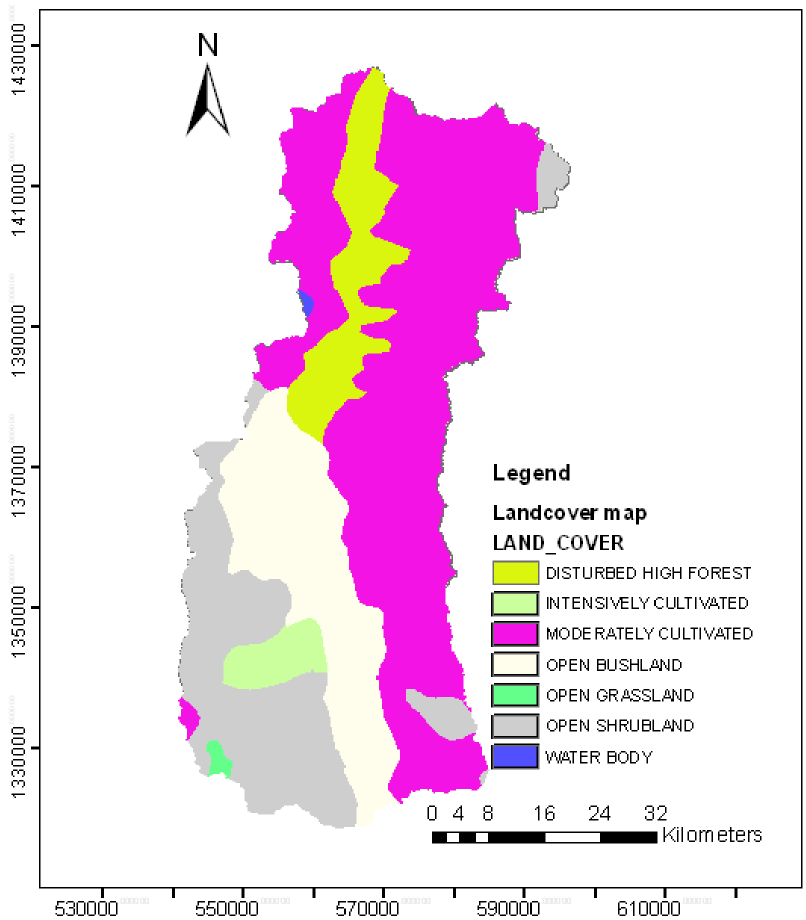

Figure 3.6 Land use of the study area (after EGS, 2002)

3.5. Water resources

3.5.1. Surface water

In the study area the surface water resources are mainly from mountain streams. These streams are not perennial rather they flow during rainy season. Some of the streams are characterized by lower dry season flow and flash floods during the rainy season. There are also a number of small springs (e.g. Waja spring) in the southern part of the project area which flow throughout the year and are used for traditional irrigation.

The dry season flow of most of the streams is totally abstracted by farmers for small traditional irrigation schemes upstream of the recently proposed irrigable areas. The Raya valley is drained by a number of streams. The annual total surface water resources generated from the upland catchment is estimated at about 114 Mm^3 (WWDSE and CECE, 2008). As we can see from the result of DEM hydroprocessing the drainage density of the study area is mainly concentrated along slopes. In the valley the drainage density is lower than the mountainous area. The result of the DEM hydroprocessing is explained further in detail in chapter 4.

3.5.2. Groundwater

Groundwater resources are believed to be a large water resource in the project area. The dominant groundwater flow directions are north south and west east. The depth of groundwater varies from less than 20 m in Waja to over 60 m in the northern part of the project area. The average groundwater recharge in the project area is estimated to be 85.6 Mm^3yr^{-1} and the static groundwater reserve is estimated at 7,150 Mm^3. However, the total sustainable quantity of groundwater per year in the valley is estimated at about 130 Mm^3yr^{-1}. (WWDSE and CECE, 1999).

Figure 3.7 Deep well for irrigation (10km from Alamata)

Figure 3.8 Shallow hand-dug wells in Raya Valley alluvial deposits near Selember

Alluvial Aquifers

The floor of the valley in the Alamata subbasin is mostly a flat plain with decreasing slope from north toward south and it is filled with quaternary alluvial deposits derived largely from basaltic mountain ranges that are standing high on the shoulders of the valley. The alluvial deposits are composed of intercalating layers of gravel, gravely sands, silty sands, clay, silty clay with increasing coarser material towards the top (REST, 1997).

From hydrogeological view point, it can be concluded that the coarser materials (mainly sandy and gravely materials) lying at different levels are the most important aquifers through which groundwater can flow easily.

As can be observed from geological well-logs inter-bedded clay layers generally act as impervious layers, restricting vertical movement of groundwater. Wells drilled in the central part of the valleys are mostly artesian, because most wells drilled in this area encountered the aquifer after penetrating several intercalations of clay horizon.

In general it is observed that the coarser alluvial aquifer in the valley decreases in thickness from both western and eastern flanks of the valley towards the central axis of the valley. On the other hand, the less permeable aquifers increase towards the centre and in the upslope areas.

Volcanic Aquifer

The valley floor is surrounded by highly fractured and weathered essentially basaltic rocks. Furthermore outward from the valley boundaries within the limit of the basin the surfaces of the shouldering plateau are covered by extensive basaltic flows. Highly weathered acidic rocks such as Ignimbrite, Rhyolite and ash flows are found within the plateau in places. Remnants of plateau type basaltic outcrop also found as a small island of hills that protrude out of the valley floor (REST, 1997).

The basaltic rocks are highly jointed fractured and weathered and consequently the open joints are dominantly filled with secondary minerals such as clayey. From hydrogeological point of view, the volcanic bedrock in the basin is not very important. In this terrain there is no coherent body of groundwater since this water bearing formation is limited to the weathered and local fracture zones of low storage and limited transmissivity.

Springs

Perennial springs of considerable yield are emerging from Western Mountains of the valley. The mountain front recharge along the western mountain slopes seems to provide the source of these springs. Of the seven cold springs which have been identified in the whole of the project area, four are found in the vicinity of Waja. They have a combined yield of about 100 ls^{-1}. The others have a very low yield, with the exception perhaps of the seepage zone at Gerjele, 10 km north of Alamata. They generally emerge at the contact between the colluvium and the less permeable alluvial deposits of the basin fill (REST, 1997).

4. Data Analysis

4.1. Introduction

Daily meteorological data were collected from the Meteorological Agency of Ethiopia. The temporal data include rainfall, wind speed, temperature, and relative humidity. Table 4.1 below gives a summary of the stations and the parameters measured at each station, whereas a location map is given in Figures 4.1 and 4.2. Data were collected for twenty-one year period from 1985 to 2005. However, there are many gaps in the data as will be discussed further in the sections below (sections 4.2, 4.3 and 4.4).

The weather stations are grouped into two categories: the valley stations (Waja, Alamata, Kobo, Zobel) and the highland stations (Maichew, Korem and Muja). The general climatological and hydrometeorological aspects were discussed in two reports (Metaferia, 2008; REST, 2007) and in this chapter use is made of the analysis presented in these reports. Although more climatic data were obtained, for example for the stations Chercher and Woldia, these data are not further discussed here.

Discharge is measured in only two stations. There is one station measuring the discharge of the Golina River near Kobo Town, while the other measures the discharge of the Alwuha River. Both river catchments lie to the south of the Raya Valley. The raw discharge data was collected from the Ministry of Water resources. As was already reported by Metaferia (2008) and REST (2007) the data are rather poor. There are many gaps in the data and the processed data also contain many outliers. The processing of the river discharge data is discussed in section 4.5.

It is important to employ good procedures to fill gaps in the data series, because of the many gaps in the data. Here use is made of the monthly climatic time series which was patched by WWDSE and CECE (2008).The data allow making a comparison of the evapotranspiration determined by the Penman-Monteith and the Hargreaves methods. Moreover the monthly time series may be applied in the construction of weather generation files for use with the SWAT model (section 4.6). SWAT uses a stochastic weather generator to fill gaps in the daily data (see chapters 5 and 6). For this reason a discussion is given of the monthly climatic parameters of a valley and a highland station (respectively, Kobo and Maichew) and the way they may be used in the preparation of the SWAT weather generator files.

Spatial data include a digital elevation map at 30 m resolution obtained from the global ASTER DEM database (http://www.gdem.aster.ersdac.or.jp/search.jsp). Moreover, soil and land cover maps were collected from Ethiopian geological survey. The DEM was processed with the ILWIS hydroprocessing tool, leading to accurate delineation of all subcatchments in the area and whole catchment of the valley (sees Figure 4.1 and section 4.7). This section also briefly describes the main steps of the hydroprocessing. ASTER images in the visible domain were used in combination with the DEM to delineate the subcatchments accurately, resolving some small problems on the southern and northern boundaries of the Raya Valley watershed.

Table 4.1 Summary of meteorological and river discharge stations used in this study

					Availability of climate, rainfall and river discharge data							
					Temperature							
nr	Station name	Lat (degree)	Long (degree)	Elev (m)	Tmax	Tmin	Rainfall	RH	Sunshine hour	Wind speed	Solar radation	Discha
	Rainfall and climate data											
1.	Alamata	12.42	39.56	1545	x	x	x	x	x	x	x	
2.	Kobo	12.15	39.64	1498	x	x	x	x	x	x	x	
3.	Waja	12.28	39.60	1469		x	x					
4.	Korem	12.51	39.52	2483	x	x	x	x				
5.	Maichew	12.78	39.54	2432	x	x	x	x	x			
6.	Muja	12.00	39.29	2780			x					
	River Discharge data											
7	Golina	12.07	39.62	1465								x
8	Allwuha	11.90	39.68	1414								x

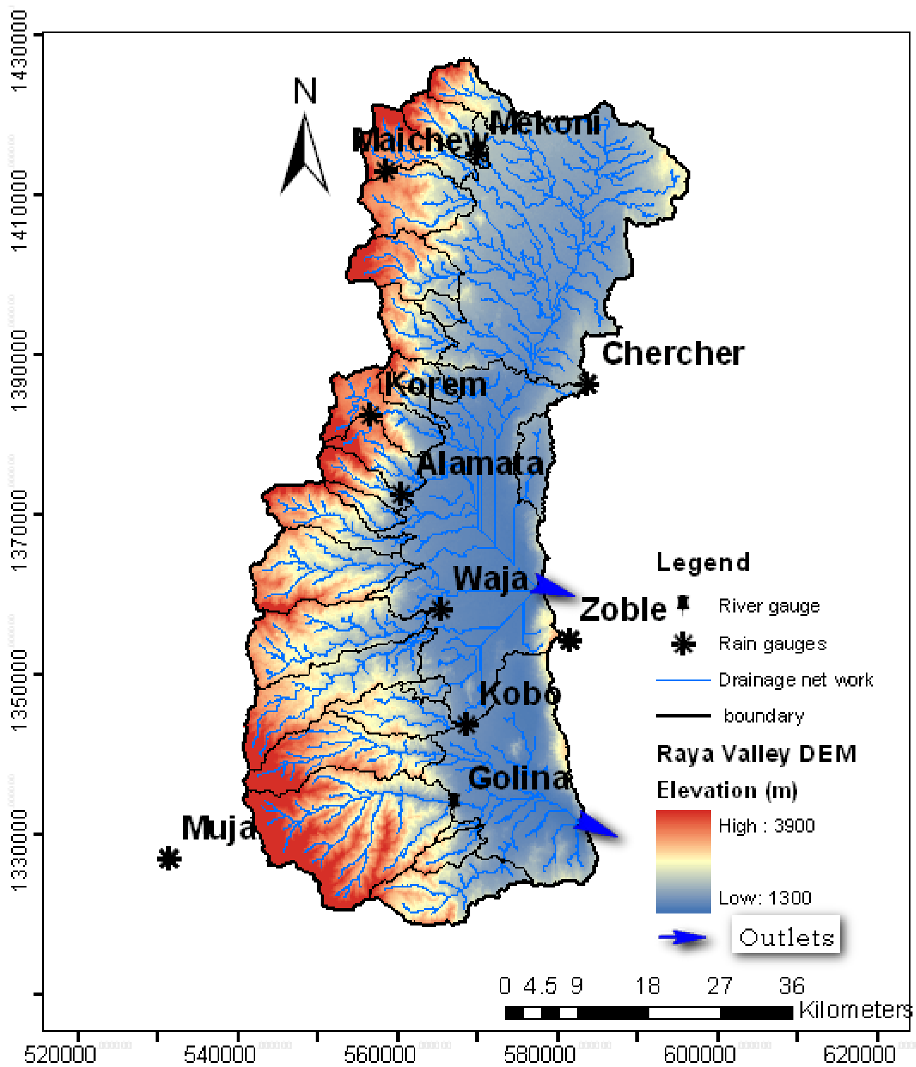

Figure 4.1 Location map of hydrometeorological stations.

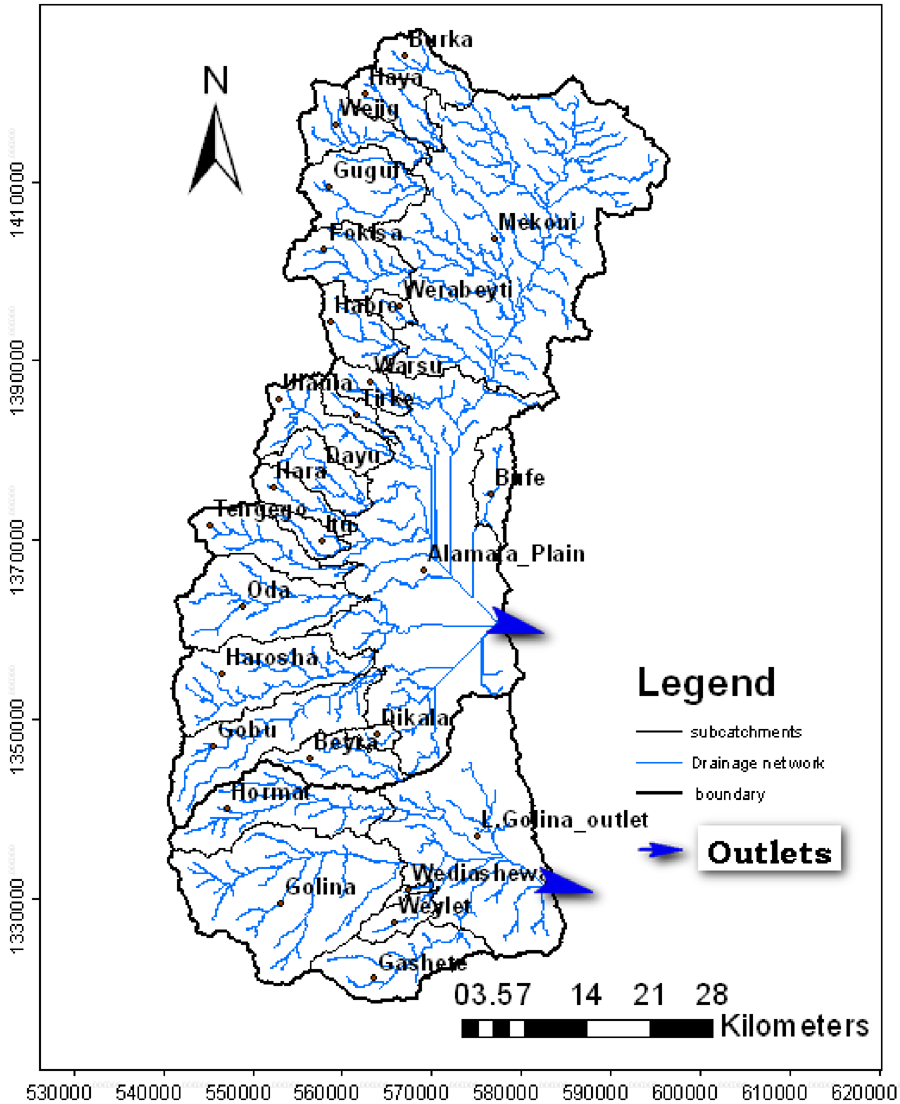

Figure 4.2 Subcatchments of the study area

The areas of the different subcatchments shown in the above figure are found in the appendix C.

4.2. Daily precipitation

Rainfall data is available from a number of stations located in and around the basin. Basically daily and monthly total rainfall time series are required to estimate the monthly water resources availability.The graphs below show distribution of daily rainfall in the study area (in high lands and low lands). As we can see from the graph the data have many missing values. The first three figures show the rainfall from valley area stations which are Alamata, Kobo and Waja. The other figures show the rainfall of the highland stations Korem, Maichew and Muja. It is obvious that there is a common data gap due to the war in the early 1990s. Fewer gaps occur in the period from 1995 onwards. A similar trend is present in all the other climatic data sets. For this reason the modelling in this thesis is restricted to a 10-year period from 1996 to 2005.

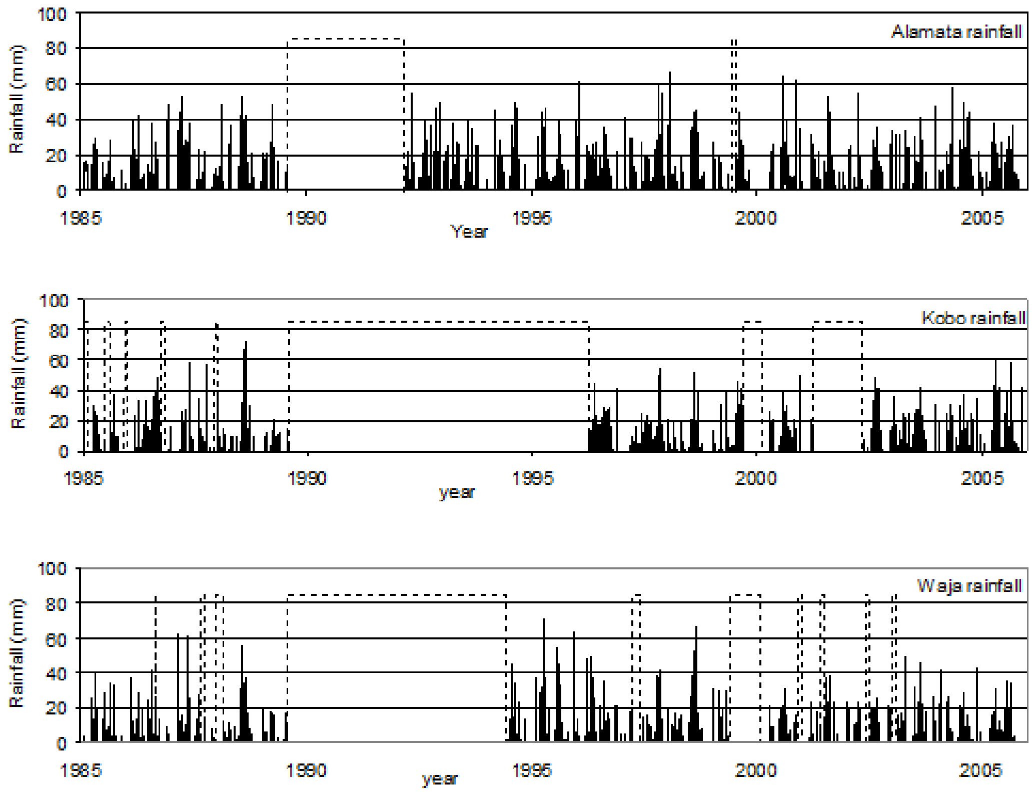

Figure 4.3 Daily rainfall of Waja, Kobo and Alamata, showing gaps in the data

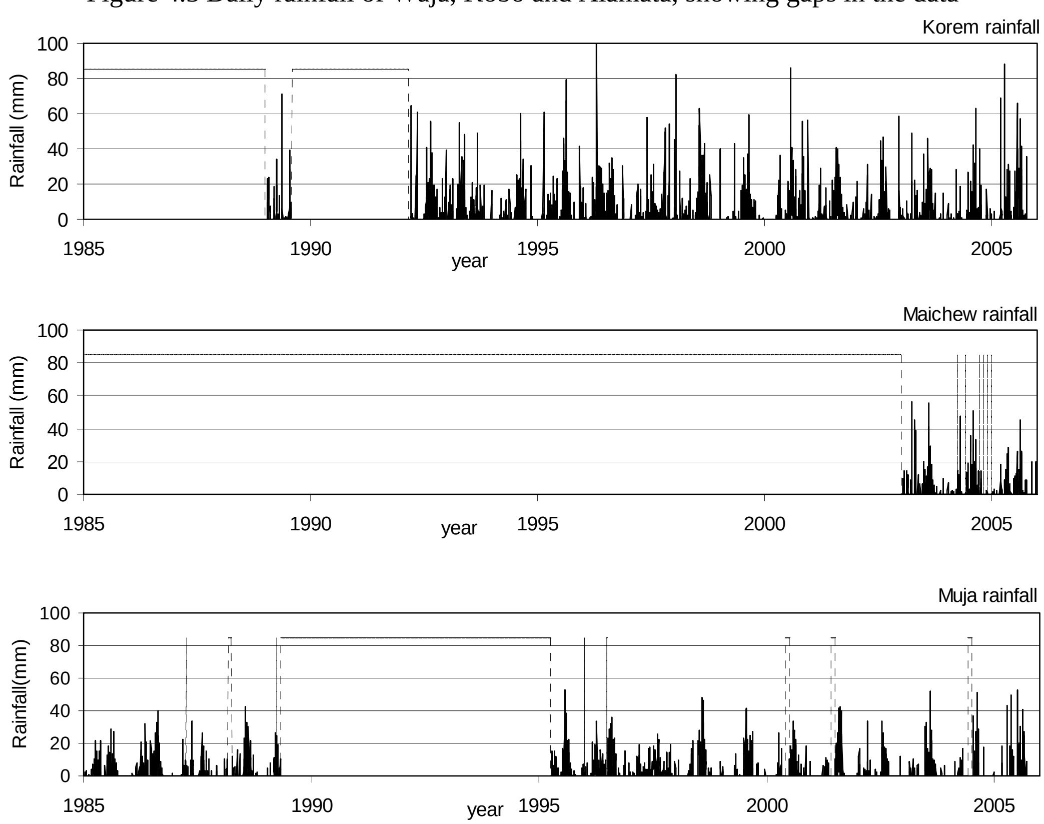

Figure 4.4 Daily rainfall of Muja, Korem and Maichew, showing gaps in the data

4.3. Temperature (maximum and minimum)

In the study area the temperature zone can be divided into two classes. These are the lower plain of the valley which has high temperature and the high land (mountainous) area which has lower temperature. Figures below show the temperature of the low land and high land areas. Of the lowland area I took as examples Alamata and Kobo and from the highland areas Korem and Maichew. The dashed lines show the missing data. The figures show again a data gap in the early 1990s. However, with the exception of Maichew, the data appear sufficient for SWAT modelling from 1996 onwards.

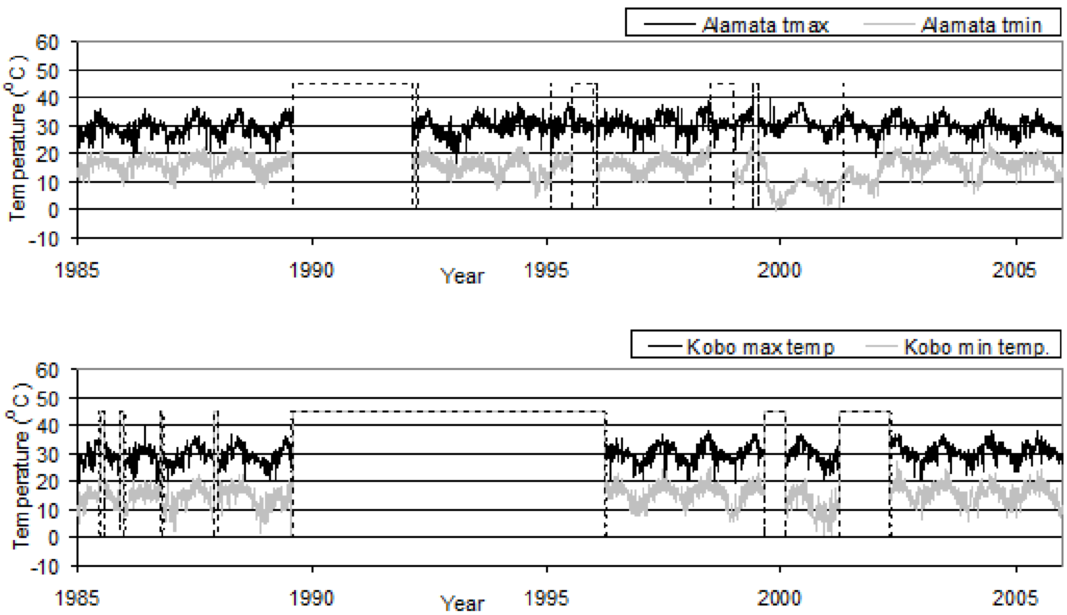

Figure 4.5 Maximum and minimum temperature of Alamata and Kobo station

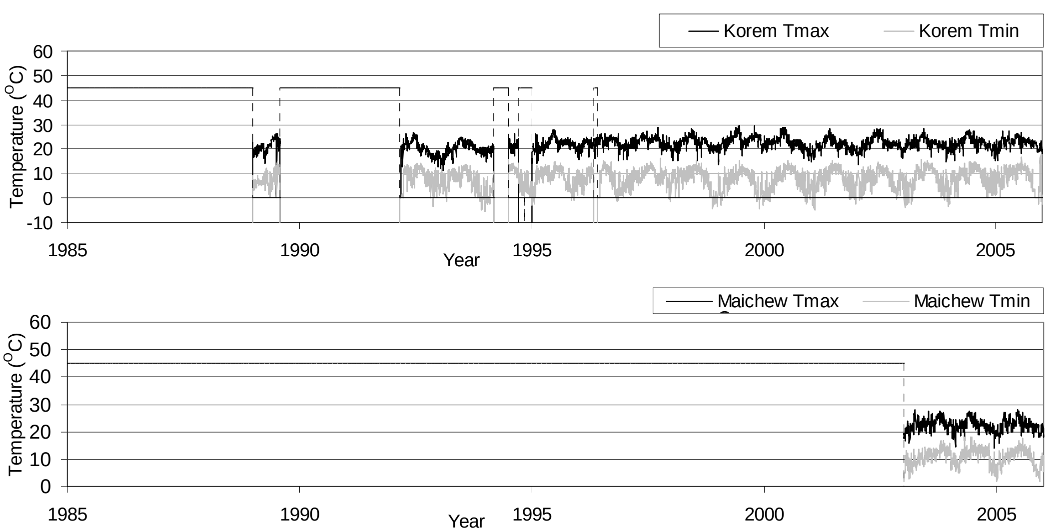

Figure 4.6 Maximum and minimum temperature of Korem and Maichew

4.4. Monthly climate data

In addition to the daily rainfall and temperature, the SWAT weather generator (*.WGN) needs the average monthly data of wind speed, solar radiation (sunshine), relative humidity and dewpoint temperature for a period of several years. These monthly data were obtained from the WWDES and CECE (2008) hydrometeorological report and the Ethiopian Meteorological Agency. The gaps in the monthly data were filled by WWDSE and CECE (2008) using correlations with adjacent stations. This interpolated average monthly data was used in the construction of the highland and lowland *.wgn SWAT files. The SWAT weather generator then generates the daily output of rainfall and temperature while filling the gaps in the temperature and rainfall files. SWAT then uses these data to produce PET, actual ET, surface runoff, river base flow and groundwater recharge. More details are found in section 4.6. Results are shown in Chapter 6.

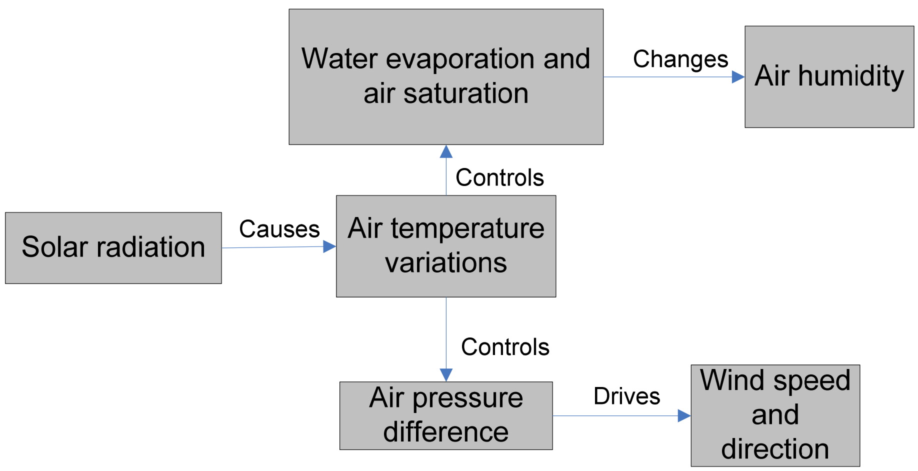

Figure 4.7 Relationship among weather variables after (Guan et al., 2007)

4.4.1. Relative humidity

Relative humidity is the gravimetric ratio of water in a unit space to the water vapour moist space can hold at that temperature (Viessman et al., 1989). Relative humidity is usually expressed as a percentage. The relative humidity is one of the weather generator inputs. In Kobo station the mean monthly relative humidity ranges from 30 to 70 % in June and January respectively. These data were also used to compare the Hargreaves and Penman-Monteith calculation of the ET_o in Maichew and Kobo areas respectively.

4.4.2. Wind speed

Air pressure gradient, or the difference between regions of high and low air pressure, impels air in the direction of lowest pressure, creating wind. The larger the air pressure gradient, the greater the wind speed. Wind speed is one of the inputs for the SWAT weather generator and for the computation of evapotranspiration. Wind is characterised by magnitude and direction. It is measured by anemometer. The mean values of Kobo wind speed vary from 1.2 ms^{-1} in September and 2.2 ms^{-1} in July.

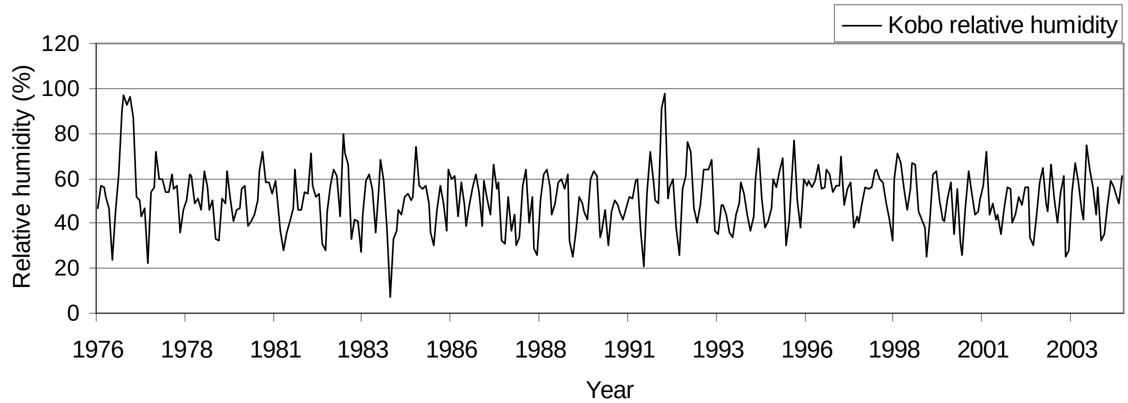

Figure 4.8 Relative humidity of Kobo station

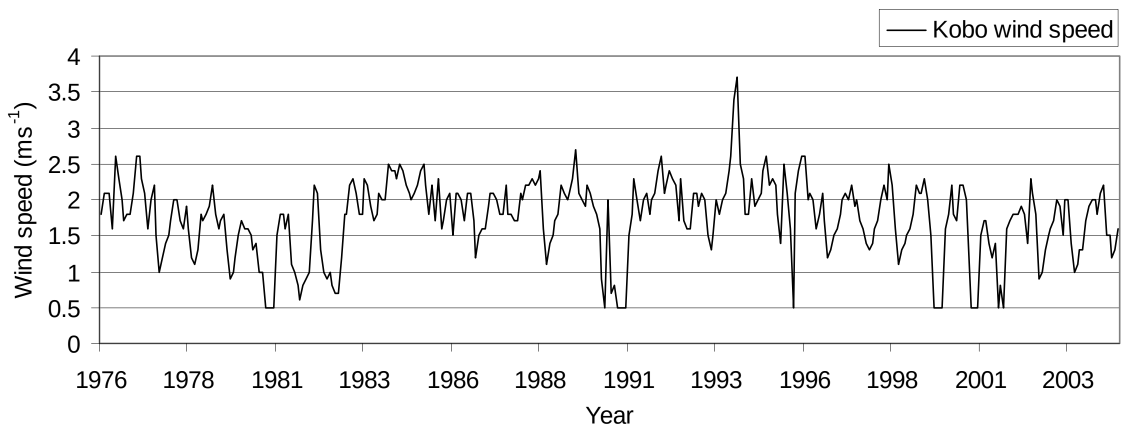

Figure 4.9 Wind speed of Kobo station

4.4.3. Solar radiation

All the sun's energy arriving at the earth's surface is at wave lengths less than 4μm, this energy is referred to as solar radiation. Water vapour absorbs some of the sun's energy in the "near infrared" range (Dingman, 2002). Solar radiation is one of the inputs for the SWAT weather generator. As it is described in the the mean shine duration of the study area is above 8.4 hours in the period of October to December and is reduced to 5.7 hours in July.

4.4.4. Dewpoint temperature

Dew-point temperature is the temperature to which a given parcel of air must be cooled at constant pressure and constant water vapour content in order for saturation to occur (Dingman, 2002) The dew point temperature is the temperature below which the air can no longer hold all of its water vapour, where the relative humidity would be 100% if the air was cooled. Theoretically, the dewpoint temperature can be as low as –273 °C (absolute zero), but at a normal atmospheric pressure it can never exceed 100 °C.

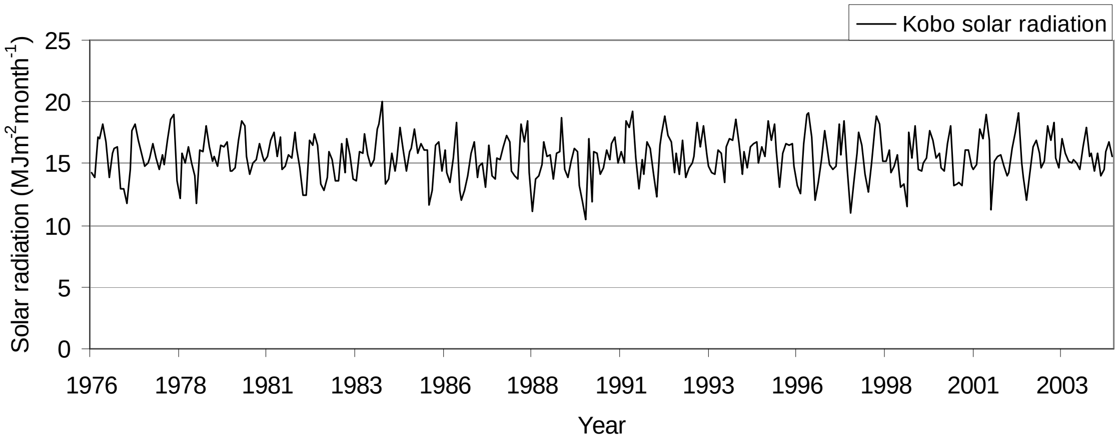

Figure 4.10 Solar radiation of Kobo station

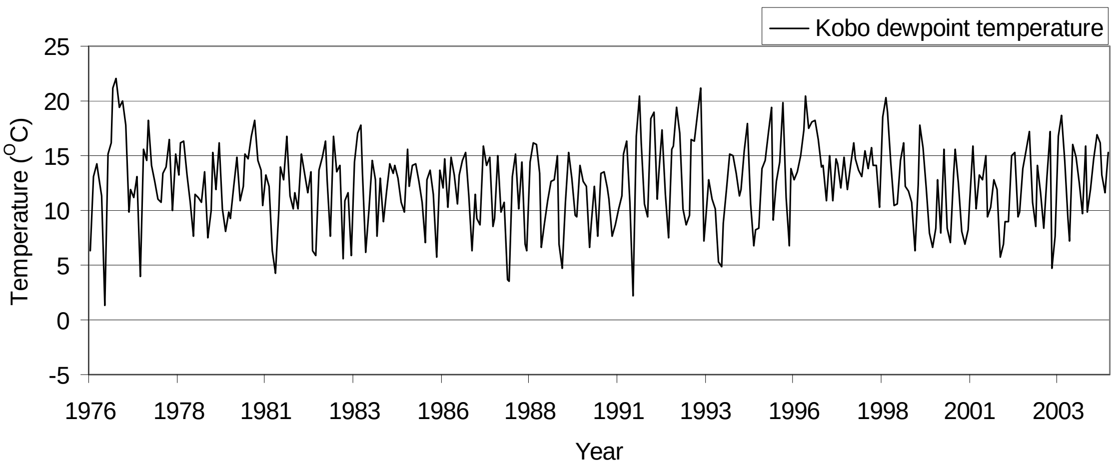

Figure 4.11 Dewpoint temperature

4.4.5. Evapotranspiration (ET)

The combination of two separate processes whereby water is lost on the one hand from the soil surface by evaporation and on the other hand from the crop by transpiration is referred to as evapotranspiration (ET) (Allen et al., 1998). The evapotranspiration of the Kobo and Maichew areas is calculated using the monthly climatic data from WWDSE and CECE (2008) report. The Hargreaves and Penman-Monteith methods were used here. As we can see from the graph below the correlation between the Penman-Montheith and Hargreaves methods is a little higher in Maichew than in Kobo.

It is important to note that the reference evapotranspiration in the valley stations is about 400 $mmyr^{-1}$ higher than in the highland stations. The modelling should take into account that rainfall generated in the highlands is less subjected to evaporation than in the valley. Consequently relatively more runoff is generated in the highland areas. Finally, the reference evapotranspiration by Hargreaves method is about 100 $mmyr^{-1}$ higher than the ET_0 determined by the Penman-Monteith method. Because in the present situation mostly only daily temperature data is available and therefore on a daily basis only the ET_0 by Hargreaves method can be evaluated, downward corrections in the order of 100 mmyr^{-1} must be considered.

Table 4.1Evapotranspiration of Kobo and Maichew meteorological stations

Stations	ETo (mm) Hargreaves	ETo (mm) Penman-Monteith
Kobo	1850	1702
Maichew	1458	1382

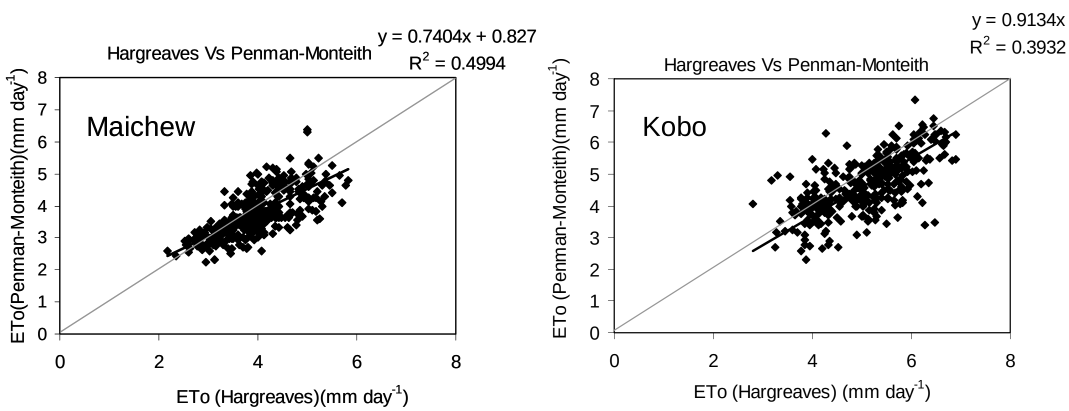

Figure 4.12 Evapotranspiration using Penman-Monteith and Hargreaves methods

4.5. Golina discharge measurements

The Raya basin is drained by quite a large number of rivers. Data on discharge are required for the model calibration on monthly basis. However, in the Raya Valley study area there are no river gauge stations. The nearest river gauge stations are located at Golina River near Kobo town, immediately to the south of Raya Valley and in the Alwuha River to the south of the Golina catchment. The raw discharge data was collected from the Ministry of Water resources for the period from 1976-2005. As was already reported by Metaferia (2008),WWDSE and CECE (2008) and REST (2007) the data are rather poor. There are many gaps in the data and the processed data also contain many outliers (see figures 4.15 and 4.16 below). The lack of quality of the discharge data, caused Metaferia (2008) to look at the discharge of a third catchment in the area i.e. Paso Mille with rainfall data from Haik.

The cumulative records of the Golina and Alwuha river flow as shown in figures 4.15 and 4.16, show that parts of the record contain discharge rates which are clearly too high. This is indicated by the near vertical slopes in the cumulative records. The flat horizontal parts in the cumulative records indicate the gaps in the records. After tentative manual correction of the outliers in the Golina and Alwuha discharge records, the cumulative records were drawn again for the period 1996 – 2005 (see Figure 4.16).

Figure 4.13 The location of Golina River gauge

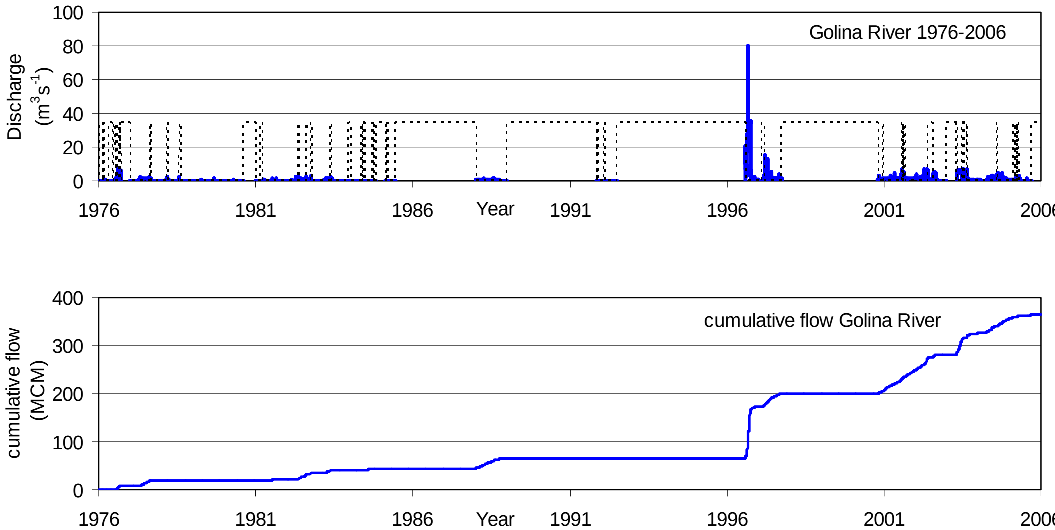

Figure 4.14 Measured Golina River discharge and cumulative discharge

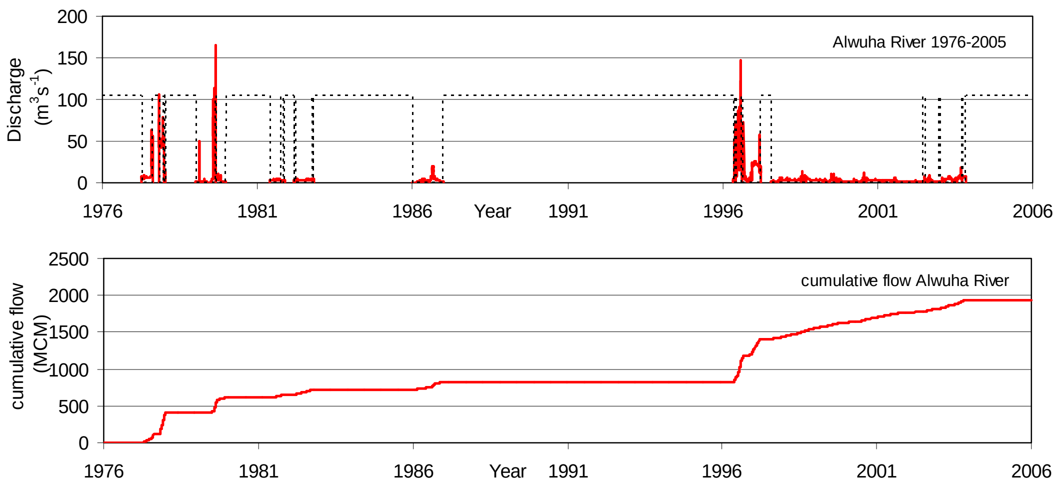

Figure 4.15 Measured Alwuha River discharge and cumulative discharge

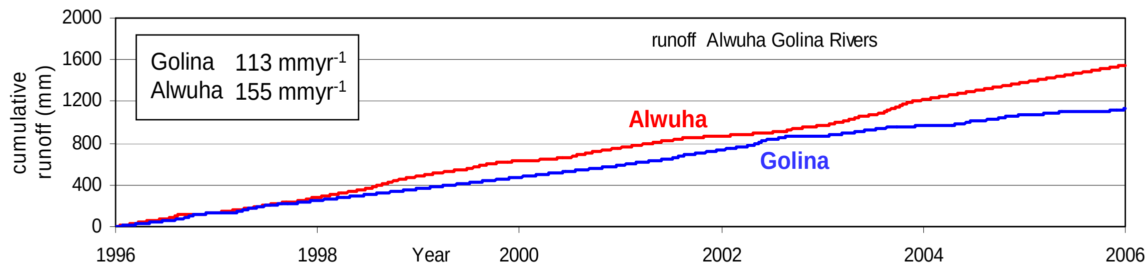

Figure 4.16 Cumulative discharges of manually corrected Alwuha and Golina records.

To be able to draw the graphs of Fig. 4.16, average discharge is assumed during periods when no data was available. It follows from the analysis that the average discharge is 113 and 155 $mmyr^{-1}$ for the Golina and Alwuha River respectively. When aggregating the corrected data on monthly time intervals, the picture of Figure 4.17 emerges. The Golina flow record does not show a clear peak in the months July and August, at the height of the rainy season. The Alwuha and Mille Rivers show this peak better. However, the baseflow of these rivers during the early months of the year appears rather high. Perhaps this is due to the fact that these rivers originate in very high mountains, with higher rainfall and possibly snowmelt effects. For the case of the Golina River it seems more realistic to assume the flow pattern indicated in the figure below as Golina2.

From observations of the hydrometric structure during the fieldwork (see Figure 4.14), it is clear that the structure is a diversion weir with offtakes on both banks. The broadcrested weir is more than 50 m wide, making it rather difficult to gauge both high and low flows. The dam upstream of the weir has completely filled with coarse river sediments, indicative of a high energy depositional environment. The discussion of the difficulties encountered in interpretation of the discharge records is continued in Chapters 6 and 7.

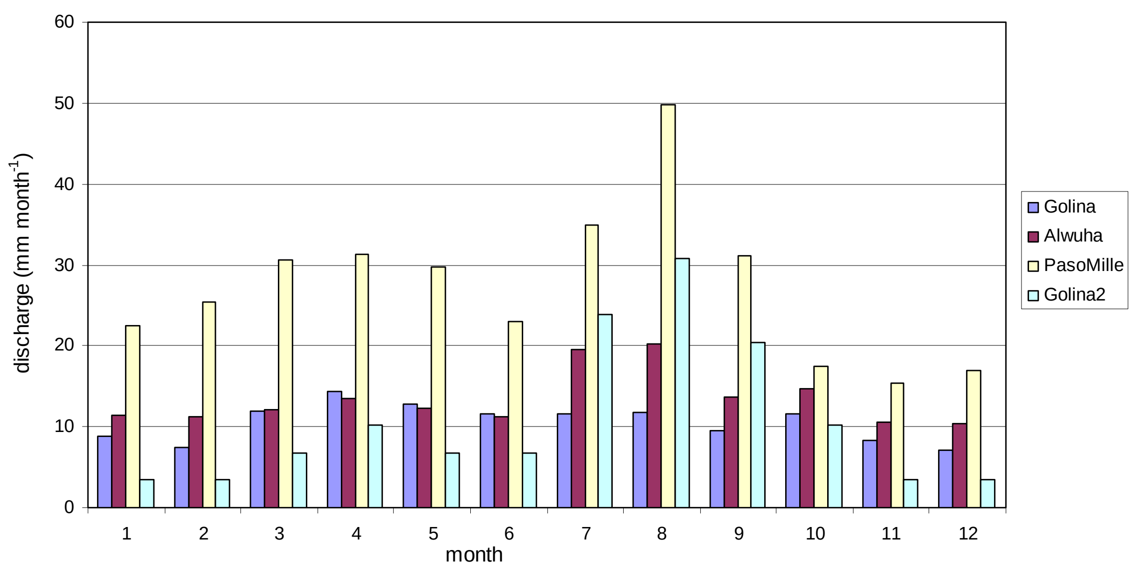

Figure 4.17 Monthly discharges of manually corrected Alwuha and Golina records

4.6. Weather generator

The weather generator input file (*.wgn) contains the long-term average monthly statistical data needed to generate representative daily precipitation data and other daily climatic variables. Generated weather inputs are calculated from tables consisting of 14 monthly climatic variables, which are derived from long-term measured weather records. Weather data definition set for the model consists of information about precipitation, temperature, solar radiation, wind speed, and relative humidity. A first order Markov-chain is used to define the day as wet or dry status of the previous day. When a wet day is generated, a skewed distribution or exponential distribution is used to generate the precipitation amount (Neitsch, 2005).

Table 4.2 Probability of wet-dry and wet-wet days in Kobo and Muja stations

Station	Probability	Jan	Feb	Mar	Apr	May	Jun	Jul	Aug	Sep	Oct	Nov	Dec
	P1WD	0.33	0.52	0.64	0.51	0.52	0.66	0.79	0.80	0.44	0.19	0.56	0.56
Muja	P1WW	0.04	0.04	0.14	0.20	0.12	0.08	0.80	0.87	0.15	0.06	0.04	0.04
Kobo	P1WD	0.41	0.48	0.46	0.40	0.28	0.51	0.66	0.60	0.47	0.38	0.41	0.37
	P1WW	0.06	0.08	0.14	0.20	0.16	0.15	0.44	0.69	0.27	0.13	0.03	0.04

Table 4.3 Maximum and minimum temperature of Kobo and Muja stations

Station		Jan	Feb	Mar	Apr	May	Jun	Jul	Aug	Sep	Oct	Nov	Dec
	Tmax	26.34	27.40	29.21	30.40	32.75	33.59	31.92	30.17	30.40	29.20	27.70	26.28
Kobo	Tmin	11.98	13.27	15.14	16.59	16.73	17.60	17.89	16.29	13.74	12.28	11.87	12.01
	Tmax	19.91	21.18	21.55	22.73	24.55	25.55	23.09	22.36	23.09	21.91	20.91	20.09
Muja	Tmin	6.55	5.64	7.82	9.27	8.91	10.36	12.36	11.91	8.55	7.27	5.45	6.27

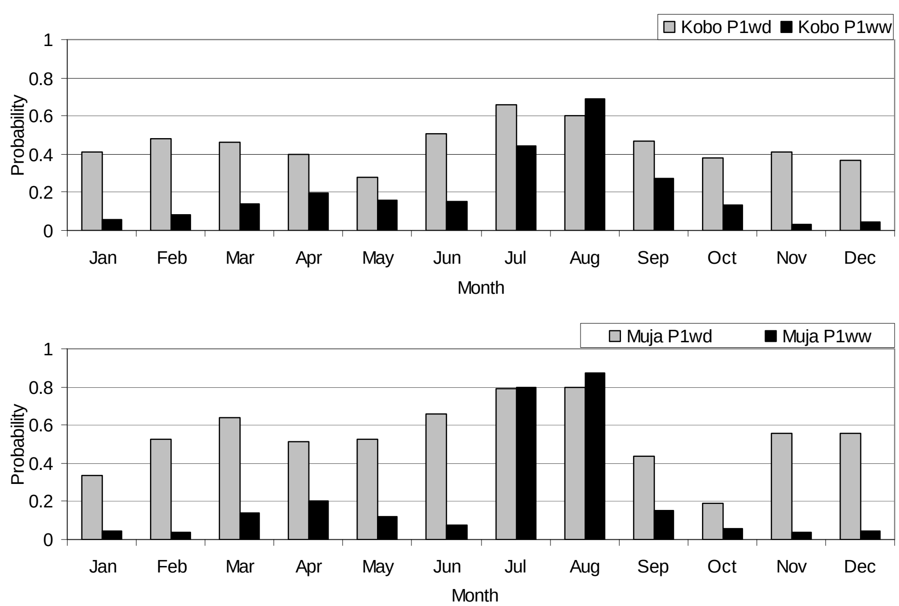

Figure 4.16 Probability of wet-dry and wet-wet days Kobo and muja stations

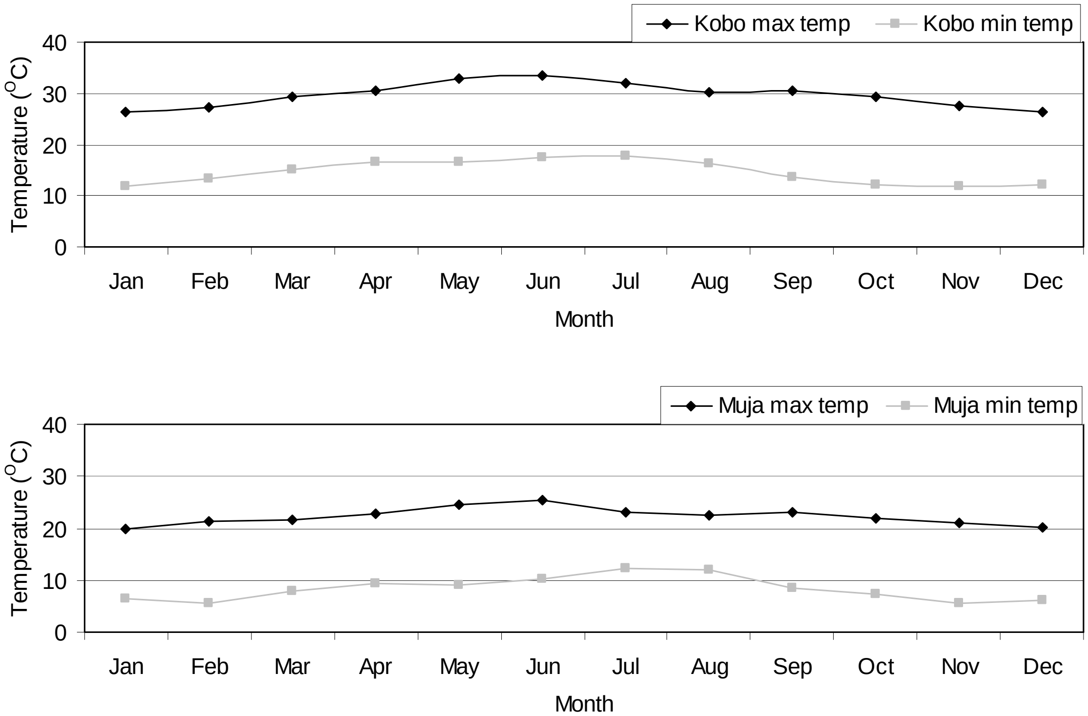

Figure 4.17 Maximum and minimum temperature of Kobo and Muja stations

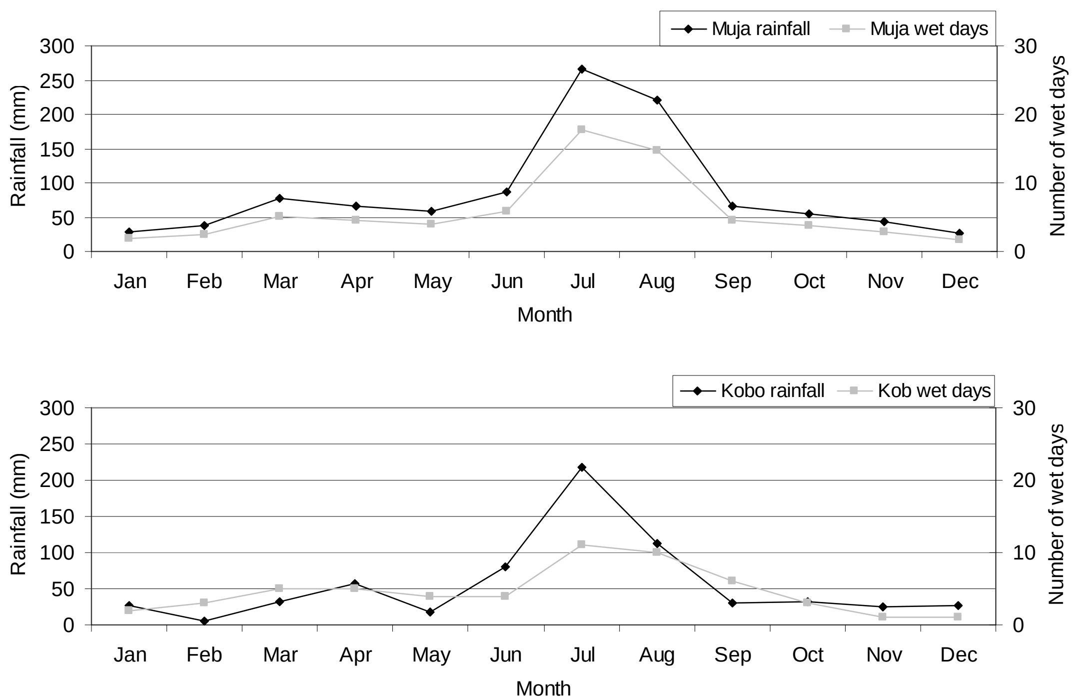

Figure 4.18 Rainfall and number of wet days of Kobo and Muja stations

Table 4.4 Average monthly rainfall and number of wet days

Month	Jan	Feb	Mar	Apr	May	Jun	Jul	Aug	Sep	Oct	Nov	Dec
Muja rainfall	27.6	38.0	77.7	67.0	58.9	87.1	265.9	220.1	66.9	55.4	43.8	25.7
Muja wet days	1.8	2.5	5.2	4.5	3.9	5.8	17.7	14.7	4.5	3.7	2.9	1.7
Kobo rainfall	26.7	5.5	31.5	56.4	18.7	80.7	218.5	113.2	29.8	33.0	24.8	27.3
Kob wet days	1.8	0.4	2.1	3.8	1.2	5.4	14.6	7.5	2.0	2.2	1.7	1.8

The above Figure 4.18 shows the probability of wet days following dry and wet days. With the first order Markov-chain model, the probability of rain on a given day is conditioned on the wet or dry status of the previous day. A wet day is defined as a day with 0.1mm of rain or more. The probability of a wet day on a day *i* given a wet day on day *i-1*, P_1 *(W/W)*, and the probability of a wet day on day *i* given a dry day on day *i-1*, P_1 *(W/D)*, for each month of the year. From these inputs the remaining transition probabilities can be derived. Rainfall is measured in discrete time intervals, say hours or days. Although the discrete time Markov chain theory is more naturally suited to the usual rainfall measurements, it is often felt that there is an important continuous time process underlying the real rainfall event series (Gieske, 1992).

$$P_1(D/W) = 1 - P_1(W/W) \qquad 4.1$$

$$P1(D/D) = 1 - P1(W/D) \qquad 4.2$$

Where $P_1(D/W)$ is the probability of a dry day on day *i* given a wet day on day *i-1* and $P_1(D/D)$ is the probability of a dry day on day *i* given a dry day on day *i-1*.To define a day as wet or dry ,SWAT first generates a random number between 0.0 and 1.0 and then uses the probability threshold values to determine whether the day is going to be wet or dry.

4.7. Watershed configuration by DEM analysis

In order to run a distributed model like SWAT, extensive information is needed. One set of information is provided through processing and analysis of digital elevation model (DEM). In addition to the climate, a DEM is used for establishing watershed boundaries, elevations, and slopes. Finally the model uses spatial data of DEM, land use and soils to establish the hydraulic response units (HRU) in the watershed. Figure 4.1 describes the result of DEM processing using ILWIS software. During ILWIS DEM processing the main steps were flow determination, flow modification and network and catchment extraction.

Flow determination

This set of routines facilitates the necessary pre-processing steps to derive a hydrologically consistent flow network. It is important to employ pit filling procedures initially, because river structures nearly always need to be continuous in a downward direction.

Flow modification

To obtain a hydrologically consistent raster based elevation representation additional modification are often required as the elevation value assigned to a pixel is an averaged representation only. The elevation of some DEM pixels may have to be changed to avoid flow in the wrong direction.

Network and catchment extraction

The raster drainage net work, extracted during the previous steps, is used as input for the drainage network ordering routines. In the drainage attribute table variables are created like upstream and downstreams coordinates; elevations, length of segment, distance between two nodes, slopes, sinuosity, upstream drainage length and Strahler and Shreve order. Figure 4.1 shows the final result of ILWIS

DEM hydroprocessing.
Watershed configuration for SWAT consists of:

- subbasins defined by Digital Elevation Model (DEM)
- hydrologic response units (HRU) in each subbasin

In SWAT, a watershed is divided into subwatersheds with unique soil/landuse characteristics called hydrologic response units (HRUs). The water balance of each HRU in the watershed is represented by four storage volumes: soil profile (0-2m), shallow aquifer (typically 2-20m), and deep aquifer (>20m). Surface runoff, sediment, nutrient, and pesticide loadings from each HRU in a subwatershed are summed, and the resulting loads are routed through channels, ponds, and/or reservoirs to the watershed outlet (Volk et al., 2008).

The first step in each hydrological analysis is the delineation of the watershed. The catchment boundary created with ILWIS has the outlet. If this outlet is known, select the outlet point. Use create shape menu by clicking at the outlet. Once the correct watershed boundary has been determined, the watershed is subdivided into subbasins required by the SWAT.

The individual subbasins have to be connected through a routing system of the river channels (reaches) in each subbasin. All reaches have their own characteristics to define ET and stream losses.

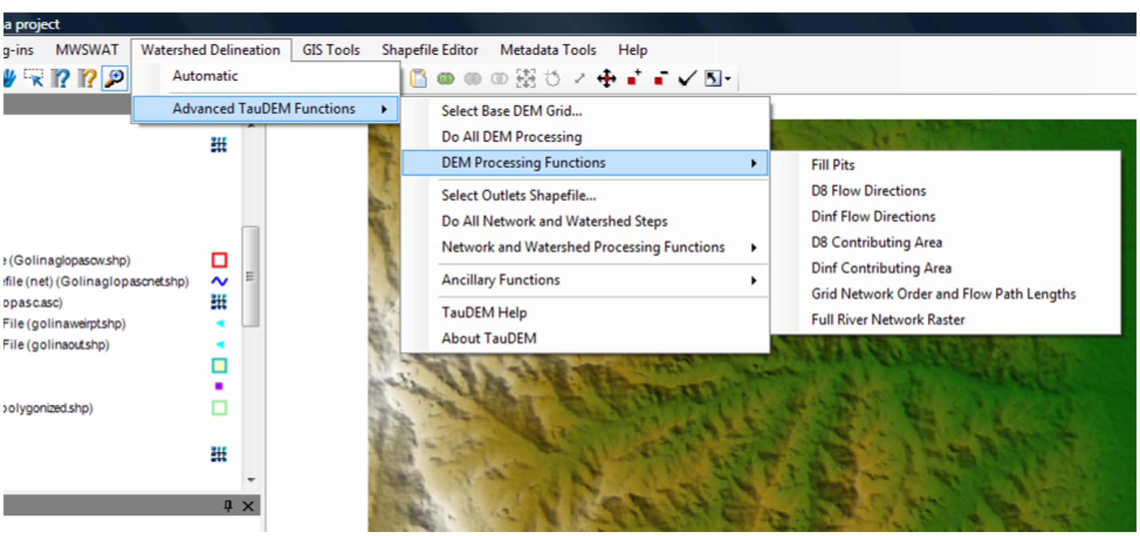

Figure 4.19 Automatic watershed delineation by MapWindows

In the MapWindow interface for SWAT 2005 there are four main steps. These are as follows:

1. Delineate watershed
2. Create hydrologic response units
3. SWAT set up and run
4. Visualization

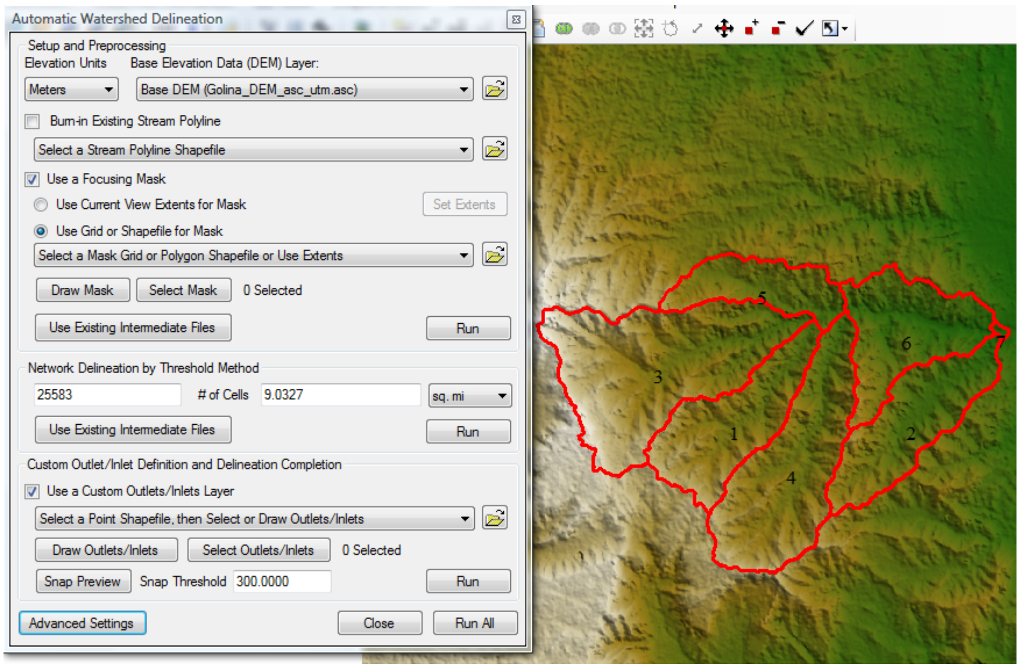

Figure 4.20 Watershed delineation using MWSWAT

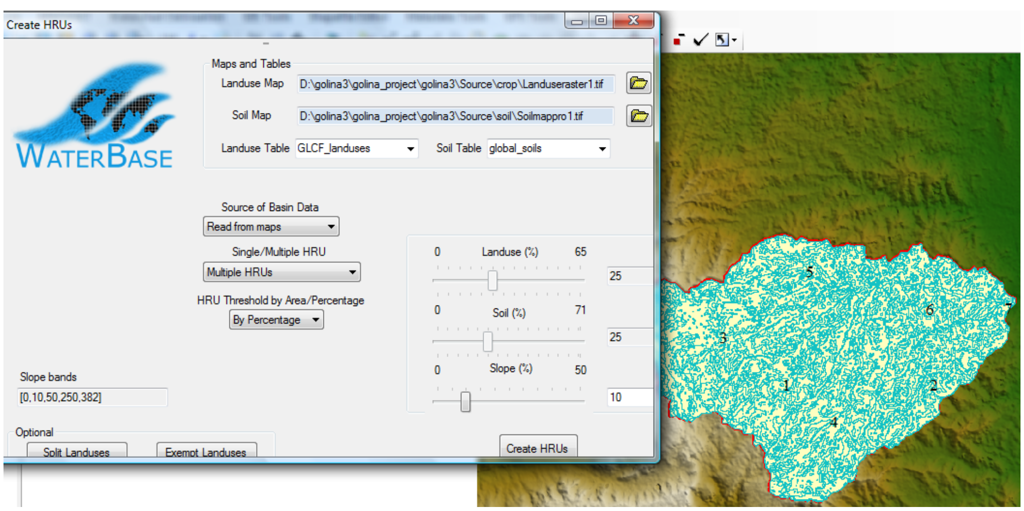

Figure 4.21 Hydrologic response units

5. SWAT Model

5.1. Introduction

SWAT model incorporates the most common hydrological equations for the simulation of flow. For the accurate implementation of these equations, detailed input data are needed. Of significant value to the simulation are the digital elevation model (DEM) of the watershed, the soil and land use data and the meteorological data of the area.

The SWAT model is a physically based input model and requires data such as weather variables, soil properties, topography, vegetation and land management practices occurring in the catchment. The model was developed for continuous simulation. The physical processes associated with water flow, sediment transport, crop growth, nutrient cycling, etc. are directly modelled by SWAT. Some of the advantages of the model includes: modelling of ungauged catchments, prediction of relative impacts of scenarios (alternative input data) such as changes in management practices, climate, and vegetation on water quality, quantity or other variables.

SWAT also has a weather simulation model that generates daily data for rainfall, solar radiation, relative humidity, wind speed and temperature from the average monthly variables of these data. This provides a useful tool to fill in missing daily data in the observed records.

In SWAT, a basin is delineated into subbasins, which are further subdivided into hydrologic response units (HRUs). HRUs consist of homogeneous land use and soil type and based on two options in SWAT, they may either represent different parts of the subbasin area or subbasin area with a dominant land use or soil type. A full model description and operation is presented in . SWAT uses hourly and daily time steps to calculate surface runoff. For hourly, the Green and Ampt equation is used and for the daily an empirical SCS curve number (CN) method is used. In this study only daily data are available and therefore the SCS curve number method has to be used here.

The hydrologic component of SWAT is based on the following water balance equation:

$$SW_t = SW_0 + \sum_{i=1}^{t}(R_i - Q_i - ET_i - P_i - QR_i) \qquad 5.1$$

where

SW_t	= soil water content at time t	[mm water]
$SW0$	= initial soil water content in day i	[mm water]
t	= the time	[days]
R_i	= amount of precipitation in day i	[mm water]
Q_i	= amount of surface runoff in day i	[mm water]
ET_i	= amount of evapotranspiration in day i	[mm water]
P_i	= percolation into the vadose zone in day i	[mm water]
QR_i	= return flow in day i	[mm water]

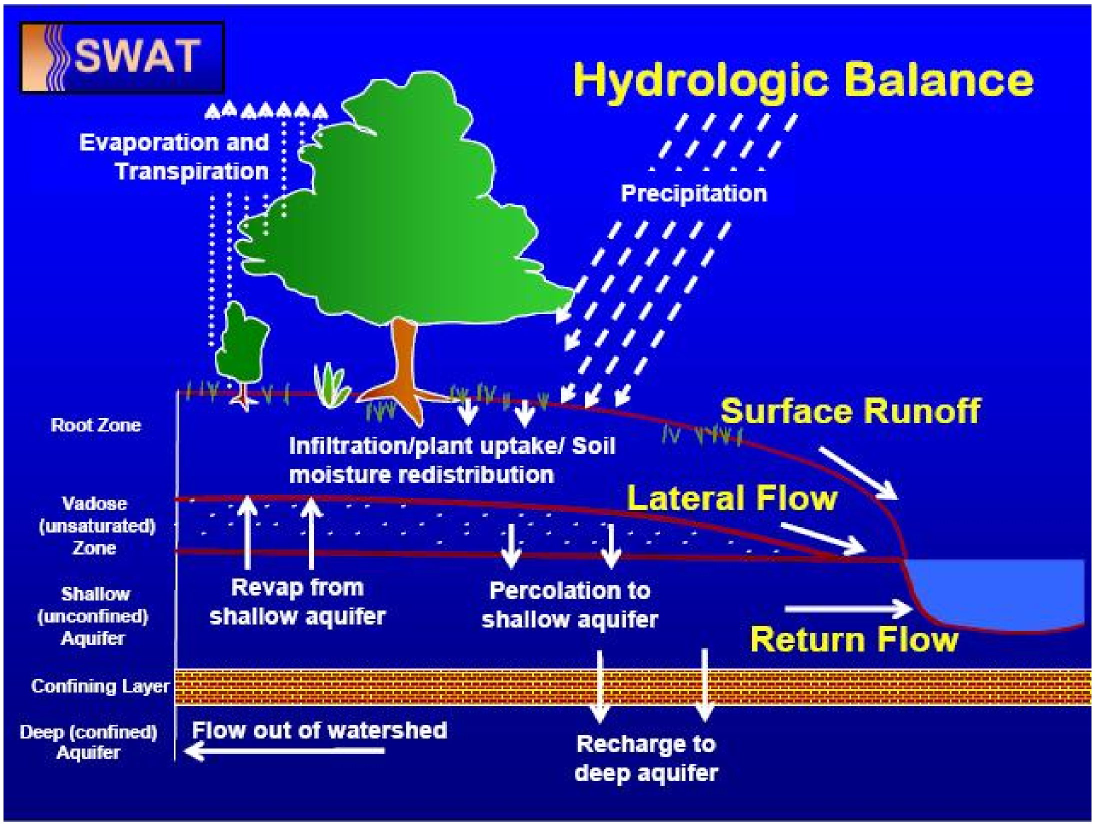

Figure 5.1 Hydrologic balance (from MapWindows/WaterBase)

5.2. SWAT concepts

5.2.1. Runoff generation

Surface runoff occurs whenever the rate of water application to the ground surface exceeds the rate of infiltration. When water is initially applied to a dry soil, the infiltration rate is usually very high. However, it will decrease as the soil becomes wetter. When the application rate is higher than the infiltration rate, surface depressions begins to fill. If the application rate is higher than the infiltration rate once all the surface depressions have filled, surface runoff will commence.

SWAT provides two methods for estimating surface runoff: the SCS curve number and the Green-Ampt infiltration method. In this study I used the SCS curve number method for estimation of runoff volume and adjust curve numbers based on antecedent moisture condition. For daily rainfall, surface runoff is predicted using the SCS curve number equation (USDA-SCS, 1972).

$$Q_{surf} = \frac{(R_{day} - 0.2S)^2}{R_{day} + 0.8S}, R_{day} > 0.2S \qquad 5.2$$

$$Q_{day} = 0.0, R_{day} < 0.2S \qquad 5.3$$

Where

Q_{surf}	=	accumulated runoff	[mm water]
R_{day}	=	rainfall depth for the day	[mm water]
S	=	soil retention parameter	[mm water]

The retention parameter varies spatially due to changes in soil water content and is defined as:

$$S = 25.4\left[\frac{1000}{CN} - 10\right] \qquad 5.3$$

Where: *CN* is the curve number for the day. The initial abstractions, I_a, is commonly approximated as 0.2S. The SCS curve number is a function of the soil's permeability, land use and antecedent soil water conditions. SCS defines three antecedent moisture conditions: 1 – dry (wilting point), 2 – average moisture, and 3 – wet (field capacity). The moisture condition 1 curve number is the lowest value that the daily curve number can assume in dry conditions. The curve numbers for moisture conditions 2 and 3 are calculated from equations 5.5 and 5.6.

$$CN_1 = CN_2 - \frac{20(100 - CN_2)}{(100 - CN_2 + \exp[2.533 - 0.0636(100 - CN_2])} \qquad 5.4$$

$$CN_3 = CN_2 \exp[0.00673(100 - CN_2)] \qquad 5.5$$

In which CN_1 is the moisture condition 1 curve number, CN_2 is the moisture condition 2 curve number, and CN_3 is the moisture condition 3 curve number.

Typical curve numbers for moisture condition 2 are listed in various tables which are appropriate to slope less than 5%. But in the Raya valley basin there are areas with slopes greater than 5%. To adjust the curve number for higher slopes an equation developed by William was used as in equation 5.7 (Neitsch et al., 2005).

$$CN_{2s} = \frac{(CN_3 - CN_2)}{3}[1 - 2\exp(-13.86 slp)] + CN_2 \qquad 5.6$$

In which CN_2 is the moisture condition II curve number for the default 5 % slope, CN_3 is the moisture condition III curve number for the default 5 % slope, CN_{2S} is the moisture condition II curve number adjusted for slope and slp is the average percent slope of the sub basin.

5.2.2. Evapotranspiration

Evapotranspiration (ET) is the process whereby water, originating from a wide range of sources, is transferred from the soil and/or vegetation layer to the atmosphere. ET includes evaporation (E) from surface water bodies, from land surfaces, from soil, sublimation from snow and ice and plant transpiration or plant water consumption. A general segregation of ET is plant transpiration, soil evaporation and evaporation of intercepted canopy water (INTC). The importance of evapotranspiration can be identified at different levels. A well known aspect of ET is that a large part of it supports plant growth. Other water consuming systems are evaporation losses from man-made reservoirs. They can reach very high magnitudes. Processes depending on ET are for instance antecedent moisture conditions since last rainfall, water erosion, and rainfall-runoff. Rough estimates of ET can lead to large errors in the calculation of the components of the hydrological cycle such as runoff, groundwater table, available water for irrigated and rain fed vegetation and drinking water (Verstraeten et al., 2005). Actual soil water evaporation is estimated as a function of potential ET and leaf area index (area of plant leaves relative to the soil surface area) by using exponential relationships of soil depth and water content. Plant water evaporation is simulated as a linear function of potential ET, leaf area index and root depth and can be limited by soil water content. It is assumed that 30% of total plant uptake comes from the upper 10% of the root zone and roots can compensate for water deficits in certain layers by using more water in layers with adequate suppliers.

Depending on the input data availability SWAT model offers three options for estimating actual evapotranspiration and potential evapotranspiration. These are Penman-Monteith, Hargreaves and Priestley-Taylor. The Penman-Monteith method requires solar radiation, air temperature, relative humidity and wind speed. The Priestley-Taylor method requires solar radiation, air temperature and relative humidity. Hargreaves method requires air temperature. In this research the Hargreaves method was used.

5.2.3. Soil water

Water that enters the soil may move along one of several different pathways. The water may be removed from the soil by plant uptake or evaporation. It can percolate past the bottom of the soil profile and ultimately become aquifer recharge. A third option is that water may move laterally in the profile and contribute to stream flow. Of these different pathways, plant uptake of water removes the majority of water that enters the soil profile. Water in the soil can flow under saturated or unsaturated conditions. In saturated soils, flow is driven by gravity and usually occurs in a downward direction. Unsaturated flow is caused by gradients arising due to adjacent areas of high and low water content. Unsaturated flow may occur in any direction (Arnold et al., 2000).

SWAT directly simulates saturated flow only. The model records the water contents of the different soil layers but assumes that the water is uniformly distributed within the given layers. This assumption eliminates the need to model unsaturated flow in a horizontal direction. Unsaturated flow between layers is indirectly modelled with the depth distribution of plant water uptake (equation 5.8) and the depth distribution of soil water evaporation (equation 5.9).

$$W_{up,z} = \frac{E_t}{[1-\exp(-\beta_w)]}[1-\exp(-\beta_w \frac{z}{z_{root}})] \qquad 5.7$$

where:

$W_{up,z}$ = potential water uptake from the soil surface to depth, z , on a given day [mm water]
E_t = maximum plant transpiration on a given day [mm water]
β_w = water use distribution parameter, z is the depth of root development [mm water]

$$E_{soil,ly} = E_{soil,zl} - E_{soil,zu} \qquad 5.8$$

where:

$E_{soil,ly}$ = the evaporative demand for layer [mm water]
$E_{soil,zl}$ = evaporative demand at the lower boundary of the soil layer [mm water]
$E_{soil,zu}$ = evaporative demand at the upper boundary of the soil layer [mm water]

The soil percolation component of SWAT uses a storage routing technique to predict flow through each soil layer in the root zone. Downward flow occurs when field capacity of a soil layer is exceeded if the layer below is not saturated. The downward flow is governed by the saturated conductivity of the soil layer. Upward flow may occur when a lower layer exceeds field capacity. Movement from a lower layer to an adjoining upper layer is regulated by the soil water to field capacity ratios of the two layers. Percolation is also affected by soil temperature. If the temperature in a particular layer is 0^0C or below, no percolation is allowed from that layer (Arnold et al., 2000).

5.2.4. Groundwater

The simulation of groundwater is partitioned into two aquifer systems i.e. an unconfined aquifer (shallow) and a deep-confined aquifer in each sub basin. The unconfined aquifer contributes to flow in the main channel or reach of the sub basin. Water that enters the deep aquifer is assumed to contribute to streamflow outside the watershed (Arnold et al., 1998). In SWAT2005 the water balance for a shallow aquifer is calculated with equation 5.10.

$$aq_{sh,i} = aq_{sh,i-1} + w_{rchg} - Q_{gw} - W_{revap} - W_{deep} - w_{pump,sh} \qquad 5.9$$

where
$aq_{sh,i}$ = amount of water stored in the shallow aquifer on day i [mm water]
$aq_{sh,i-1}$ = amount of water stored in the shallow aquifer on day *i-1* [mm water]
w_{rchrg} = amount of recharge entering the aquifer on day *i* [mm water]
Q_{gw} = groundwater flow, or base flow, into the main channel on day i [mm water]
W_{revap} = water moving to soil zone by water deficiencies on day i [mm water]
W_{deep} = water percolating from shallow aquifer into deep aquifer on day *i* [mm water]
$w_{pump,sh}$ = amount of water removed from shallow aquifer by pumping on day *i* [mm water]

The steady-state response of groundwater flow to recharge is estimated by equation 5.11 (Neitsch et al., 2005).

$$Q_{gw} = \frac{800 K_{sat}}{L^2_{gw}} h_{wtbl} \qquad 5.10$$

where
Q_{gw} = groundwater flow or base flow, into the main channel on day i [mm water]
K_{sat} =..saturated hydraulic conductivity of the aquifer [mm day^{-1}]
L_{gw} = distance from subbasin divide for ground water system to main channel [m]
h_{wtbl} = water table height [m]
Although SWAT does not currently print groundwater height in the output files, the water table height is updated daily bay model. Groundwater height is related to groundwater flow by equation (5.12)

$$Q_{gw} = \frac{800K_{sat}}{L_{gw}^2} h_{wtbl} = \frac{8000\mu}{10} \frac{10K_{sat}}{\mu L_{gw}^2} h_{wtbl} = 800\mu\alpha_{gw} h_{wtbl} \qquad 5.11$$

where:

μ = specific yield of the shallow aquifer [-]

α_{gw} = baseflow recession constant [day^{-1}]

The baseflow recession constant α_{gw} is therefore defined as

$$\alpha_{gw} = \frac{10K_{sat}}{\mu L_{gw}^2} \qquad 5.12$$

5.3. Map Windows (WaterBase) Grapher User Interface (GUI)

SWATPlot and SWATGraph are companion tools to the MWSWAT tool that generates inputs for and runs the SWAT watershed modelling program. SWATPlot is a tool designed to make it easy to select SWAT output values from the files output.rch, output.sub, output.hru, output.rsv and output.wtr. The normal way to plot such values is to import the SWAT output file into Excel, use an Excel filter to select the reach, subbasin, hru, reservoir or wtr, respectively, and then use Excel graphing facilities to draw graphs or histograms. This is a relatively tedious process, especially if you want to use outputs from different runs to compare them. SWATPlot makes this process much simpler (George, 2008).

5.4. Model parameterization

Parameterization is a technique for assigning specific models and model parameters to the spatial units in the watershed. For this study, a ‘representative subbasin’ is selected, for which the model assumes homogeneity of parameters and variables. A relationship between required parameters of this representative modelling unit and corresponding parameters of other homogeneous units (e.g. subbasins) is developed using available information about the parameters. In this way, the definition of variables in the representative subbasin enables determination of a corresponding parameter in other subbasins.

Sensitivity tests and preliminary model runs can be carried out to identify the most sensitive model parameters. To avoid over parameterization, only the most sensitive parameters are adjusted in the model calibration. Using SWAT-CUP ten sensitive parameters were normally identified: four of these mainly affect base flow generation (GW_REVAP, REVAPMN, GW_DELAY, ALFA_BF) while the other parameters (CN2, SOL_K, SOL_AWC, SOL_AWC, EPCO, ESCO) affect surface runoff formation.

Parameters and parameter ranking ranges used in th sensitivity analysis and sensitivity ranking (with Gw.=groundwater,Evap.=evaporation, Geom=Geomorphology

Name	Min	Max	Definition	Process
ALPHA_BF	0	1	Baseflow alpha factor (days)	Gw.
BIOMIX	0	1	Biological mixing efficiency	Soil
Blai	-50	50	Leaf area index for crop	Crop
Canmx	0	10	Maximum canopy index	Runoff
CH_K2	0	150	Effective hydraulic in main channel alluvium(mm/hr)	Channel
Ch_n	-20	20	Manning coefficient for channel	Channel
CN2	-50	50	SCS runoff curve number for moisture condition II	Runoff
Epco	-50	50	Plant evaporation compensation factor	Evap.
ESCO	0	1	Plant evaporation compensation factor	Evap.
GW_DELAY	0	100	Groundwater delay (days)	Gw.
GW_REVAP	0.02	0.2	Groundwater "revap"coefficient	Gw.
GWQMN	0	1000	Threshold depth of water in the shallow aquifer for return flow to occure(mm)	Soil
Rchrg_dp	0	1	Groundwater recharge to deep aquifer (fractu)	
REVAPMN	0	500	Threshold depth of water in the shallow aquifer for "revap" to occur (mm) return flow to occure (mm)	Gw.
SLOPE	-50	50	Average slope steepness(m/m)	Geom.
SLSUBBSN	-50	50	Average slope length(m/m)	Geom.
SMFMN	0	10	Minimum melt rate for snow (mm/^{O}C/day)	Snow
SMFMX	0	10	Maximum melt rate for snow (mm/^{O}C/day)	Snow
SMTMP	-2	2	Snow base temperature (^{O}C)	Snow
Sol_alb	0	1	Moist soil albedo	Soil
SOL_AWC	-50	50	Available water capacity (mm/mm soil)	Soil
Sol_k	-50	50	Soil conductivity (mm/hr)	Soil
Sol_z	-50	50	Soil depth	Soil
Surlag	0	10	Surface runoff lag factor	Runoff
TIMP	0.01	1	Snow pack temperature lag factor	Snow
TLAPS	-50	50	Temperature lapse rate (^{O}C/km)	Geom.

Table 5.1 Main model parameters in the SWAT setup. Source (Holvoet et al., 2005)

6. Modelling Results

6.1. Introduction

As described in Chapter 4 the hydrological and hydrometeorological data in the area are scarce and generally poor in quality. Therefore there are large data gaps. In this study, the SWAT daily weather generator algorithm used the monthly climate data for ten years (1996-2005) to generate the missing daily climatic data for the same period. The mixed exponential distribution was used throughout the modelling.

Modelling of the area was carried out in two phases. An initial model simulation was made for the Golina catchment for the period from 1996 – 2005. This was followed by modelling of the Alamata catchment, just north of the Golina catchment, for the same period. It was necessary to model the discharges of the Golina River first, because no river gauge has ever been operational in the Alamata and Mekoni basins.

The Map Window SWAT 2005 (MWSWAT) interface was used for watershed delineation, input map characterization and processing, stream and outlet definition, the computation of the different geomorphologic characteristics and characterization of land cover and soil. Surface runoff was modelled based on the SCS- curve number approach for both the Golina and the Alamata cases.

This chapter first describes modelling the Golina catchment, followed by modelling of the Alamata and Mekoni basins together with Golina catchment. Only a few indicative scenarios are presented for the Alamata and Mekoni catchments, based on the Golina catchment analysis with SWAT.

6.2. Golina River catchment

6.2.1. Golina model setup

In this study the SWAT model for the Golina catchment was developed first, because the only hydrometeorological station in the study area is found here. Calibration of the Golina River discharges proved to be difficult because of the poor quality of the discharge data. It was only possible to construct an approximate monthly runoff curve after correcting for outliers and systematic errors, as was discussed extensively in Chapter 4 (see section 4.5). In the Golina River model, the two weather stations are Muja and Kobo. The Korem temperature data was used also. The monthly simulated discharges of the Golina River were calibrated against the average monthly runoff curve (see Fig. 4.17). Calibration was done with SwatCup2 (Abbaspour, 2009) using the SUFI method and Swatshell4.0 (Gieske, 2010) using the GML method. The calibrations, however, have to be considered only approximative, because of the uncertain nature of the observed discharges.

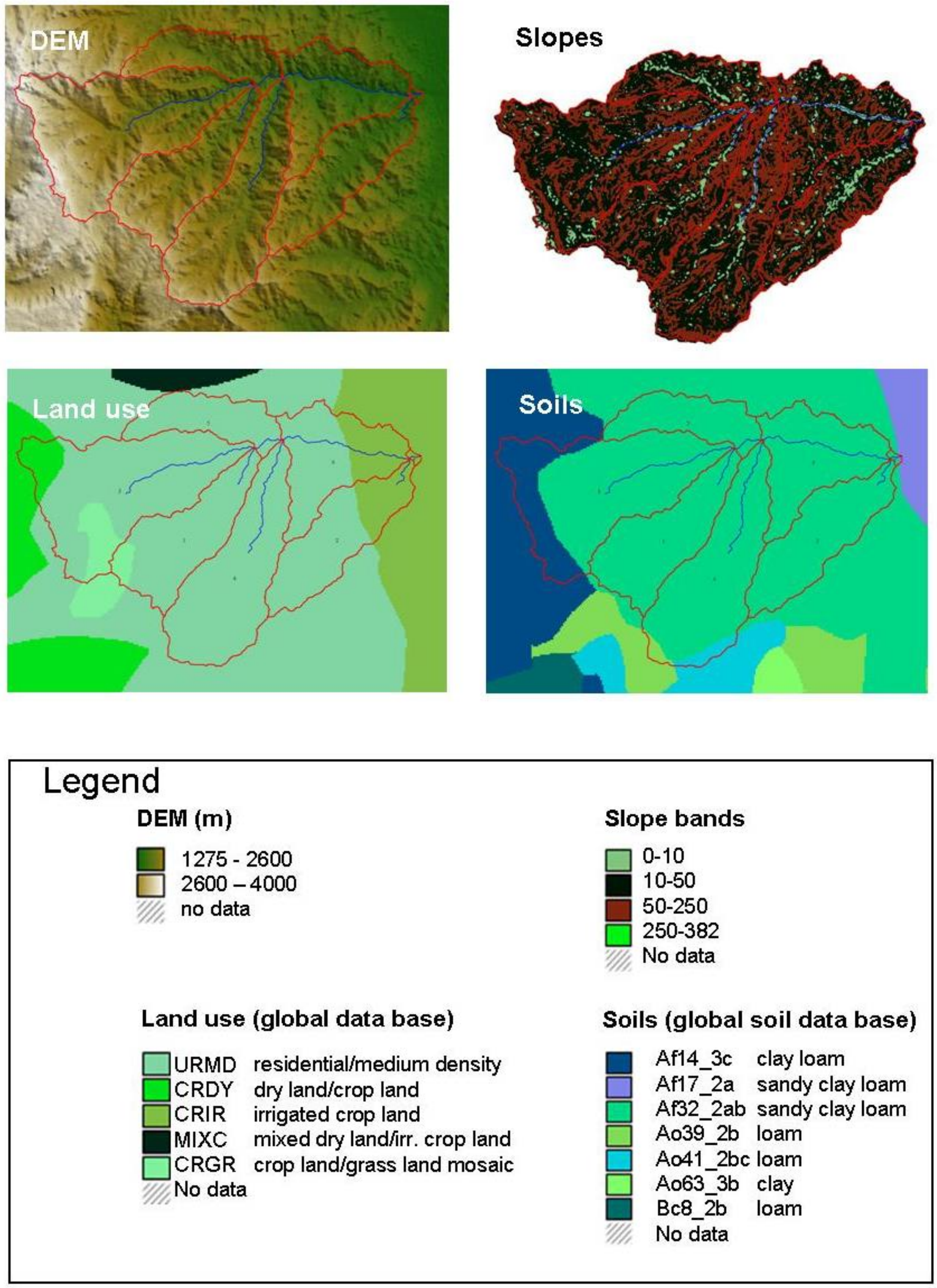

Figure 6.1 DEM, slope map, land cover and soil map of the Golina River catchment

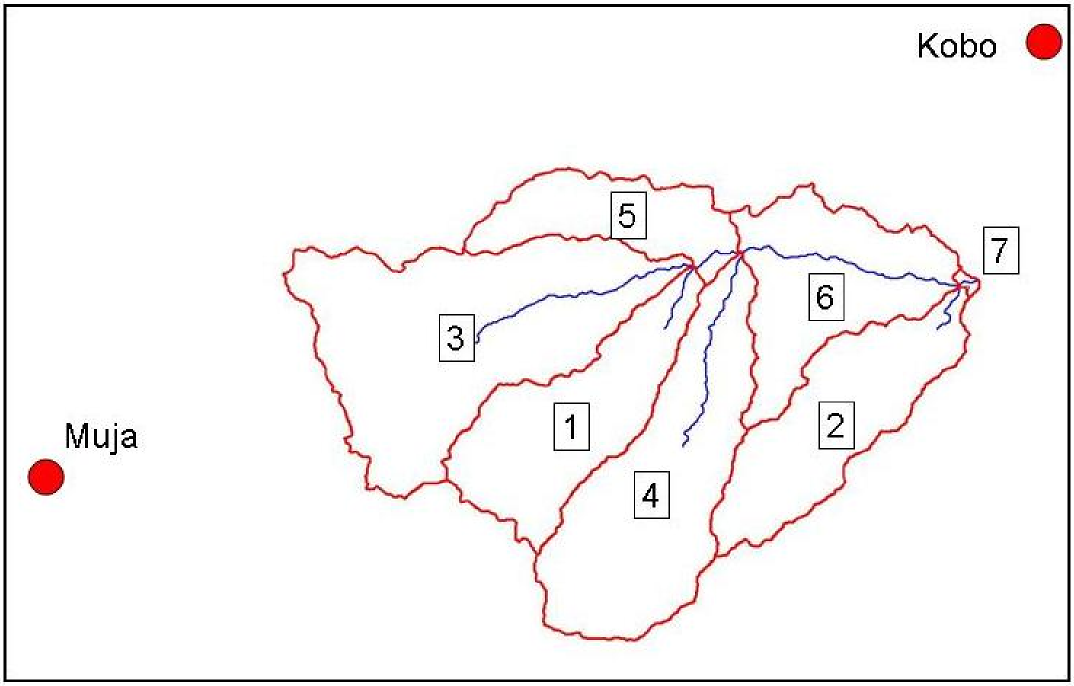

Figure 6.2 Seven sub-basins of the Golina SWAT model.

Figures 6.1 and 6.2 show the three main model input maps (DEM, land use and soils). The DEM is derived from the 30m resolution ASTER global database (see Figures 1.1 and 3.1). The slope map is determined in the MapWindows pre-processing package. The land use map is derived from the global land use database while the soil map was extracted from the global soil database both provided by the Ethiopian Geological Survey Department. The predominant land use can be classified as medium density crop land, while the main soils in the area are sandy clay loams. There is not much distinction between the HRUs in the area, and for this reason the HRUs have been chosen to coincide with the 7 sub-basins. The total area is about 285 km^2 (see Table 6.1) while the elevation lies between 1483 and 3934 m. Main land use type is URMD (87%), whereas the soils are predominantly classified as sandy clay loams (Af32-2ab-3, 91 %). The proper qualification should not be residential, but rather dry land/crop/forest, where the coniferous forest occurs on the slopes

Table 6.1 Golina main basin parameters

						area (km^2)	%
elevation	min		1483	m	sub1	41.15	14.44
	max		3934	m	sub2	39.47	13.85
	mean		2439	m	sub3	79.53	27.91
slope	0	-10	7	%	sub4	59.86	21.01
	10	-50	55	%	sub5	24.28	8.52
	50	-250	38	%	sub6	40.10	14.07
	250	-382	0	%	sub7	0.54	0.19
land use	URMD		87	%			
soil	Af32-2ab-3		91	%	total	284.93	100.00

6.2.2. SWAT model initial parameters

The preprocessing with MapWindows yields a complete set of input files, making it possible to run SWAT. However, SWAT input files contain a large number of parameters with regard to climate, plant and tree growth, agricultural management, groundwater, and surface water. This study is restricted to hydrological modelling without information on agricultural practices and crop patterns and without data on natural vegetation. For this reason a parameter subset was selected initially which only contains the main hydrological parameters. Table 6.2 shows the 22 parameters selected initially. Further selection was made after manual and automatic calibration. The parameters of the basin (*.bsn), channel (*.rte and *.sub) and hydrological response units (*.hru) were as much as possible left at their default values. The calibration process is focusing here on the parameters of the soil (*.sol), the runoff (*.mgt) and the groundwater (*.gw). Within the set of groundwater parameters, the deep recharge (RECH_DP) should be set to zero, because the mountainous catchments are assumed to have only shallow groundwater, while the valley areas can be modelled as unconfined/semi-confined single layer aquifers (Mohamedsultan, 2010). The parameter SHALLST (initial shallow aquifer storage) is only important in the first couple of start-up years, and not after that. In the modelling a start-up time of two years was used. For this reason it was left out of the initial list in Table 6.2 below.

Table 6.2 SWAT hydrological parameters

var nr	name	file	description	r_min	r_max	default	unit
1	CN2	mgt	curve number II	30	95	77	-
2	ESCO	bsn	soil evap compensation	0.01	1	0.95	-
3	EPCO	bsn	plant uptake compensation	0.01	1	1	-
4	SURLAG	bsn	surface runoff lag coeff	0.01	5	4	-
5	CN_coef	bsn	plant ET coef	0.5	20	1	-
6	CH_N2	rte	Manning main channel	0.025	0.1	0.014	-
7	CH_K2	rte	hydraul. cond main channel	0.025	500	1	$mmhr^{-1}$
8	ALPHA_BNK	rte	bank storage alpha	0	1	0	-
9	CH_K1	sub	hydraul. cond. trib channel	0.025	500	500	$mmhr^{-1}$
10	CH_N1	sub	Manning trib. channel	0.025	0.1	0.014	-
11	SOL_BD1	sol	soil bulk density	1.1	1.9	1.4	-
12	SOL_AWC1	sol	av. water hold. cap. layer 1	0	1	0.15	-
13	SOL_K1	sol	sat hydraul.cond, soil layer 1	0.025	500	6	$mmhr^{-1}$
14	GW_DELAY	gw	unsat zone delay time	1	50	31	day
15	ALPHA_BF	gw	shallow baseflow alpha	0.1	1	0.048	day^{-1}
16	GW_QMN	gw	threshold return flow	1	50	0	mm
17	GW_REVAP	gw	shallow revap coef	0	1	0.02	-
18	REVAPMN	gw	threshold re-evaporation	1	50	1	mm
19	RECHRG_DP	gw	fraction of deep recharge	0	1	0.05	-
20	GW_SPYLD	gw	specific yield shallow aquifer	0.001	0.3	0.003	-
21	SLSUBBSN	hru	average slope length	1	100	30	m
22	OV_N	hru	Manning overland flow	0.01	0.6	0.1	-

6.2.3. SWAT calibration

Manual calibration

As mentioned already in the introduction to this chapter, calibration of the Golina River discharges proved to be difficult because of the poor quality of the discharge data. An approximate average monthly runoff curve was constructed after correcting for outliers and systematic errors, as was discussed in section 4.5. In the Golina River model, the two weather stations Muja – with precipitation only – and Kobo –with precipitation and temperature data - were used as a source for the weather generator package. The Korem temperature data was used as representative data for Muja. The monthly simulated discharges of the Golina River were calibrated against the average monthly runoff curve (see Fig. 4.17) for the period 1996-2005.

Several objective function criteria can be used to determine the performance of the simulation in comparison to the observed discharge. For the GML method the objective function is chosen as the square root of the average of the squared deviations between modelled and simulated discharges (RMSE)

$$RMSE = \sqrt{\frac{\sum \left(Q_{obs,i} - Q_{sim,i}\right)^2}{n}} \qquad 6.1$$

where:

$Q_{obs,i}$ = measured average daily streamflow in month i (m^3s^{-1})
$Q_{sim,i}$ = predicted average daily streamflow in month i (m^3s^{-1})
n = number of months of observations

Alternatively the Nash-Sutcliffe coefficient NS (Nash and Sutcliffe, 1970) can be used to measure the goodness-of-fit between observed and simulated daily stream discharge:

$$NS = 1 - \frac{\sum_{i=1}^{n} (Q_{obs,i} - Q_{sim,i})^2}{\sum_{i=1}^{n} (Q_{obs,i} - Q_{obs,avg})^2} \qquad 6.2$$

where:

$Q_{obs,avg}$ = average monthly discharge (m^3s^{-1})

Minimization of the RMSE is equivalent to the optimization of the NS coefficient. The Nash-Sutcliffe coefficient, however, is more frequently used by hydrologists. The results of the modelling with the default parameter set are shown in Figure 6.3

Automatic calibration

Automatic calibration of the modelled discharges against the constructed monthly average discharges was attempted with SWATSHELL4.0 and with SWAT_CUP2. As mentioned before, the modelling should be regarded as indicative only, because of the poor quality of the observed data (see section 4.5). The results are illustrated in Tables 6.3 and 6.4, while Figure 6.3 shows the monthly rainfall with the modelled and observed discharges. Three modelling runs can be distinguished. First, the results are shown as obtained with the parameter values produced by MapWindows pre-processing. Next, the manual corrections are made based on adjusting the parameter set in accordance with our understanding of the hydrology and hydrogeology of the area. Finally, four main parameters were selected for the automatic calibration process. Table 6.3 shows the reduction of the RMSE and NS values during the modelling process. The default parameter set gave an NS value of -0.69, which was improved from 0.9 to 0.63 during steps two and three. Table 6.4 illustrates the changes in the parameter values during the modelling process. SWATSHELL4.0 integrates Gauss-Marquardt-Levenberg (GML) non-linear optimization with the SWAT processing. The process is very similar to combining SWAT with PEST. However, SWATSHELL4.0 only produces error estimates based on the parameter covariance matrix. The final four modelling errors are also indicated in Table 6.4. The GW_REVAP parameter was increased from 0.02 to 0.3 during the second step (manual correction), because this improved the NS value immediately, The deep groundwater recharge was reduced to zero, because it is assumed that there are only shallow, single layer aquifers in the area. The specific yield of the unconfined aquifer was set fixed at 0.03, which is considered a better estimate in the area. The parameter changes were applied to all sub-basins in the same way, because the soil and land use are clearly dominated by a single type. Obviously, the lack of data makes it advisable to keep the modelling as simple as possible.

Table 6.3 RMSE and NS values for Default, Manual and Calibrated parameter sets

	Parameter sets			
	Default	Manual	GML	unit
Qobs	125.91	125.91	125.91	m^3s^{-1}
Qsim	155.40	129.24	97.86	m^3s^{-1}
RMSE	1.68	1.23	0.79	m^3s^{-2}
NS	-0.69	0.09	0.63	-

Table 6.4 Parameter values for the three different runs

var nr	var name	file	optpar	default	manual	optimized	error
1	CN2	mgt	1	77.000	80.000	67.8314	1.0705
2	ESCO	bsn	0	0.950	0.950	0.9500	
3	EPCO	bsn	0	1.000	1.000	1.0000	
4	SURLAG	bsn	0	4.000	4.000	4.0000	
5	CN_coef	bsn	0	1.000	1.000	1.0000	
6	CH_N2	rte	0	0.014	0.014	0.0140	
7	CH_K2	rte	0	1.000	1.000	1.0000	
8	ALPHA_BNK	rte	0	0.000	0.000	0.0000	
9	CH_K1	sub	0	500.000	500.000	500.0000	
10	CH_N1	sub	0	0.014	0.014	0.0140	
11	SOL_BD1	sol	0	1.400	1.400	1.4000	
12	SOL_AWC1	sol	0	0.150	0.150	0.1500	
13	SOL_K1	sol	1	6.000	6.000	5.4337	0.5845
14	GW_DELAY	gw	1	31.000	31.000	19.5648	0.9303
15	ALPHA_BF	gw	0	0.048	0.050	0.0500	
16	GW_QMN	gw	0	0.000	0.000	0.0000	
17	GW_REVAP	gw	1	0.020	0.300	0.8403	0.0907
18	REVAPMN	gw	0	1.000	1.000	1.0000	
19	RECHRG_DP	gw	0	0.050	0.000	0.0000	
20	GW_SPYLD	gw	0	0.003	0.030	0.0300	
21	SLSUBBSN	hru	0	30.000	30.000	30.0000	
22	OV_N	hru	0	0.100	0.100	0.1000	

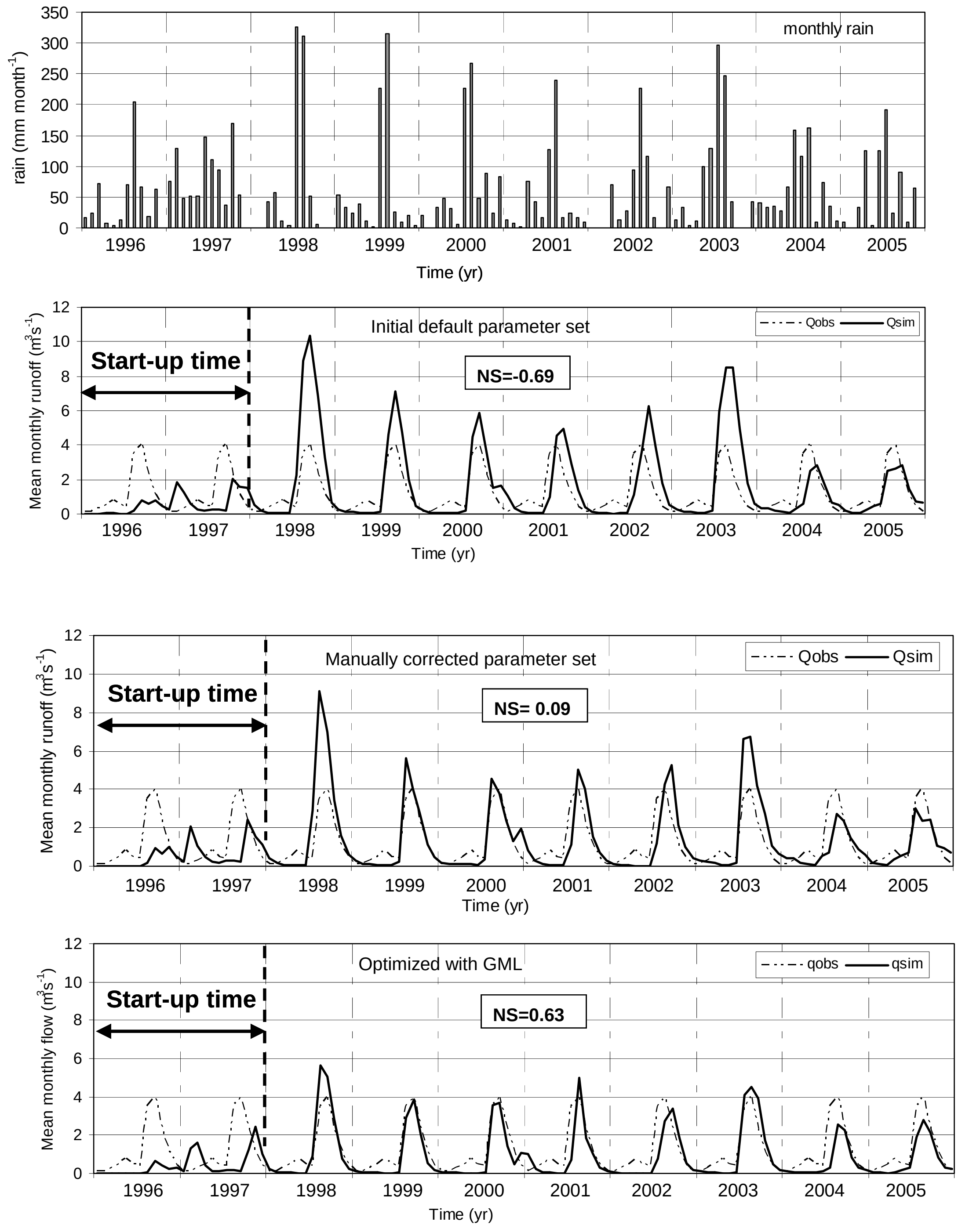

Figure 6.3 Monthly rain, modelled and observed discharges 1996-2005

In general the modelled monthly discharges follow the rain pattern. The rains of July and August (Kremt) have the largest impacts. The years with high rainfall (1998, 1999 and 2003) also produce high monthly river flow. The early rains (Belg) are not visible in the runoff pattern, unlike in the case of the Alwuha and PasoMille discharges. These rivers are probably more influenced by snowmelt, because their source areas are higher up in the mountains. The constructed Golina discharge pattern of Fig. 4.17 should probably be corrected for the small rainy period. The final modelled discharge equals approximately 100 $mmyr^{-1}$ for the period 1998 to 2005. If the constructed monthly discharge pattern would be corrected for the "Belg" influence, then the RMSE would go down to about 0.7 and the NS coefficient would go up to around 0.8.

The most important parameters in this modelling exercise are the curve number CN2 and the shallow soil and groundwater re-evaporation coefficient GW_REVAP. These parameters reflect the nature of the catchment, where a relatively large amount of rain is stored initially. This appears to be caused by the forest on the slopes and the ploughed land on the agricultural fields. If the storage capacity is exceeded during heavy rains, then large runoff events will occur.

However, these events will be of short duration (see also Figure 6.4). This pattern also suggests why accurate flow gauging has proved to be difficult. The flow observations are made at a fixed time during the day, whereas peak flows may occur anytime during the day and are probably of short duration. Moreover, some daily recorded peak flows have apparently been extrapolated to monthly duration. It would be advisable to let the observers not only measure staff gauges but also write some short notes on the duration and frequency of the peak flows, while recording flood marks on bridges and river banks.

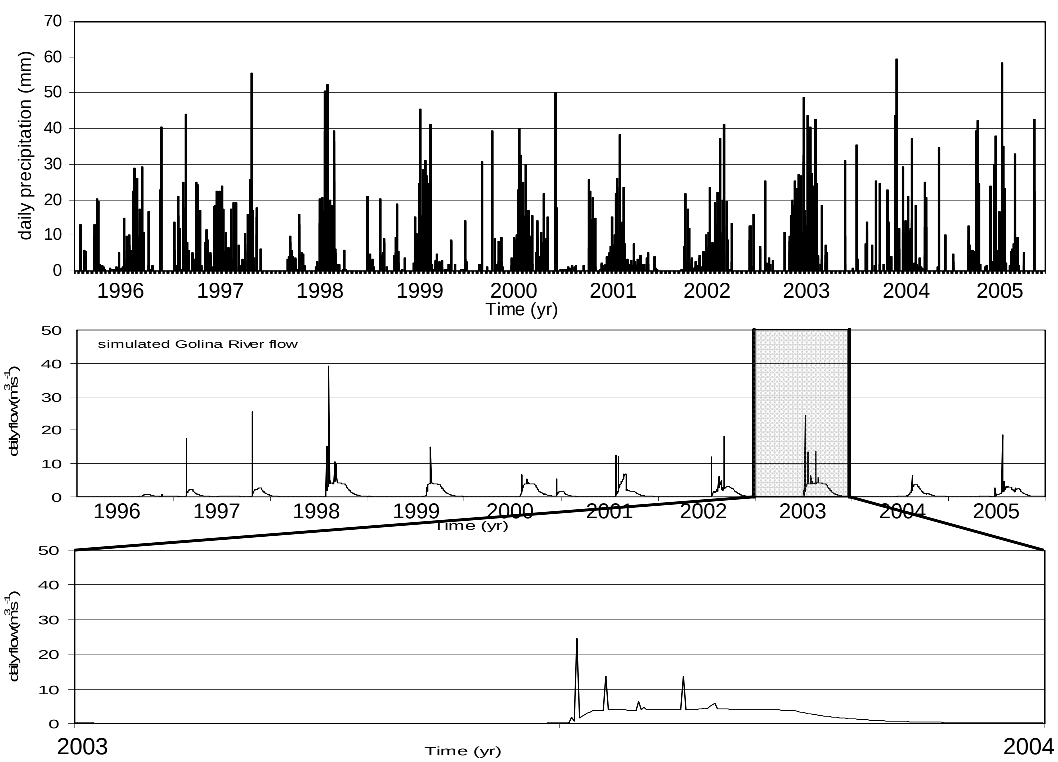

Figure 6.4 Simulated daily rainfall and river outflow of the Golina sub-basin near Kobo

.

Calibration with Sequential Uncertainty Fitting (SUFI) was also attempted by means of the SWAT-CUP software (Abbaspour, 2009). The approach is based on Latin Hypercube Sampling (McKay et al., 1979). Figure 6.5 and 6.6 illustrate the results. The blue line is the (constructed) observed discharge, the red line indicates the best estimated discharges and the green band gives the uncertainty interval,

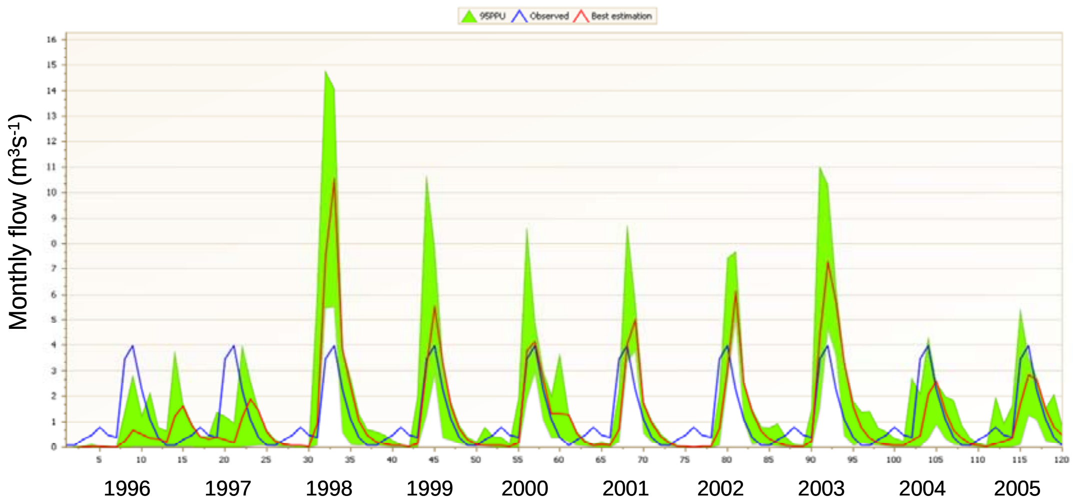

Figure 6.5 Monthly observed flow and simulated flow with SWAT-CUP (SUFI).

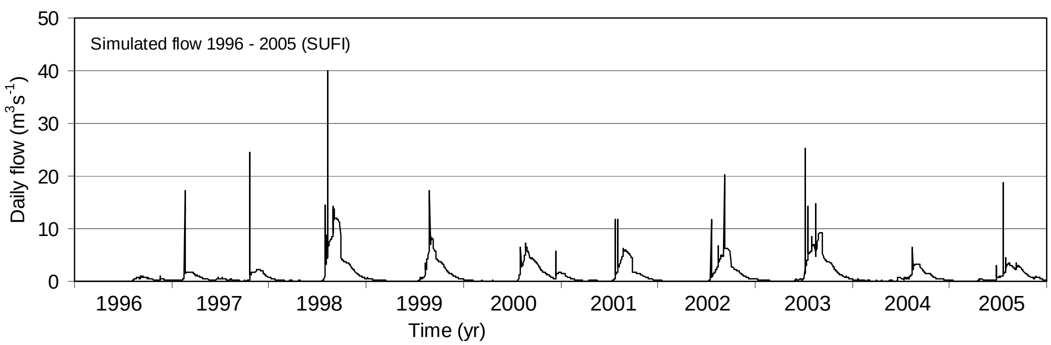

Figure 6.6 Daily simulated flow with parameters calibrated by SUFI (see Figure 6.5)

The resulting parameters are: CN2 = 67.83 (the same as the GML optimized value in Table 6.4), SOL_K (1) = 7.4, SOL_K(2) = 16.0, GW_REVAP=0.2 and GW_DELAY=37.3. The Nash-Sutcliffe value NS = -0.14 and R^2 = 0.42. Differences with the GML optimization are also caused by the fact that no start-up time was used here. For this simulation the average simulated flow has gone up from 98 $mmyr^{-1}$ (GML) to 140 $mmyr^{-1}$ (SUFI) (see also the discussion on the water balance in the next section. The daily flow pattern simulated with SUFI parameters (Figure 6.6) is remarkably similar to the daily flow simulated with GML parameters. In both cases the maximum flow is 40 m^3s^{-1}. The presence of one or more peak events per year is also very clear.

6.2.4. Discussion of results and Golina water balance

Figures 6.8 and 6.9 show the average monthly rainfall and the average simulated monthly response of the Golina River discharge. The figure shows that the modelled discharges are lagging the July-August rains by about a month.

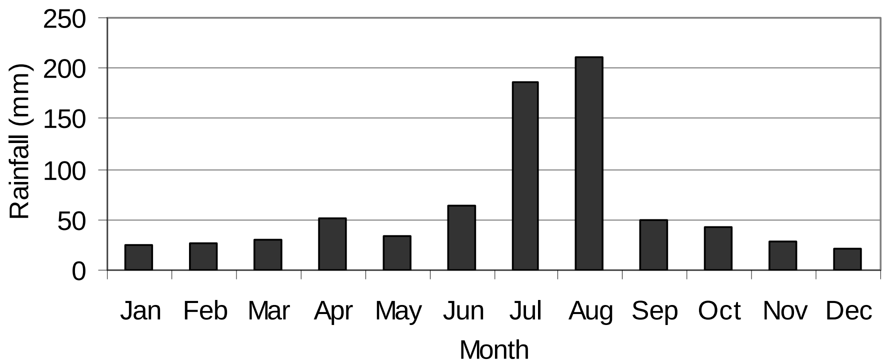

Figure 6.7 Monthly average rainfall of the Golina catchment

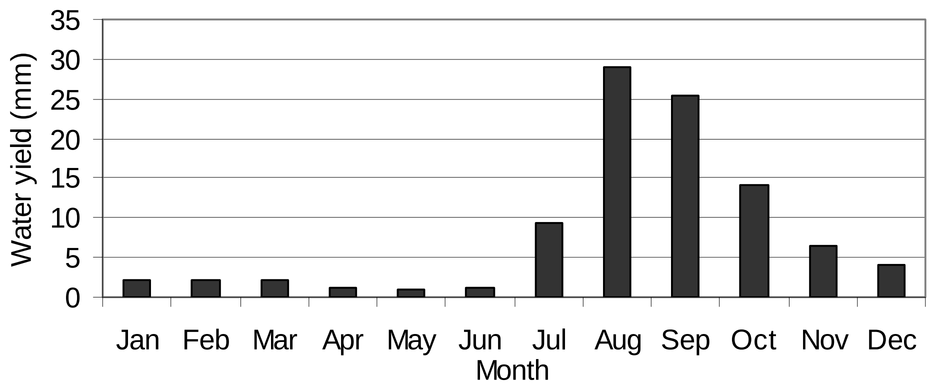

Figure 6.8 Monthly simulated average water yield of the Golina catchment

The water balance of the Golina catchments is presented in the Tables 6.5 and 6.6 below on monthly and annual basis. Figure 6.10 shows the main SWAT flow components in a diagram. The balance shows that a large amount of the rainfall is lost through evapotranspiration. This includes both the common evapotranspiration and the evapotranspiration from the shallow aquifer. Note that it was assumed that there is only a shallow aquifer and no deep aquifer in the area. A large amount of water (76mm) is released back into the atmosphere by evapotranspiration from soil/aquifer storage. The main difference between the GML and the SUFI derived parameters is in the GW_REVAP values. The lower REVAP values in the SUFI calibration lead to higher river flow. The different water yield values can be compared to average Golina and Alwuha discharges, estimated in Chapter 4 at respectively 113mmyr^{-1} and 155 mmyr^{-1} (see Figure 4.16).

Table 6.5Annual water balance values obtained with GML optimization

Annual water balance component values			
Precipitation	Preci	767.7	mm
Surface runoff	SurQ	37.03	mm
Lateral soil flow	Q	24.69	mm
Shallow groundwater flow	(SHALAQ)	64.89	mm
REVAP (shall aquifer) soil/plants	Evapo	76.39	mm
Deep aquifer recharge	DAQ	0	mm
Total aquifer recharge	AQ	141.24	mm
Total water yield	WATER	98.08	mm
Percolation out of soil	Q	112.73	mm
Evapotarnspiration	ET	587.8	mm
Potential evapotranspiration	PET	1996.2	mm
Transmission losses	Q	28.53	mm

Table 6.6 Average monthly water balance components (GML optimization)

	Average monthly basin values					
Month	Rain (mm)	SurfQ (mm)	LatQ (mm)	Water yield (mm)	ET (mm)	PET (mm)
January	24.16	0.04	1.09	2.24	26.98	130.82
February	26.62	1.36	0.81	2.07	34.78	154.87
March	29.30	0.00	0.76	2.19	97.60	181.98
April	51.52	0.21	0.75	1.09	54.49	189.35
May	34.19	0.00	0.83	1.05	31.85	200.82
June	63.28	0.51	0.92	1.14	31.17	186.07
July	186.27	11.13	2.18	9.31	70.77	211.44
August	210.98	17.87	5.05	29.10	92.55	155.67
September	50.50	2.61	4.97	25.35	59.32	182.28
October	41.69	1.69	3.39	14.08	39.50	155.92
November	28.37	0.75	2.29	6.44	26.30	128.30
December	21.42	0.90	1.67	4.07	23.33	122.46
Total	768.30	37.07	24.71	98.13	588.64	1999.98

ET=Evapotranspiration, SURQ=Surface runoff, LATQ=Lateral flow to stream GW_Q = Groundwater contribution to streamflow, Water yield=SURQ+LATQ+GW_Q-LOSSES

Table 6.7 Water balance components obtained with the SUFI calibration

Water balance		SUFI	fitting
precipitation	=	767.70	mm
surface runoff	=	35.40	mm
lateral soil flow	=	38.22	mm
shallow aquifer outflow	=	94.59	mm
revap from soil/plants	=	38.11	mm
deep aquifer recharge	=	0.00	mm
total aquifer recharge	=	132.65	mm
total water yield	=	140.70	mm
percolation to aquifer	=	105.38	mm
ET	=	583.40	mm
PET	=	1996.20	mm
transmission losses	=	27.50	mm

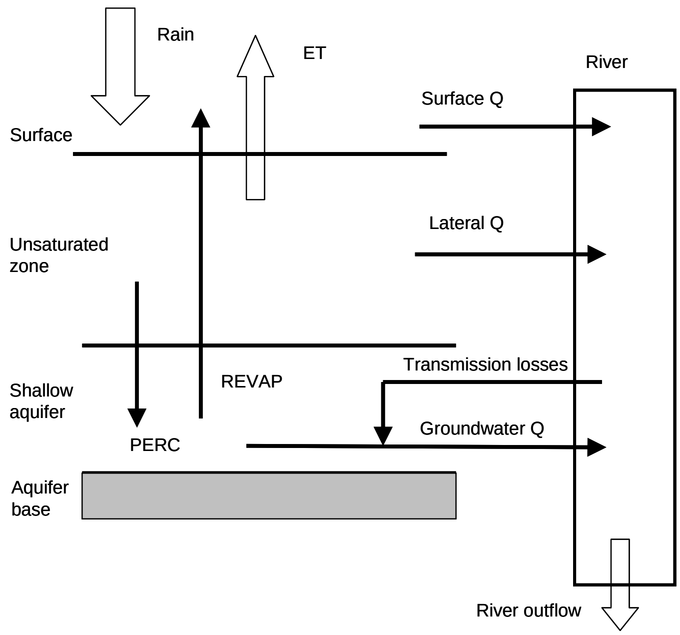

Figure 6.9 Diagram of main SWAT water balance components

.

6.3. SWAT Alamata/Mekoni Model

6.3.1. Introduction

The Alamata and Mekoni sub-basins are designated development corridors in northern Ethiopia. Federal and Regional governments are planning to utilize the groundwater resources in the area for irrigation purposes. Many deep wells have been drilled in the valley area (see MohamedSultan, 2010). The meteorological stations of the study area are well distributed and reasonably accurate, although there are many gaps in the data. Out of the ten stations in the area, only five stations have been used here (Alamata, Kobo, Korem, Waja and Zobel). Using the rainfall and temperature data of these stations, the water balance components of the area have been determined with the SWAT model, as described in the next sections.

6.3.2. Modelling the Alamata and Mekoni sub-basins

Raya Valley with the Alamata and Mekoni sub-basins was the main target for this study. Because there are no river gauges in these sub-basins, it was decided to do the initial modelling for the Golina sub-basin first. This catchment is just south of the Alamata sub-basin and it has a river gauge station near Kobo. The modelling was described in section 6.2. In this section a model is described that combines the Golina, Alamata and Mekoni sub-basins, with the use of the SWAT model parameters derived from the analysis of the Golina catchment. Figures 6.11 and 6.12 below show the catchment divided into sub-basins based on elevation, soil and land cover. The Golina catchment has become one sub-basin in this model set-up. The entire area has nine types of soils and nine land cover classes.

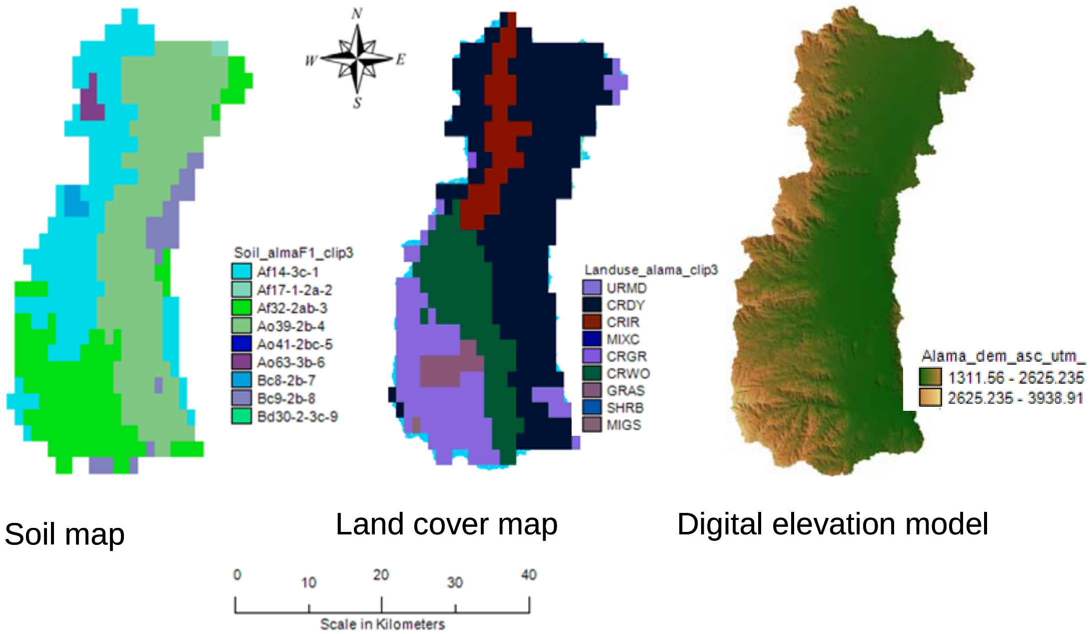

Figure 6.11 Soil, Land cover map and DEM of Alamata, Mekoni and Golina

Table 6.8 Land use and soil types derived from the data base (Ethiopian Geological Survey)

		Soil type definition
nr	SWAT code	TEXTURE
1	Af14-3c	CLAY_LOAM
2	Af17-1-2a	SANDY_CLAY_LOAM
3	Af32-2ab	SANDY_CLAY_LOAM
4	Ao39-2b	LOAM
5	Ao41-2bc	LOAM
6	Ao63-3b	CLAY
7	Bc8-2b	LOAM
		Land cover classes definition
	SWAT code	Definition
1	URMD	RESIDENTIAL / MEDUIM DENSITY
2	CRDY	DRYLAND CROPLAND and PASTURE
3	CRIR	IRRIGATED CROPLAND AND PASTURE
4	MIXC	MIXED DRYLAND/IRRIGATED CROPL
5	CRGR	CROPLAND/GRASSLAND MOSAIC

Based on the major classes of soils and land cover 36 hydrologic response units (HRUs), which are the same as the number of sub-basins, were created (see Figure 6.12). The SWAT codes for soil and land cover are given in Table 6.8 above. MWSWAT automatically assigns different parameters such as Manning‘s roughness coefficient and curve number to each sub-basin during the watershed delineation. The default parameters were adjusted according to the conceptual situation before the model was run. The rainfall and temperature data were used from five stations (903609, 903610, 903613, 903602 and 903606). The measured data have many missed data; these gaps were filled using the weather generator which is produced from monthly data. Climate data such as solar radiation, relative humidity and wind speed were generated using the weather generator, as described before. As can be seen in Figure 6.12, there are two outlets through which surface runoff leaves the catchment. The Golina river cuts through the eastern hill in sub-basin 25, while the location of the Golina river gauge is in sub-basin 18. The Alamata and Mekoni sub-basins are drained by the Sulula River which cuts through the hills at Selember in sub-basin 36.

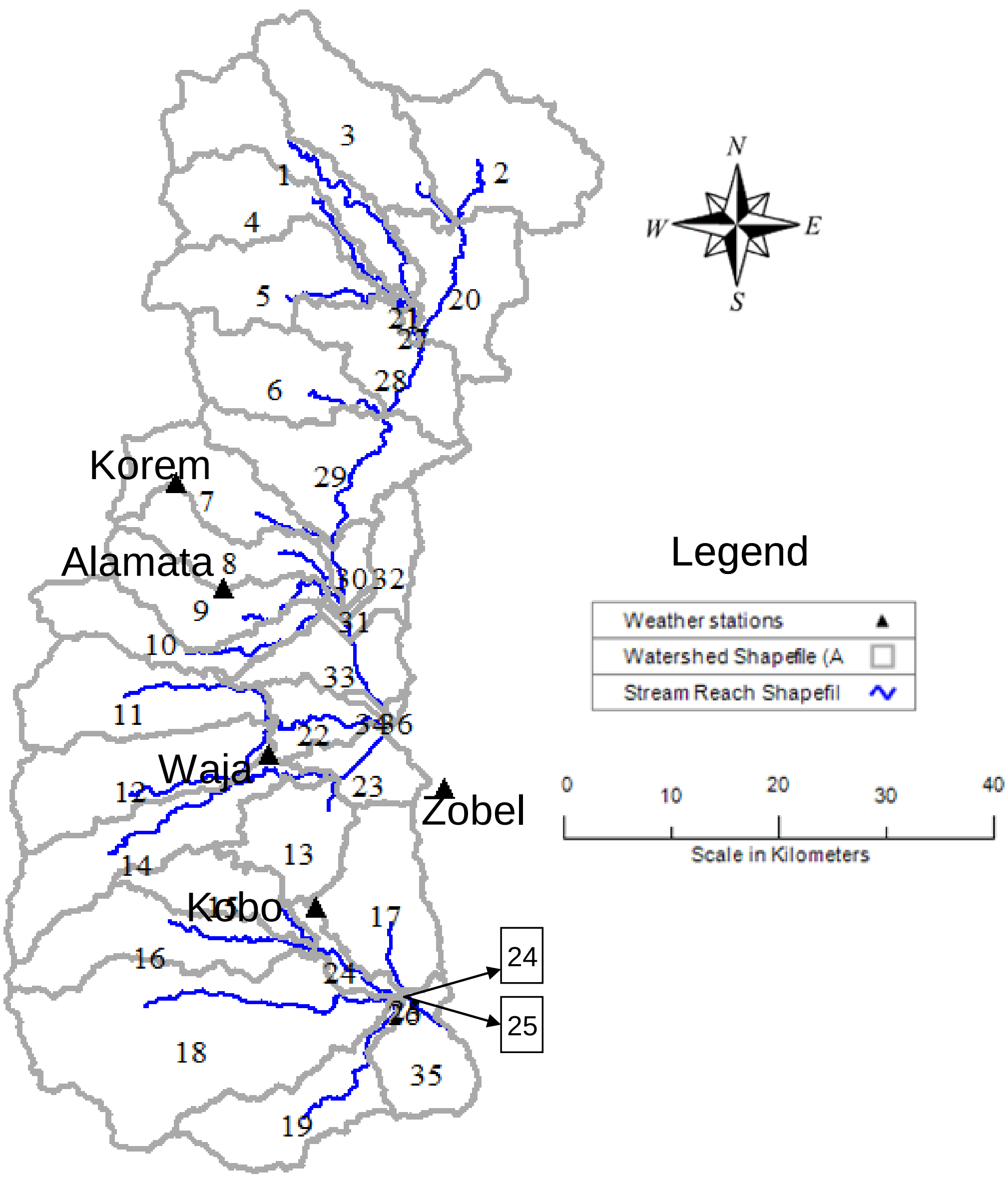

Figure 6.12 MWSWAT output sub-basins of the study area

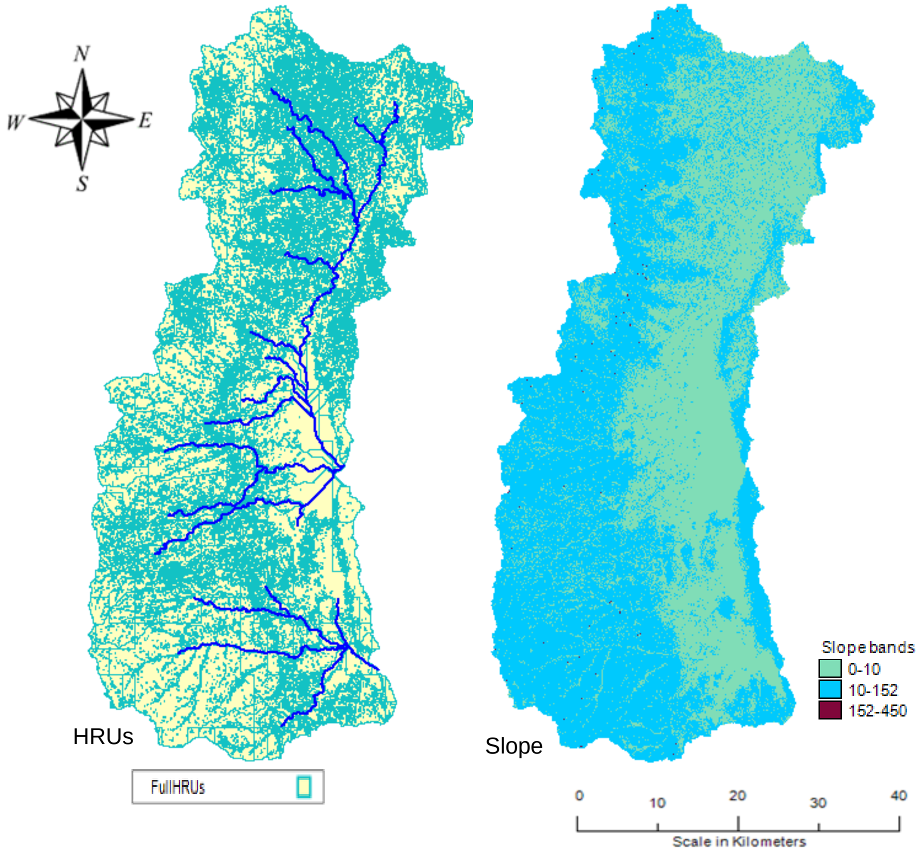

Figure 6.13 MWSWAT hydrologic response units and slope bands

6.3.2 SWAT model parameters for the Alamata/Mekoni model

According to Section 6.2, the model parameters were divided into two parts. The first part consisted of parameters that have kept fixed during the calibration of the Golina catchment. The values have been chosen to correspond with our understanding of the area's hydrological characteristics (see Table 6.9 below). The second part consisted of parameters, with values varying during the calibration processes. The parameter values found with the GML procedure produced lower flow rates than the parameter set resulting from the SUFI calibration. The larger Golina/Alamata/Mekoni model was now run with the two parameter sets. All other parameters were kept fixed at the values of Table 6.4. The model is called the Alamata model for reasons of brevity.

Table 6.9 The SWAT parameters for high and low flow scenarios

	low flow GML	high flow SUFI	remarks
CN2	67.83	67.83	
SOL_K	5.43	11.50	for SUFI K1 (7.4) K2(16.0)
GW_DELAY	31.00	37.30	
GW_REVAP	0.84	0.20	for SUFI fixed at 0.2

6.3.3 Monthly discharges of the Golina and Alamata/Mekoni sub-basins

The Alamata model produces the high and low flow values for the Golina catchment which is now modelled as a single sub-basin (reach number 18, Figure 6.12). The area is larger now (383 km^2) because some additional tributaries were included by the automatic delineation process. Figure 6.14 show the results for both scenarios. The constructed constant average monthly flow pattern is again shown as a dashed line. Modelled discharges are shown as solid line. The modelled discharges are similar to the simulations of the separate Golina catchment with seven sub-basins, discussed in section 6.2. It is also clear from the graphs that the monthly rain is an important factor in the runoff generation.

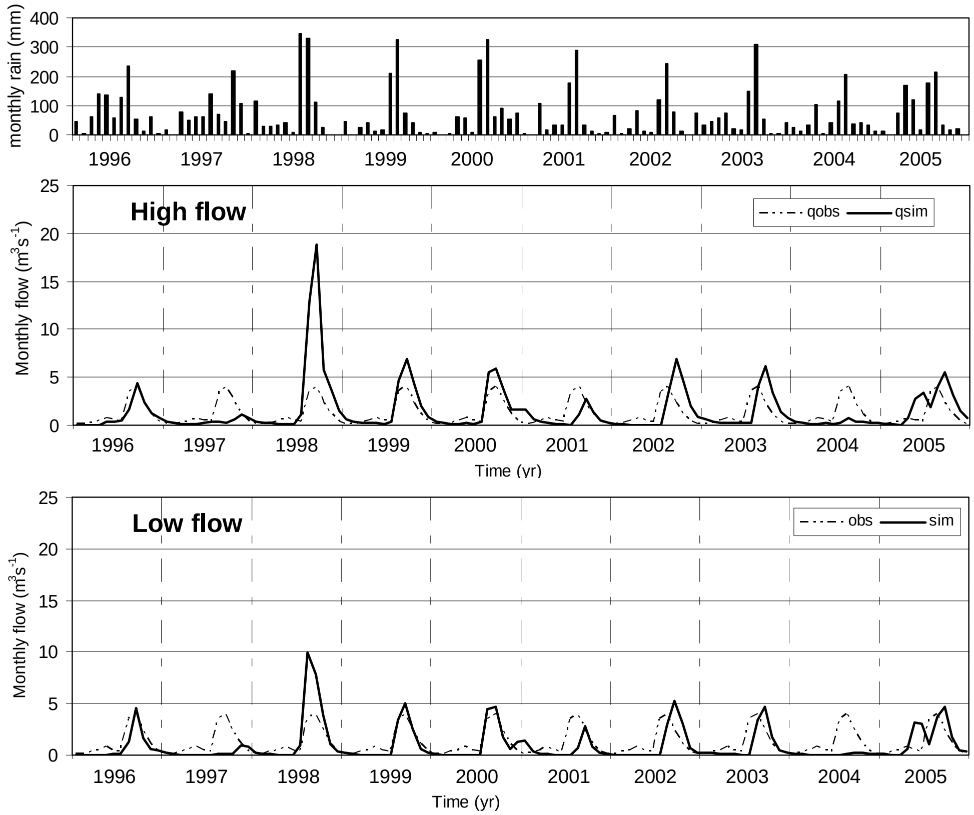

Figure 6.10 High and low flow value for Golina sub-basin 18

high flow	area (km^2)	reach	m^3s^{-1}	Mm^3yr^{-1}	$mmyr^{-1}$
Golina	383	18	1.46	46.07	120.30
Mekoni	1084	28	8.29	261.40	241.20
Selember	2481	36	15.38	485.00	195.50

low flow	area (km^2)	reach	m^3s^{-1}	Mm^3yr^{-1}	$mmyr^{-1}$
Golina	383	18	0.93	29.41	76.78
Mekoni	1084	28	5.48	172.85	159.45
Selember	2481	36	9.92	313.00	126.16

Table 6.10 Average flow rates for the low and high flow scenarios

Maximum runoff occurred in 1998, when both July and August rainfall were very high. There was very low runoff in 1997 and 2004. Table 6.10 shows the average flow rates for the Alamata and Mekoni sub-basins, respectively reaches 28 and 36. Both the values for the high and low flow scenarios are given. The monthly flow patterns are given in Figure 6.15 below. The table shows that the Mekoni sub-basin has a relatively high runoff rate. This is probably because the rains in the area were overestimated. Not many rainfall records are available in the area and therefore the model relies on the Alamata and Korem gauges in the Mekoni area. Both these gauges have higher annual rainfall than the other stations. The low flow scenario is in better agreement with values derived from the groundwater modelling which suggest about 100 mmyr^{-1} for the entire Alamata catchment (including the Mekoni).

Figures 6.14 and 6.15 also show the large variability of the runoff. Large runoff occurred in 1998, while the simulated river flow nearly ceased in 2002 and 2004. The flow rates are probably more indicative of recharge to the valley aquifer, than of real river flow. It should be remembered that a large part of the river water transported by the western catchments is infiltrating to the groundwater, after which it flows as groundwater to the Sulula River which acts as the valley drain. A large part of the groundwater is perhaps also taken out by evapotranspiration. The GW_REVAP coefficient should perhaps attain larger values here than is the usually the case. It is recommended to improve the modelling of the valley water balance modelling when more monitoring data have become available.

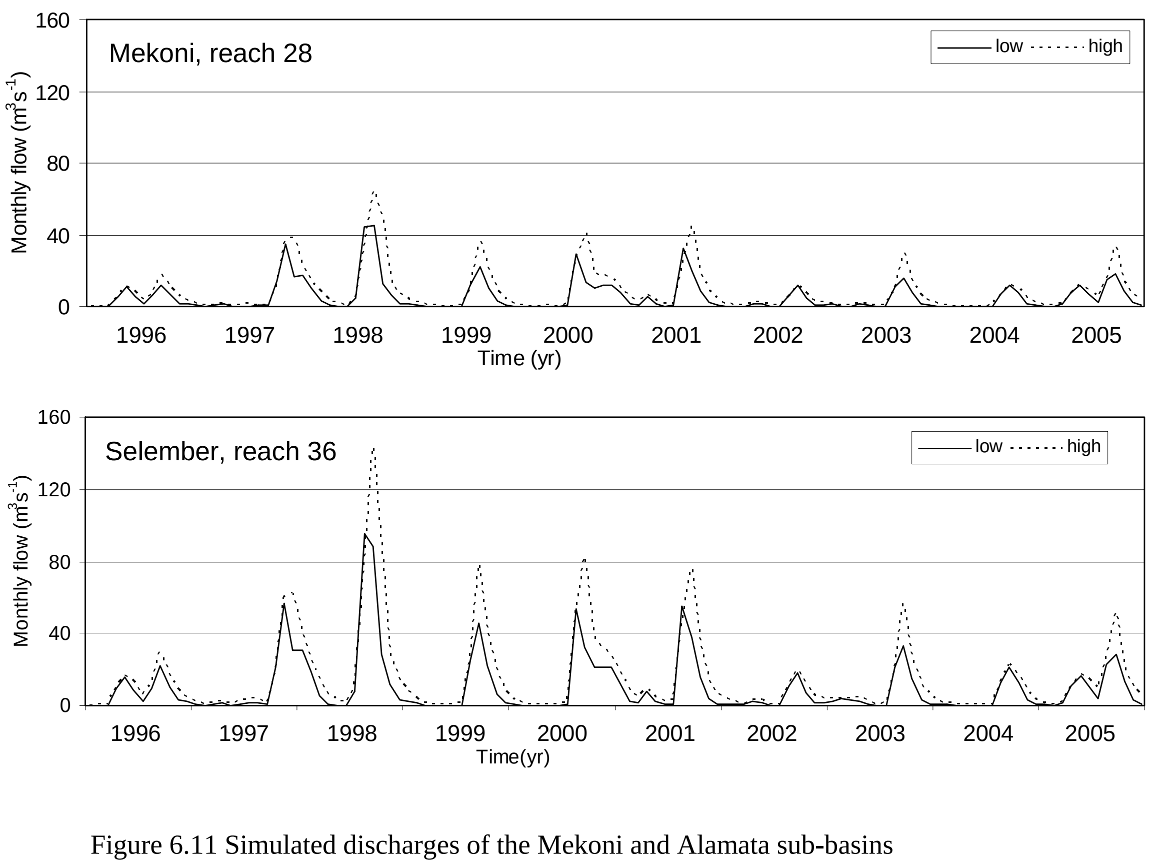

Figure 6.11 Simulated discharges of the Mekoni and Alamata sub-basins

6.3.5 Water balance of the Alamata/Mekoni sub-basins

The most important elements of water balance of a basin are precipitation, surface runoff, lateral flow and evapotranspiration. The predicted values of surface runoff, lateral flow, base flow, water yield and evapotranspiration by the calibrated model is shown in the tables below. It can be seen that the major portion of the rainfall received by the basins lost as evapotranspiration. According to the Immerzeel et al. (2008) the SWAT model is able to analyze the entire water balance as well as biomass and crop growth processes. The monthly water balance was derived from the results of the calibrated model. Balance closure refers to the sum of net change in groundwater and soil storage and model inaccuracies. In the study area the water balance components obtained from SWAT model were categorized into three sub-basins with respect to their areas.

Tables 6.11 and 6.12 show simulated water balance components on annual average basis. Individual components were put separately and the magnitude with comparison of the annual rainfall. The water balance of the study area was divided in to three sub-basins: Mekoni, Alamata and Golina. The main water balance components of the three sub-basins include: the total amount of precipitation falling on the sub-basin during the time step, actual evapotranspiration from the basin and the net amount of water that leaves the basin and contribute to stream flow in the reach. The water yield includes surface runoff contribution to stream flow, lateral flow contribution to the stream flow (water flowing within the soil that joins the main channel).

Tables 6.11 and 6.12 describe the water balance of the study area on monthly basis for both the low and high flow scenarios. In the study area a large amount of the precipitation is lost through evapotranspiration. In the dry season the monthly flow is very small.

Table 6.11 Monthly hydrological water balance for the low flow scenario

	Average monthly basin values					
Month	RAIN (mm)	SURF Q (mm)	LAT Q (mm)	Water yield (mm)	ET (mm)	PET (mm)
January	34.86	2.51	0.83	4.83	27.83	113.95
February	9.36	0.13	0.57	2.67	22.05	132.75
March	49.38	0.86	0.52	1.62	70.74	154.58
April	77.69	2.9	0.67	3.68	95.23	161.92
May	51.91	1.1	0.82	4.32	58.43	177.24
June	24.73	0.12	0.63	2.68	33.73	171
July	180.54	7.32	0.94	2.68	75.73	163.11
August	255.11	24.58	2.9	31.17	91.94	148.69
September	61.13	3.27	3.21	33.14	60.33	160.83
October	48.6	4.52	2.25	17.41	39.39	146.09
November	29.46	2.35	1.59	10.47	26.02	123.5
December	23.15	1.51	1.17	6.34	22.76	114.3

Table 6.12 Monthly hydrological water balance components for the high flow scenario

Average monthly basin values						
Month	RAIN (mm)	SURF Q (mm)	LAT Q (mm)	Water yield (mm)	ET (mm)	PET (mm)
January	34.86	2.47	1.06	7.75	27.63	113.95
February	9.36	0.12	0.63	4.28	21.9	132.75
March	49.38	0.84	0.8	3.16	70.42	154.58
April	77.69	2.79	1.54	4.66	94.52	161.92
May	51.91	1.06	1.84	5.35	57.59	177.24
June	24.73	0.12	1.1	3.82	33.41	171
July	180.54	6.73	2.42	4.66	75.04	163.11
August	255.11	23.17	8.59	30.42	91.02	148.69
September	61.13	3.08	7.29	53.8	59.66	160.83
October	48.6	4.19	3.42	30.26	38.99	146.09
November	29.46	2.25	2.06	18.25	25.73	123.5
December	23.15	1.48	1.34	13.17	22.53	114.35

ET=Evapotranspiration, PERC= percolation below root zone (Groundwater recharge), SURQ=Surface runoff, LATQ=Lateral flow in to stream GW_Q=Groundwater contribution to the stream flow, WYLD=SURQ+LATQ+GW_Q-LOSSES,

Tables 6.13 and 6.14 describe the annual water balance of the entire catchment. The value of total water yield matches with the reported studies. These tables represent the high and low flow scenarios. The tables show once again that the difference between the low and high flow is mainly caused by the evapotranspiration from the shallow aquifer (coefficient GW_REVAP) and by the outflow from the groundwater into the river channels.Tables 6.15 to 6.18 show the water balance components for the individual sub-basins, while a summary is given in Tables 6.19 and 6.20.

Table 6.13 Annual hydrological water balance of low flow scenarios

Annual water balance components			
Precipitation	PRECIP	845.7	mm
Surface runoff	SURQ	51.16	mm
Lateral soil flow	LATQ	16.09	mm
Shallow groundwater flow	SHALAQ	97.43	mm
REVAP	(SHAL AQ)	97.36	mm
Deep aquifer recharge	DAQ	0	mm
Total aquifer rechrage	AQ	194.75	mm
Total water yield	WATER	120.93	mm
Percolation out of soil	Q	151.02	mm
Evapotranspiration	ET	623.7	mm
Potential evapotranspiration	PET	1764.8	mm
Transmission losses	Q	43.75	mm

Table 6.14 Annual hydrological water balance components of high flow scenarios

Annual water balance components			
Precipitation	PRECIP	845.7	mm
Surface runoff	SURQ	48.3	mm
Lateral soil flow	LATQ	32.09	mm
Shallow groundwater flow	SHALAQ	140.55	mm
REVAP	(SHAL AQ)	44.37	mm
Deep aquifer recharge	DAQ	0	mm
Total aquifer rechrage	AQ	184.87	mm
Total water yield	WATER	179.48	mm
Percolation out of soil	Q	143.79	mm
Evapotranspiration	ET	617.9	mm
Potential evapotranspiration	PET	1764.8	mm
Transmission losses	Q	41.47	mm

Table 6.15 Annual water balance components of Mekoni's high flow scenario

	nr	Subbasins	Area km^2	Slope (%)	CN2	Rainfall (mm)	ET (mm)	PERC (mm)	SURQ (mm)	TLOSS (mm)	LATQ (mm)	GW_Q (mm)	WYLD (mm)	SWin (mm)
	1	1	142.41	10-152	64.3	1021.6	677.7	213.8	66.0	62.8	62.6	214.6	280.4	93.68
	2	2	175.00	0-10	70.2	1021.6	677.3	240.9	87.5	69.6	14.2	242.6	274.7	95.06
	3	3	156.96	0-10	70.2	1021.6	676.2	232.4	86.9	76.9	24.5	241.6	276.1	94.89
	4	4	109.62	10-152	64.3	1021.6	677.8	214.6	66.0	61.9	61.6	214.5	280.3	93.69
Mekoni	5	5	136.04	10-152	64.2	1021.6	676.7	207.5	65.5	56.0	70.4	203.9	283.7	93.55
	6	6	121.01	10-152	61.5	1021.6	651.0	233.5	77.2	64.4	58.9	231.8	303.5	84.25
	7	20	128.56	0-10	70.3	1021.6	677.8	244.0	87.8	71.8	10.4	246.8	273.2	95.12
	8	21	2.50	0-10	70.3	1021.6	678.2	246.1	87.9	62.5	7.8	241.0	274.2	95.17
	9	27	5.00	0-10	70.3	1021.6	678.3	247.0	88.0	61.3	6.6	240.8	274.1	95.18
	10	28	106.67	0-10	70.2	1021.6	677.5	242.6	87.6	75.6	12.2	248.7	272.9	95.08
		Total	1083.78			1021.6	674.31	229.0	78.5	67.5	38.2	231.0	280.2	93.33

Table 6.16 Annual water balance components of Alamata's high flow scenario

	nr	Subasins	Area km^2	Slope (%)	CN2	Rainfall (mm)	ET (mm)	PERC (mm)	SURQ (mm)	TLOSS (mm)	LATQ (mm)	GW_Q (mm)	WYLD (mm)	SWin (mm)
	1	7	106.38	10-152	64.2	1021.6	677.2	210.7	65.7	56.0	66.4	206.5	282.6	93.60
	2	8	86.99	10-152	65.1	821.8	641.2	117.7	37.3	34.9	22.2	115.1	139.8	74.87
	3	9	101.74	10-152	59.7	821.8	656.9	92.3	23.6	21.9	47.2	86.3	135.2	75.39
	4	10	99.28	10-152	59.7	821.8	656.1	90.7	23.5	22.0	49.7	85.1	136.2	75.26
	5	11	155.89	10-152	59.6	821.8	654.6	87.7	23.3	21.1	54.5	82.1	138.7	75.02
	6	12	162.80	10-152	56.6	668.4	576.4	41.8	11.6	10.6	35.6	38.5	75.2	59.23
	7	13	90.34	0-10	64.0	706.0	587.5	75.1	26.8	22.9	9.5	69.1	82.6	70.60
	8	14	158.37	10-152	60.7	668.4	562.2	62.5	18.1	16.9	22.7	58.1	81.9	65.73
Alamata	9	22	52.18	0-10	63.2	668.4	570.0	71.7	21.5	19.2	2.3	66.8	71.4	66.91
	10	23	53.78	0-10	67.6	905.4	646.8	165.5	72.9	54.7	14.8	158.7	191.7	84.57
	12	29	158.72	0-10	70.2	1021.6	676.7	236.0	87.1	63.0	20.1	233.1	277.4	94.94
	13	30	25.86	0-10	62.7	821.8	645.2	130.4	32.7	27.5	10.2	119.4	134.8	75.44
	14	31	4.10	0-10	65.3	821.8	647.0	130.8	38.4	29.6	2.2	121.6	132.7	75.60
	15	32	52.24	0-10	62.7	821.8	644.4	128.3	32.5	29.3	13.2	119.0	135.5	75.34
	16	33	80.93	0-10	63.2	668.4	568.7	70.0	21.3	19.5	5.4	65.8	73.0	66.74
	17	34	4.92	0-10	67.6	905.4	650.1	175.3	73.8	56.1	0.8	167.1	185.5	84.92
	18	36	2.92	10-152	65.0	905.4	649.2	164.1	65.2	34.5	21.6	142.5	194.8	84.14
	Total		1397.4			817.2	625.3	111.6	35.5	29.6	30.8	106.7	143.4	75.2

Table 6.17 Annual water balance components of Mekoni's low flow scenario

	nr	Subbasins	Area km2	Slope (%)	CN 2	PRECIP (mm)	ET (mm)	PERC (mm)	REVAP (mm)	SURQ (mm)	TLOSS (mm)	LATQ (mm)	GW_Q (mm)	WYLD (mm)	Swin (mm)
Mekoni	1	1	142.41	10-152	64.466	1021.6	681.455	238.348	148.783	68.763	65.389	31.211	154.976	189.561	94.26
	2	2	175	0-10	70.434	1021.6	682.772	236.757	150.735	93.129	73.543	7.227	159.582	186.395	95.86
	3	3	156.96	0-10	70.41	1021.6	682.071	232.557	152.253	92.695	81.695	12.525	162.016	185.542	95.764
	4	4	109.62	10-152	64.468	1021.6	681.514	238.773	148.474	68.8	64.382	30.695	154.704	189.816	94.265
	5	5	136.04	10-152	64.439	1021.6	681.002	234.954	144.141	68.465	58.362	35.337	149.199	194.639	94.185
	6	6	121.01	10-152	61.783	1021.6	653.256	257.404	159.111	80.318	66.66	29.354	164.974	207.986	85.373
	7	20	128.56	0-10	70.44	1021.6	683.013	238.318	152.339	93.287	75.855	5.282	161.852	184.566	95.887
	8	21	2.5038	0-10	70.446	1021.6	683.19	239.396	148.713	93.399	65.898	3.926	156.599	188.026	95.911
	9	27	5.0012	0-10	70.448	1021.6	683.263	239.867	148.436	93.447	64.547	3.338	155.995	188.233	95.921
	10	28	106.67	0-10	70.434	1021.6	682.893	237.611	153.792	93.211	80.035	6.182	163.872	183.23	95.864
		Total	1083.775			1021.6	678.90	238.93	151.05	82.91	70.91	19.16	158.80	189.96	94.10

Table 6.18 Annual water balance components of Alamata's low flow scenario

	nr	Subbasins	Area km^2	Slope (%)	CN 2	PRECIP (mm)	ET (mm)	PERC (mm)	REVAP (mm)	SURQ (mm)	TLOSS (mm)	LATQ (mm)	GW_Q (mm)	WYLD (mm)	Swin (mm)
Alamata	1	7	106.38	10-152	64.443	1021.6	681.242	236.68	144.882	68.611	58.313	33.245	150.134	193.677	94.205
	2	8	86.986	10-152	65.311	821.834	648.314	118.69	79.356	40.166	37.641	11.251	77.024	90.8	75.547
	3	9	101.74	10-152	60.04	821.834	663.787	107.128	64.314	24.987	23.211	23.514	66.075	91.366	76.43
	4	10	99.282	10-152	60.024	821.834	663.436	106.235	64.136	24.917	23.363	24.848	65.512	91.914	76.376
	5	11	155.89	10-152	59.994	821.834	662.771	104.552	62.796	24.784	22.526	27.368	64.332	93.958	76.272
	6	12	162.8	10-152	57.028	668.444	585.18	49.885	32.007	12.675	11.532	17.584	29.458	48.186	60.702
	7	13	90.341	0-10	64.095	706.016	592.798	73.242	51.691	28.259	23.934	4.708	45.475	54.508	70.921
	8	14	158.37	10-152	60.863	668.444	568.475	66.294	44.602	19.357	18.101	11.263	39.839	52.358	66.368
	9	22	52.182	0-10	63.197	668.444	573.013	68.731	47.125	22.534	19.93	1.142	41.582	45.328	66.908
	10	23	53.783	0-10	67.714	905.354	653.982	162.169	123.855	76.324	57.061	7.458	95.419	122.141	85.193
	11	29	158.72	0-10	70.412	1021.6	682.377	234.351	147.03	92.87	66.614	10.28	153.953	190.488	95.777
	12	30	25.861	0-10	62.859	821.834	648.482	130.339	80.69	34.667	29.284	4.955	78.981	89.32	75.806
	13	31	4.1004	0-10	65.404	821.834	651.24	125.225	79.111	40.871	31.477	1.117	77.639	88.15	75.921
	14	32	52.242	0-10	62.847	821.834	648.061	129.348	81.294	34.566	31.165	6.463	79.267	89.132	75.759
	15	33	80.925	0-10	63.177	668.444	572.403	67.901	46.902	22.434	20.45	2.674	41.496	46.154	66.83
	16	34	4.9189	0-10	67.758	905.354	655.615	167.133	128.364	76.831	58.502	0.378	97.315	116.021	85.37
	17	36	2.9208	10-152	65.218	905.354	655.735	165.497	114.244	68.1	35.833	10.703	87.13	130.101	84.732
			1397.4421			817.17	631.56	118.38	75.74	37.67	31.36	15.40	74.04	95.76	76.01

Table 6.19 Summary of water balance components of sub-basins of low flow scenario

Subbasin	Area km^2	Unit	PRECIP	ET	PERC	REVAP	SURQ	TLOSS	LATQ	GW_Q	WYLD	SWin
Mekoni	1083.78	$mmyr^{-1}$	1021.6	678.90	238.93	151.05	82.91	70.91	19.16	158.80	189.96	94.10
		Mm^3yr^{-1}	1107.18	735.77	258.95	163.71	89.85	76.85	20.76	172.11	205.88	101.98
		m^3s^{-1}	35.11	23.33	8.21	5.19	2.85	2.44	0.66	5.46	6.53	3.23
Alamata	1397.44	$mmyr^{-1}$	817.17	631.56	118.38	75.74	37.67	31.36	15.40	74.04	95.76	76.01
		Mm^3yr^{-1}	1141.95	882.58	165.43	105.84	52.64	43.82	21.52	103.47	133.81	106.22
		m^3s^{-1}	36.21	27.99	5.25	3.36	1.67	1.39	0.68	3.28	4.24	3.37
Golina	968.19	$mmyr^{-1}$	706	550.41	99.72	68.48	35.10	31.25	13.64	62.50	80.00	79.82
		Mm^3yr^{-1}	683.54	532.90	96.55	66.31	33.99	30.25	13.20	60.51	77.45	77.28
		m^3s^{-1}	21.67	16.90	3.06	2.10	1.08	0.96	0.42	1.92	2.46	2.45

Table 6.20 Summary of water balance components of subbasins

Subbasin	Area km^2	Unit	PRECIP	ET	PERC	REVAP	SURQ	TLOSS	LATQ	GW_Q	WYLD	SWin
Mekoni	1083.78	$mmyr^{-1}$	1021.6	674.31	229.0	64.9	78.5	67.5	38.2	231.0	280.2	93.33
		Mm^3yr^{-1}	1107.18	730.81	248.19	70.33	85.12	73.13	41.38	250.30	303.68	101.15
		m^3s^{-1}	35.11	23.17	7.87	2.23	2.70	2.32	1.31	7.94	9.63	3.21
Alamata	1397.44	$mmyr^{-1}$	817.2	625.3	111.6	34.4	35.5	29.6	30.8	106.7	143.4	75.2
		Mm^3yr^{-1}	885.63	677.69	120.94	37.30	38.49	32.13	33.39	115.64	155.39	81.51
		m^3s^{-1}	28.08	21.49	3.83	1.18	1.22	1.02	1.06	3.67	4.93	2.58
Golina	968.19	$mmyr^{-1}$	706.016	544.11	94.86	35.76	32.91	29.41	27.11	88.22	118.83	79.01
		Mm^3yr^{-1}	765.16	589.69	102.81	38.75	35.67	31.88	29.38	95.61	128.78	85.63
		m^3s^{-1}	24.26	18.70	3.26	1.23	1.13	1.01	0.93	3.03	4.08	2.72

7. Conclusions and recommendations

7.1. Conclusions

This study is applied for the water balance the Rata Valley, Tigray, Ethiopia. The area of the study is 2840 km^2 and has one outlet. The hydrologic simulation used DEM, landuse and soil and hydrometeorological data. Watershed distributed hydrological model (SWAT) was used. The area is prone to data scarcity so that I have prepared weather generator from the monthly climatic data which was obtained from previous report. An important improvement in the model setup was the change from the use of the poor quality and missed measured weather data to the use of daily generated data based on monthly climate data. To use the measured precipitation and temperature (maximum and minimum) data as input to the SWAT model I made some data analysis and preparation. Using the weather data obtained from the weather generator and measured data (precipitation and temperature); the SWAT calculated the hydrologic components. The calibration of the model was done using the SWAT-CUP and SWATSHELL4a. The discharge data which was used for the calibration was very poor. By correcting some errors based on the previous works I used for the calibration of the model.

Using the MWSWAT 2005 interface the hydrologic response units and subbasins were created. For the creation of the hydrologic response units I have used the major soil classes and land cover. SWAT produces water balance for each hydrologic response units. In addition to the simplification made for the soil and landcover maps to represent subbasin, there are also many other processes which were neglected (e.g., Reservoirs, water use, irrigation) due to the limited available information. Given all uncertainties in the model input, the parameters, and especially in the conceptual model, I tried to run the model.

After the model was run it has to be calibrated. Here in this study there were two options of calibration which are manually and automatic. Before I started calibration the parameters were selected based on their sensitivity. A manual calibration is more or less a processes trial and error. In general parameter value has to be changed and the model has to be rerun. Based on the parameters I obtained using manual calibration I used the automatic calibration using GML and SUFI2. The automatic calibration needs only requires two input files to be filled once. These files contains the information controlling the program, the measured and modelled values are used to compare with and decelerations of the parameter constraints and interdependencies. A program using a relatively small number of simulations to perform calibration and uncertainty analysis was essential for such a computationally extensive model. Initial calibration was done for Golina. The study showed that surface water model parameters are more sensitive and have more physical meaning especially the CN2 and SOL_K. The result which was obtained from this calibration was good. The objective functions for this calibration were the Nash-sutcliff and RMSE. For Golina catchment based on these two values, the result was comparable. The large amount of the rainfall is lost from the basin through evapotranspiration.

The next modelling was done for the Alamata subbasin as it was my target area. Here the only option I had was to use the parameters which were obtained during calibration of the Golina catchment. Because the catchment has no any measured river discharge data. The simulated result obtained from this result was comparable with previous study of the area. Here also the maximum part of the rainfall of the basin was lost through the evapotranspiration. As it is known SWAT needs many parameters but for this study very limited amount of data were used. The rest was as taken as default therefore further study has to be done by taking additional detailed data. SWAT is the powerful software for the catchment wise water balance modelling especially for the ungauged catchment like Raya Valley. Here I had to use but I did not use is calibration of the model using evapotranspiration obtained fro the satellite using SEBS algorithm.

7.2. Recommendations

This study is not the end of water balance modelling of the area but it can be used as a base for the future study. By adding and refining the data water balance modelling is possible, which is expected to improve the accuracy of the model. Good quality of the daily climate data will increase the capability of to understand the hydrological processes therefore more data loggers 3hich can measure daily data should be installed in the area.

The following are further recommendations for the study area.

- Soil and water assessment tool (SWAT) is one of the hydrological models which can represent the water balance components of each subbasin of the catchment, but it requires daily data so that further investment on the gauging stations should be given an emphasis.
- In this study the soil parameters were not exactly known so that for further study the soil properties and land use type should be defined in detail.
- The quality of hydrometeorological data is the main factor to understand the hydrological processes so in this study area the distributed river gauge stations should be well studied.
- The amount of water extracted from shallow and deep aquifer must be differentiated and regulated.
- To understand the relationship between the bed of the river and the flowing water along the river SWAT and Modflow must be used together in one catchment.
- One gauged station must be in between the Mekoni and Alamata basin to understand the relationship of these two basins
- Another river gauge stations have to be in the Sulula, Selember, Harosha and oda rivers.
- Data collection should be assessed and evaluated for all the rain gauge and river gauge stations of the study area.
- The integration of the remote sensing in the calibration of the distributed hydrological models in areas where there is limited data availability is very helpful.
- The water balance modelling has to be done for different scenarios that is for land use and climate change.

8. References

Abbaspour, K.C., 2009. SWAT Calibration and Uncertainty Programs. A user Manual,EWAG,Swiss federal Institute of Aquatic Science and technology,duebendorf,Swizerland Version 2: pp.95.

Allen, R.G., Pereira, L.S., Raes, D. and Smith, M., 1998. Guidelines for computing crop water requirements FAO (Food and Agriculture Organization of the United Nations) irrigation and drainage paper, 56: pp.134.

Arnold, J.G., Muttiah, R.S., Srinivasan, R. and Allen, P.M., 2000. Regional estimation of base flow and groundwater recharge in the Upper Mississippi river basin. Journal of Hydrology, 227(1-4): 21-40.

Arnold, J.G., Srinivasan, R., Muttiah, R.S. and Williams, J.R., 1998. Large area hydrological modelling and assessment. Journal of the American Water Resources Association, 34(1): 73-89.

Bärlund, I., Kirkkala, T., Malve, O. and Kämäri, J., 2007. Assessing SWAT model performance in the evaluation of management actions for the implementation of the Water Framework Directive in a Finnish catchment. Environmental Modelling and Software, 22(5): 719-724.

Birhanu, B.Z., 2009. Hydrological modelling of the Kihansi river catchment in South Central Tanzania using SWAT model. International Journal of Water Resources and Environmental Engineering, Vol. 1 (1): (http://www.academicjournals.org/IJWREE/PDF/Pdf2009/Oct/Birhanu.pdf Accessed on December,2009) pp.10.

Birhanu, B.Z., Ndomba, P.M. and Mtalo, F.W., 2007. Application of SWAT Model for Mountainous Catchment. (University of Dar es Salaam, Water Resources Engineering): 182-187.

Dagnew, B., 2007. Assesement of causes and extent of land degradation in Hashenge catchment ,Southern Tigray. MSc Thesis, Addis Abeba, Ethiopia: (http://etd.aau.edu.et/dspace/handle/123456789/1840 Accessed on December 2009) pp.66.

Dessie, N.H., 2003. Aquifer Characterisation and Hydrochemical Investigation in Raya Valley, Northern Ethiopia. PhD Thesis: 1-248.

Dingman, S.L., 2002. Physical hydrology. Prentice Hall, Upper Saddle River, 646 pp.

George, C., 2008. SWAT Output Plotting and Graphing Tools (SWATPlot and SWATGraph). Manual for Graphing Tools in SWAT, Version 1.1.

Gieske, A.S.M., 1992. Dynamics of Groundwater recharge: A case study in Semi-Arid Eastern Botswana. PhD Thesis: pp.285.

Gieske, A.S.M., 2010. SWATSHELL4.0, Integration of SWAT with Gauss-Marquardt-levenberg optimization procedures. Alpha version 4.0, ITC, Enschede, The Netherlands.

Govender, M. and Everson, C.S., 2005. Modelling streamflow from two small South African experimental catchments using the SWAT model. Hydrological Processes, 19(3): 683-692.

Guan, L., Yang, J. and Bell, J.M., 2007. Cross-correlations between weather variables in Australia. Building and Environment, 42(3): 1054-1070.

Immerzeel, W.W., Gaur, A. and Zwart, S.J., 2008. Integrating remote sensing and a process-based hydrological model to evaluate water use and productivity in a south Indian catchment. Agricultural Water Management, 95(1): 11-24.

Kidan, H., 2009. Community spate irrigation in Raya Valley: The case study of free spate irrigation systems. MScThesis Addis Abeba University,Ethiopia: (http://www.spate-irrigation.org/librar/documents/MSc-Socio-economic_spate.pdf Accessed on November 2009) pp.85.

Kjell, E., Tor-Gunnar, V., Yibabe, T. and Mitiku, H., 2002. Soil Conservation in Tigray,Ethiopia. Report Number 5(Agricultural University of Norway): (http://www.umb.no/statisk/noragric/publications/reports/2002_nor_rep_5_bodytxt.pdf Accessed on December 2009) pp.21.

Leon, L.F., 2009. Map Window Interface for SWAT(MWSWAT). Main report: pp.70.

McKay, M.D., Beckman, R.J. and Conover, W.J., 1979. A comparison of three methods for selecting values of input variables in the analysis of output from a computer code. Technometrics, 21: 239-245.

Metaferia, C.E., 2008. Kobo-Girana pressurized irrigation system study and detail design project water resources. Draft report, Volume one: (FREMWR , Federal Republic of Ethiopia Ministry of Water resources) pp.45.

Michael, M.G. and Seleshi, B.A., 2007. Irrigation practices in Ethiopia: Characteristics of selected irrigation schemes. IWMI (International Water Management Institute), working paper124: pp.80.

Mohamedsultan, 2010. Groundwater flow modelling assissted by GIS and remote sensing techniques (Raya Valley,Ethiopia). MSc Thesis,ITC,Enschede: pp.114.

Mulungu, D.M.M. and Munishi, S.E., 2007. Simiyu River catchment parameterization using SWAT model. Physics and Chemistry of the Earth, 32(15-18): 1032-1039.

Neitsch, S.L., Arnold, J.G., Kiniry, J.R., Srinivasan,R.,Williams, J.R., 2005. Soil and water Assessment tool input/output files documentation. . user's Manual,Temple,Texas,USA, Version 2005: pp.541.

Neitsch, S.L., Arnold, J.G., Kiniry, J.R., Williams, J.R., 2005. Soil and water Assessment tool theoretical documentation. . User's manual,Temple,TX,USA, Version 2005: pp.476.

Ouessar, M., Bruggeman, A., Abdelli, F., Mohtar, R.H., Gabriels, D. and Cornelis, W.M., 2008. Modelling water-harvesting systems in the arid south of Tunisia using SWAT. Journal Hydrology and Earth System Sciences, 5: 1863–1902.

Pikounis, M., Varanou, E., Baltas, E., Dassaklis, A. and Mimikou, M., 2003. Application of the SWAT model in the Pinio River Basin under different land use scenarios. The international Journal of hydrology, 5: 71-79.

REST, 1996. Raya Valley development study project. Reconnaissance phase report, Phase I: (http://www.eap.gov.et/content/files/Documents/EAP%20Documents/Extension%20Development/Raya%20Valley%20Development%20Study%20Project.pdf Accessed on November 2009) pp.37.

REST, 1997. Hydrogeology of Raya Valley. Main report, Phase two: (REST, Relief Society of Tigray): pp.61.

REST, 2007. Raya pressurized irrigation project. Water resources Hydrometeorology Draft report, (REST) Relief Society of Tigray, (FDREMWR) Federal Republic Ministry of Water Resources): pp.86.

Schuol, J. and Abbaspour, K.C., 2007. Using monthly weather statistics to generate daily data in a SWAT model application to West Africa. Ecological Modelling, 201(3-4): 301-311.

Shimelis, G.S., Ragahavan, S., Assefa, M.M. and Dargahi, B., 2009. SWAT model application and prediction uncertainty analysis in the Lake Tana Basin, Ethiopia. Hydrological Processes, 10: pp.14.

USDA-SCS, 1972. National Engineering Handbook. Section 4 - Hydrology. Washington, D.C.: USDA-SCS.

Verstraeten, W.W., Veroustraete, F. and Feyen, J., 2005. Estimating evapotranspiration of European forests from NOAA-imagery at satellite overpass time: Towards an operational processing chain for integrated optical and thermal sensor data products. Remote Sensing of Environment, 96(2): 256-276.

Viessman, W., Lewis, G.L. and Knapp, J.W., 1989. Introduction to hydrology. Harper & Row, New York etc., 780 pp.

Volk, M., J.G. Arnold, D.D. Bosch, P.M. Allen and Green, C.H., 2008. Watershed Configuration and Simulation of Landscape Processes with the SWAT Model. Conference: 2383-2389.

WWDSE and CECE, 1999. Agronomy feasibility study. Report (WWDSE, Water works Design and Specification Enterprise ,(CECE, Concert Engineering and Consulting Enterprises): pp.100.

WWDSE and CECE, 2008. Raya pressurised irrigation project water resources hydrometeorology. Feasibility study report: Report (WWDSE, Water works Design and Specification Enterprise ,(CECE, Concert Engineering and Consulting Enterprises) pp.111.

Appendices A Photographs of the study area

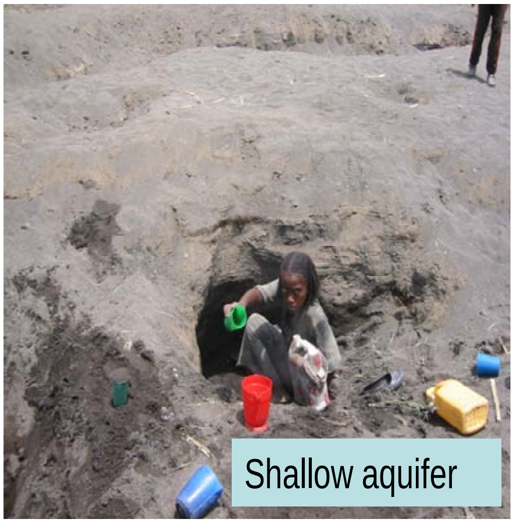

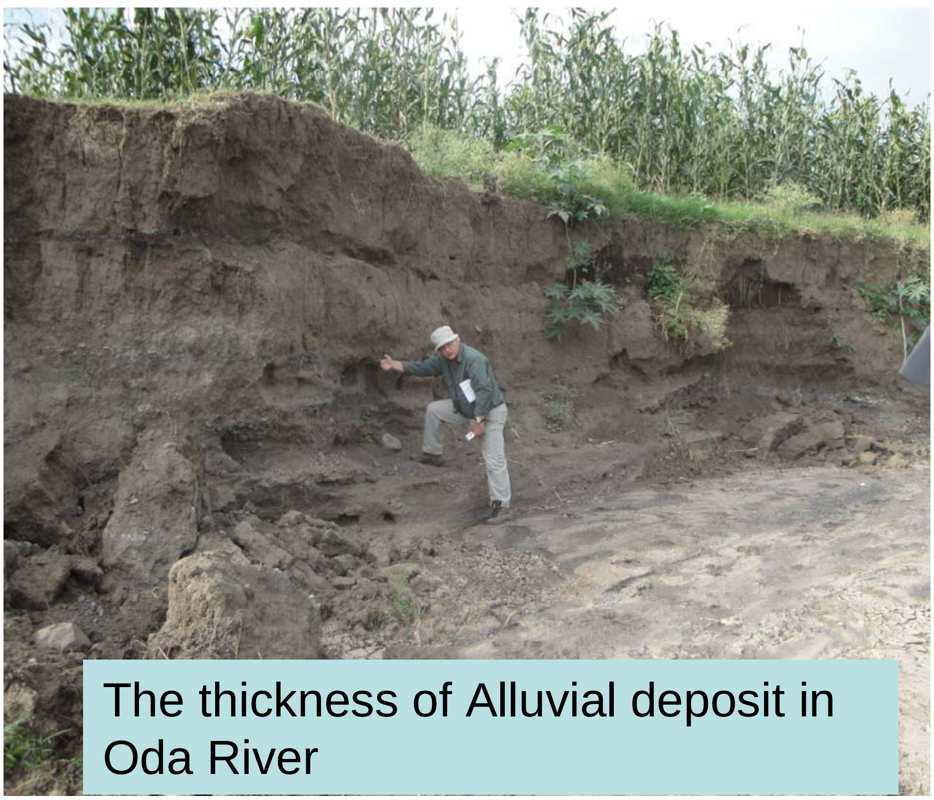


Forest West of Alamata


River bank soil deposit


Forest in the Valley plain area


Artesian well in Kobo valley

Appendices B Ground control points for Landcover classification

Ground control points taken during field work

nr	Landcover	Longitude	Latitude	Elevation
1	Agricultural area	562003	1370012	1508
2	Irrigation	561985	1370058	1505
3	Waja spring	563584	1360322	1468
4	Grass land	563606	1360257	1462
5	Forest	564498	137205	1474
6	Residense area	564563	1372185	1475
7	Forest	564718	1371973	1473
8	Bare land	566778	1372356	1440
9	Forest	570820	1373013	1399
10	Bare land	573147	1373325	1407
11	Residense and forest area	564343	1363663	1495
12	Outlet(Selem Ber)	577317	1360821	1377
13	Residense area	574007	1361812	1399
14	Forest	572927	1362529	1408
15	Forest	570517	1363537	1417
16	Forest	573175	1335387	1411
17	Gergele grass land(Swampy)	566624	1375845	1432
18	Grass land	567088	1375229	1433
19	Alamata	560781.32	1372723.94	1559
20	Korem	556475.06	1382919.79	2462
21	Hashenge	554360.56	1391307.94	2438
22	Maichew	558408	1412993.59	2429
23	Mekoni	570060.15	1415185.99	1773
24	Kobo	568673.06	1343949.25	1509

Appendices C Area of the Alamata subbasin subcatchments

nr	Latitude(m)	Longitude (m)	Elev (m)	Catchment name	Area(Km^{-2})
1	567405	1330755	1466	Wediashewa	5.87
2	561615	1383795	1472	Tirke	21.07
3	563145	1347435	1504	Warsu	12.10
4	564015	1396845	1612	Werabeyti	15.67
5	565965	1327185	1473	Weylet	27.35
6	555345	1370865	1517	Itu	25.25
7	553425	1375365	1488	Hara	37.59
8	576645	1375005	1414	Beyra	44.24
9	561855	1386555	1498	Dikala	28.30
10	558345	1343955	1509	Bufe	65.40
11	569445	1422615	1700	Burka	48.58
12	558735	1397655	1618	Habro	53.71
13	564435	1419105	1716	Haya	52.18
14	560685	1407225	1703	Guguf	93.87
15	562725	1414635	1710	Wejig	67.58
16	557955	1377435	1482	Dayu	54.07
17	555525	1384365	1451	Ulaula	75.36
18	560955	1399455	1633	Fokisa	80.44
19	558195	1322145	1461	Gashete	100.51
20	553575	1368225	1489	Tengego	73.43
21	551655	1362705	1486	Oda	137.19
22	551595	1349385	1453	Gobu	144.63
23	554085	1341405	1493	Hormat	131.03
24	552135	1353555	1455	Harosha	142.53
25	554685	1334265	1478	Golina	292.83
26	576585	1339575	1322	L.Golina outlet	356.21
27	583155	1404945	1463	Mekoni	701.45
28	573345	1381785	1404	Alamata Plain	604.93

Appendices D Weather generator statistic value of different stations

Alamata

OID 903609
Latitude(deg) 12.42 Longitude(deg) 39.56
Elevation(m) 1545
Rain years 10

	Jan	Feb	Mar	Ap	May	Jun	Jul	Au	Se	Oct	Nov	De
maxtemp	16.35	18.48	20.60	21.22	23.67	22.34	22.57	21.04	23.66	20.15	17.94	16.94
min temp	11.92	12.84	14.58	15.79	16.98	17.92	17.60	16.04	20.56	14.14	12.73	11.79
stdev.max	5.83	5.83	5.45	5.70	3.34	7.36	6.11	4.41	11.87	4.18	6.29	5.82
stdev.min	3.45	3.39	3.35	2.91	2.45	2.20	2.26	2.37	21.67	3.23	3.54	3.51
av.mon.prec	38.60	28.07	85.53	100.94	50.57	10.84	125.40	211.21	51.72	22.80	19.99	29.90
stdv.daily prec	5.85	5.52	7.52	7.73	4.89	3.85	7.93	10.72	5.09	4.81	4.45	5.03
skew.daily prec	6.73	4.08	4.09	3.38	4.32	6.54	2.91	1.80	4.11	7.66	10.17	6.77
pwd	0.08	0.06	0.14	0.14	0.11	0.07	0.23	0.24	0.17	0.06	0.03	0.05
pww	0.40	0.84	0.83	1.48	0.63	0.35	2.37	2.67	0.71	0.29	0.14	0.33
no.of wet days	3	4	5.67	7.67	4.33	2.62	12.38	13.48	6.19	2.14	1.05	2.19
max.0.5 hr rain	66.20	48.50	55.40	58.00	38.00	40.00	64.70	52.30	46.50	58.50	62.40	48.50
av.daily sol.rad	9.43	12.28	16.42	19.40	22.96	25.01	24.51	23.13	19.23	15.54	11.40	9.05
av.daily dewpt	3.15	4.20	5.95	8.05	4.55	2.75	13.00	14.15	6.50	2.25	1.10	2.30
av.daily windsp	2.89	2.06	2.11	1.90	1.68	1.94	1.92	1.60	1.20	1.30	1.46	1.61

Kobo

OID 903610
Latitude (deg) 12.15 Longitude (deg) 39.64
Elevation (m) 1498
Rain year 10

	Jan	Feb	Mar	Ap	May	Jun	Jul	Au	Se	Oct	Nov	De
maxtemp	26.34	27.40	29.21	30.40	32.75	33.59	31.92	30.17	30.40	29.20	27.70	26.28
min temp	11.98	13.27	15.14	16.59	16.73	17.60	17.89	16.29	13.74	12.28	11.87	12.01
stdev.max	1.12	1.89	1.73	1.27	1.55	2.95	1.79	1.92	1.39	1.40	1.26	1.32
stdev.min	2.72	2.08	1.41	1.17	1.45	2.01	1.66	1.97	3.03	2.24	2.67	3.95
av.mon.prec	19.2	8.13	33.64	52.29	32.12	65.07	214.88	153.99	33.62	42.38	28.50	18.09
stdv.daily prec	5.71	4.21	4.16	5.44	7.28	6.47	14.89	9.66	6.23	5.76	4.44	4.10
skew.daily prec	9.89	6.07	4.62	4.64	5.03	4.86	10.21	2.62	4.09	6.61	7.25	8.11
pwd	0.06	0.07	0.12	0.14	0.12	0.10	0.16	0.19	0.15	0.08	0.03	0.03
pww	0.41	0.67	1.00	0.95	0.46	1.03	3.31	2.90	1.28	0.49	0.18	0.18
no.of wet days	3.25	4.50	7.00	7.75	5.42	6.58	16.17	15.67	8.92	4.17	1.42	1.58
max.0.5 hr rain	37.50	44.20	31.10	42.30	58.90	59.40	237.80	72.20	48.50	57.00	42.40	50.20
av.daily sol.rad	18.30	19.70	21.50	22.20	22.00	18.70	17.90	18.40	19.30	21.10	19.40	18.70
av.daily dewpt	2.60	3.60	5.60	6.20	4.33	5.27	12.93	12.53	7.13	3.33	1.13	1.27
av.daily windsp	1.75	1.98	2.10	2.05	1.91	2.11	2.17	1.65	1.22	1.29	1.42	1.52

Muja

OID	903613											
Latitude (deg)	12.00	Longitude (deg)		39.29								
Elevation (m)	2780											
Rain	10											
	Ja	**Fe**	**Mar**	**Ap**	**May**	**Ju**	**Jul**	**Aug**	**Se**	**Oc**	**Nov**	**De**
maxtem	19.91	21.18	21.55	22.73	24.55	25.55	23.09	22.36	23.09	21.91	20.91	20.09
min temp	6.55	5.64	7.82	9.27	8.91	10.36	12.36	11.91	8.55	7.27	5.45	6.27
stdev.ma	2.02	1.08	1.13	1.01	1.13	1.04	0.83	0.92	1.22	1.45	1.64	0.83
stdev.min	3.62	3.26	2.48	1.62	2.51	1.63	0.67	0.54	1.57	2.10	4.03	4.08
av.mon.pre	31.26	41.49	89.88	80.16	93.18	53.42	225.91	203.28	70.01	58.97	39.48	17.95
stdv.daily prec	1.49	1.25	3.92	16.16	4.23	45.65	15.03	9.60	2.82	1.75	2.47	5.62
skew.daily	7.62	5.83	4.07	-5.38	6.16	-0.91	-3.51	1.83	4.83	7.04	5.65	-16.18
pwd	0.00	304.00	221.00	204.00	244.00	182.00	57.00	54.00	239.00	297.00	299.00	294.00
pww	0.33	0.61	3.11	2.44	1.83	1.50	10.00	10.61	1.56	0.22	0.78	0.83
no.of wet days	2.0	2.3	9.8	9.6	7.0	4.6	25.2	26.6	7.1	2.3	2.8	3.0
max.0.5 hr rain	17.00	11.70	33.90	43.50	49.50	30.30	52.70	51.90	27.30	18.00	19.50	12.00
av.daily sol.rad	18.30	19.70	21.50	22.20	22.00	18.70	17.90	18.40	19.30	21.10	19.40	18.70
av.daily	1.20	1.40	5.87	5.73	4.20	2.73	15.13	15.93	4.27	1.40	1.67	1.80
av.daily windsp	1.47	1.60	1.77	1.77	1.53	2.37	2.40	1.87	1.23	1.17	1.17	1.30

Zobel

OID	903606											
Latitude (deg)	12.25	Longitude (deg)	39.75									
Elevation (m)	2109											
Rain years	10											
	Jan	**Feb**	**Mar**	**Ap**	**May**	**Jun**	**Jul**	**Au**	**Se**	**Oct**	**Nov**	**De**
Av. Max temp	22.55	24.98	26.65	29.00	30.41	31.89	28.86	27.96	28.33	26.07	25.72	25.85
Av.Min temp	9.89	11.17	13.63	14.50	15.36	14.78	14.29	12.95	12.62	12.60	12.73	11.99
stdev.max	2.90	1.97	2.40	2.50	2.50	2.17	1.90	2.53	2.20	2.28	2.73	3.15
stdev.min	5.56	4.58	4.09	5.27	4.93	5.01	2.85	3.49	4.49	4.83	3.95	4.50
av.mon.prec	43.37	18.64	72.73	88.66	56.76	12.82	146.33	226.43	88.79	58.47	29.38	16.90
stdv.daily prec	5.03	3.68	6.67	9.80	7.29	2.54	11.04	14.54	6.25	8.88	6.34	0.46
skew.daily prec	4.27	9.26	6.25	4.74	5.55	6.18	2.10	1.75	5.23	3.17	8.24	6.60
PDW	0.10	0.07	0.19	0.23	0.16	0.11	0.30	0.36	0.19	0.16	0.04	0.02
pww	0.60	0.33	0.53	0.70	0.17	0.03	0.40	0.42	0.60	0.50	0.20	0.03
no.of wet days	3.75	2.25	4.88	6.13	3.00	1.75	11.38	15.88	5.25	6.75	1.38	0.50
max.0.5 hr rain	37.50	44.20	31.10	42.30	58.90	59.40	237.80	72.20	48.50	57.00	42.40	50.20
av.daily sol.rad	18.30	19.70	21.50	22.20	22.00	18.70	17.90	18.40	19.30	21.10	19.40	18.70
av.daily dewpt	2.60	3.60	5.60	6.20	4.33	5.27	12.93	12.53	7.13	3.33	1.13	1.27
av.daily windsp	0.1	0.13	0.12	0.1	0.14	0.16	0.18	0.15	0.12	0.13	0.1	0.12

Appendices E Monthly meteorological data

Maximum temperature of Alamata station

Year	Jan	Feb	Mar	Apr	May	Jun	Jul	Aug	Sep	Oct	Nov	Dec
1996	30	29	31	31	31	33	32	31	32	31	29	28
1997	27	30	30	30	34	35	33	34	33	30	29	29
1998	27	28	31	35	35	36	32	29	31	31	30	30
1999	29	32	31	34	36	36	31	30	30	30	30	29
2000	30	32	33	34	35	37	33	31	31	29	29	27
2001	28	30	31	31	34	34	31	29	30	30	28	28
2002	25	28	30	30	34	34	34	31	29	31	29	26
2003	26	29	29	30	33	34	31	29	30	30	28	26
2004	27	22	30	29	33	33	32	30	30	29	28	26

Maximum temperature of Kobo station

Year	Jan	Feb	Mar	Apr	May	Jun	Jul	Aug	Sep	Oct	Nov	Dec
1997	26	29	30	28	34	35	32	31	32	30	28	26
1998	28	27	30	31	35	34	33	32	32	30	30	27
1999	27	30	31	32	32	35	33	32	32	31	29	28
2000	26	28	31	31	34	36	32	30	31	28	26	26
2001	27	29	30	31	34	36	33	29	28	27	26	26
2002	24	25	30	30	33	36	33	29	30	28	27	25
2003	28	28	28	31	32	34	32	31	29	27	26	27
2004	27	27	28	31	35	36	32	31	32	30	28	26

Maximum temperature of Waja station

Year	Jan	Feb	Mar	Apr	May	Jun	Jul	Aug	Sep	Oct	Nov	Dec
1997	29	29	30	28	34	34	33	32	32	30	30	27
1998	28	31	31	32	32	36	32	31	30	28	29	28
1999	28	28	28	26	31	34	33	33	32	31	30	28
2000	29	32	30	28	32	34	32	33	31	30	29	27
2001	25	29	31	33	29	36	31	31	33	30	29	28
2002	27	28	30	31	32	31	30	31	31	29	28	27
2003	28	27	28	29	33	39	34	33	32	29	29	27
2004	27	27	25	31	32	33	32	30	31	31	31	27

Maximum temperature of Korem station

Year	Jan	Feb	Mar	Apr	May	Jun	Jul	Aug	Sep	Oct	Nov	Dec
1996	21	21	22	22	26	25	23	22	23	21	21	20
1997	22	22	21	23	29	26	22	22	23	20	21	19
1998	19	19	21	21	24	24	22	21	21	21	23	22
1999	19	20	23	28	25	23	23	22	23	20	19	17
2000	22	23	26	26	28	27	25	23	25	22	23	23
2001	24	21	22	23	26	26	26	24	26	22	21	20
2002	21	21	24	24	26	26	25	25	22	21	23	23
2003	24	22	23	23	24	25	22	22	22	20	18	17
2004	21	20	21	22	26	27	22	21	23	21	23	23

Maximum temperature of Zobel station

Year	Jan	Feb	Mar	Apr	May	Jun	Jul	Aug	Sep	Oct	Nov	Dec
1996	24	26	28	28	34	30	30	28	27	24	23	26
1997	29	28	28	27	32	31	27	28	27	23	23	23
1998	21	24	24	29	33	30	28	26	27	26	25	24
1999	23	27	25	28	10	31	27	26	26	24	24	23
2000	23	25	27	28	29	31	28	27	27	25	23	23
2001	20	23	24	28	29	30	29	27	27	24	23	23
2002	21	23	27	28	30	32	28	28	27	25	24	22
2003	21	25	26	27	34	28	30	27	28	24	24	22
2004	27	27	27	29	30	31	29	28	28	26	25	22

Minimum temperature of Alamata station

Year	Jan	Feb	Mar	Apr	May	Jun	Jul	Aug	Sep	Oct	Nov	Dec
1996	15	13	16	16	16	16	17	16	16	14	13	12
1997	13	13	16	16	18	19	18	18	17	16	16	13
1998	15	15	17	18	18	20	17	13	17	15	15	12
1999	12	12	13	17	20	21	19	17	10	6	4	2
2000	2	5	7	8	10	11	12	9	9	8	7	6
2001	4	6	9	10	12	14	12	11	10	11	8	7
2002	10	14	17	18	19	20	20	17	17	16	15	16
2003	14	16	17	18	20	20	19	17	17	16	15	13
2004	15	9	9	16	18	20	19	17	17	15	15	15

Minimum temperature of Kobo station

Year	Jan	Feb	Mar	Apr	May	Jun	Jul	Aug	Sep	Oct	Nov	Dec
1996	16	15	16	17	17	17	18	18	16	12	12	10
1997	13	12	16	16	18	19	19	18	16	16	16	12
1998	15	15	17	18	18	21	18	17	16	15	10	8
1999	12	11	16	16	18	18	17	16	6	9	8	7
2000	6	11	14	17	16	16	15	12	7	9	8	7
2001	7	7	12	15	15	16	15	11	13	13	10	9
2002	12	14	16	17	17	19	20	18	16	13	12	15
2003	14	15	16	17	18	19	20	17	15	13	13	11
2004	15	14	15	17	17	18	19	18	16	13	16	20

Minimum temperature of Maichew station

Year	Jan	Feb	Mar	Apr	May	Jun	Jul	Aug	Sep	Oct	Nov	Dec
1996	11	8	9	12	12	14	14	13	10	8	7	8
1997	8	9	10	10	10	14	13	13	6	6	9	5
1998	6	8	8	9	10	14	14	10	8	8	6	4
1999	6	7	9	11	12	14	14	13	11	9	5	3
2000	3	7	8	9	9	9	14	13	11	7	7	4
2001	4	8	11	12	8	8	14	13	11	9	5	3
2002	3	3	7	3	10	11	13	10	2	7	5	6
2003	7	5	8	5	8	13	13	12	11	7	6	7
2004	10	9	10	12	11	13	12	13	9	10	7	8

Minimum temperature of Muja station

Year	Jan	Feb	Mar	Apr	May	Jun	Jul	Aug	Sep	Oct	Nov	Dec
1996	15	9	12	16	16	17	18	16	15	13	14	11
1997	10	11	12	12	13	16	18	16	15	12	9	8
1998	16	10	12	11	17	18	16	16	17	15	15	14
1999	13	12	16	16	17	19	19	17	14	12	11	7
2000	14	13	13	15	14	17	17	21	21	18	16	12
2001	13	11	15	13	16	17	19	18	19	17	13	13
2002	16	9	16	16	16	16	17	16	16	13	17	10
2003	16	8	11	14	14	16	18	17	15	12	11	9
2004	13	11	13	15	14	17	18	17	20	15	14	9

Minimum temperature of Zobel station

Year	Jan	Feb	Mar	Apr	May	Jun	Jul	Aug	Sep	Oct	Nov	Dec
1996	2	0	119	26	15	18	13	8	8	8	9	12
1997	14	6	127	56	26	28	9	8	6	7	1	34
1998	2	2	52	68	5	13	14	13	13	10	4	2
1999	2	1	4	3	5	5	9	7	6	4	4	2
2000	1	13	7	19	16	22	13	15	14	11	1	3
2001	8	8	13	11	14	16	16	15	12	12	16	18
2002	1	0	1	12	13	14	15	15	9	9	1	15
2003	0	0	42	64	11	12	10	10	8	6	1	66
2004	17	14	16	20	23	21	8	12	12	9	2	10

Appendices F Monthly climate data

Wind speed of Kobo station

Year	Jan	Feb	Mar	Apr	May	Jun	Jul	Aug	Sep	Oct	Nov	Dec
1996	2.6	2	2.1	2	1.6	1.8	2	1.7	1.2	1.3	1.5	1.6
1997	1.8	2	2.1	2	2.2	1.9	2	1.7	1.6	1.4	1.3	1.4
1998	1.6	1.7	2	2.2	2	2.5	2	1.6	1.1	1.3	1.4	1.5
1999	1.6	1.8	2.2	2.1	2.1	2.3	2	1.5	0.2	0.5	1.3	1.4
2000	1.6	1.8	2.2	1.8	1.7	2.2	2	2	1.5	1.6	1.5	1.2
2001	1.5	1.7	1.7	1.4	1.2	1.4	1	0.8	0.2	1.6	1.7	1.8
2002	1.8	1.8	1.9	1.8	1.4	2.3	2	1.8	0.9	1	1.3	1.5
2003	1.6	1.7	2	1.9	1.5	2	2	1.4	1	1.1	1.3	1.3
2004	1.7	1.9	2	2	1.8	2.1	2	1.5	1.5	1.2	1.3	1.6
2005	2	2.1	2.2	2	1.6	1.9	2	1.8	1.2	1.2	1.3	1.5

Sunshine of Kobo station

Year	Jan	Feb	Mar	Apr	May	Jun	Jul	Aug	Sep	Oct	Nov	Dec
1996	6.8	5.3	7.9	9.6	9.9	8.5	4	5.1	6.8	9.6	9.9	8.8
1997	8	7.3	9.3	6.9	9.4	6.2	3	5.1	7.3	9.5	9.7	8.1
1998	6.3	7.5	8.9	9.5	9.2	6.8	7	7.4	6	7.1	9	7
1999	6.9	4.4	8.7	6.6	9.1	6.3	6	6.5	7	9.6	10	9.3
2000	9.3	7.2	6.1	7.6	9.1	5.1	5	5.1	5.1	8.2	9.3	8.7
2001	8	7.4	8.9	7.9	9.8	8.3	3	6.6	7.1	7.9	8.1	7.9
2002	7.8	8.6	8.7	9.7	6.5	5.7	4	5.8	7.7	8.9	9.1	8.5
2003	8.7	10	8.1	9	6.8	6.4	8	7.1	6.7	7.3	8.6	9
2004	8.1	8.7	9	6.8	7.2	6.1	7	5.6	6.2	8.1	9.9	9.4

Wind speed of Maichew station

Year	Jan	Feb	Mar	Apr	May	Jun	Jul	Aug	Sep	Oct	Nov	Dec
1996	1.1	1.3	1.3	1.3	1.3	2.9	4	2.7	1.2	1.2	1.2	1.2
1997	1.1	1.3	1.3	1.3	1.5	1.9	3	2	1.3	1.2	1	1
1998	0.9	1	1.2	1.4	1.4	1.9	4	2.6	1.2	1.2	1.3	1.3
1999	1.2	1.4	1.4	1.5	1.6	2	3	2.2	1.1	0.9	1.1	1.1
2000	1.2	1.3	1.3	1.4	1.4	2.2	3	2.8	1.1	0.9	0.9	1
2001	1.2	1.3	1.3	1	1.2	2.4	3	2.5	1.1	1.2	1.1	1.1
2002	0.9	1.2	1.2	1.3	1.3	2.4	3	2.5	1.1	1.2	1.2	1.1
2003	1.1	1.3	1.3	1.3	1.3	1.8	3	2.7	1.4	1.2	1.2	1.1
2004	1.2	1.3	1.3	1.2	1.6	1.9	3	2.3	1.2	1.2	1.2	1.2
2005	1.1	1.2	1.3	1.4	1.3	3	3	2.7	1.2	1.2	0.9	1

Sunshine of Maichew station

Year	Jan	Feb	Mar	Apr	May	Jun	Jul	Aug	Sep	Oct	Nov	Dec
1997	7.9	8.8	5.5	7.2	8.2	6.2	6	6.2	6.7	6.2	6.6	8.4
1998	5.2	6.3	7.4	8.7	8.7	6.9	4	4.3	7.3	8.5	9	9.3
1999	7.4	9.8	7.2	10	9.7	7.3	4	4.9	7	6	8.9	7.7
2000	9	9.8	9.7	7.3	9.2	6.3	5	5.5	5.9	7.1	7.8	6.3
2001	4.4	7.9	4.4	6.2	7.2	12	5	5	7	7.9	6.9	8.3
2002	8.2	8.2	7.6	9.4	9.3	6.3	6	6.3	6.7	7.8	7.7	6.7
2003	6.4	8	6.3	9.9	9	6	5	4.4	7.3	9.4	8	7.9
2004	6.9	8	8.6	7.6	10.5	5.9	5	5.4	6.3	8	8.3	7.4

Solar radiation of Maichew station

Year	Jan	Feb	Mar	Apr	May	Jun	Jul	Aug	Sep	Oct	Nov	Dec
1996	14	15	15	17	17	17	14	14	16	15	14	14
1997	15	17	14	16	17.5	15	14	15	15	14	13	15
1998	12	14	16	18	18.1	16	13	13	16	17	16	16
1999	14	18	16	20	19.3	16	12	14	16	14	16	14
2000	16	18	19	17	18.7	15	14	14	15	15	15	13
2001	11	16	13	15	16.3	22	13	14	16	16	14	15
2002	15	16	17	19	18.8	15	15	15	15	16	15	13
2003	13	16	15	20	18.5	15	13	13	16	18	15	14
2004	14	16	18	17	20.3	15	14	14	15	16	15	14

Dewpoint temperature of Maichew station

Year	Jan	Feb	Mar	Apr	May	Jun	Jul	Aug	Sep	Oct	Nov	Dec
1996	12	7.2	11	11	13.5	9.9	11	11	8.5	6.4	7.6	6.8
1997	10	6.8	10	9.8	11.3	10	11	9.7	7.1	8.5	12	7.2
1998	10	9.4	9.8	6.7	10.9	5.4	11	11	9.3	8.7	6.6	3.1
1999	5.8	0.2	8.5	8.6	4.94	2	13	12	12	10	4.5	4.2
2000	4.9	2.7	6.6	7.2	7.82	4.6	13	13	12	11	11	10
2001	11	6.1	11	9.1	9.06	8.5	15	14	14	9.8	7.1	5.2
2002	10	5.6	10	7.7	6.09	5.6	10	12	8	6.9	7.2	12
2003	11	10	8.7	4.9	3.97	5.2	10	12	10	7	4.5	7.4
2004	9.8	6.6	5.9	12	3.67	7.9	9	11	9	8.6	8.9	11

Appendices G Monthly rainfall data of different stations

Monthly and annual precipitation

	Jan	Feb	Mar	Apr	May	Jun	Jul	Aug	Sep	Oct	Nov	Dec	annual
Muja	6.85	12.93	42.40	51.41	49.36	31.85	214.23	239.86	34.11	9.63	11.63	8.15	712.41
Korem	35.81	21.21	59.71	92.23	78.07	26.64	203.42	290.25	86.66	53.77	29.96	35.31	1013.04
Maichew	14.50	15.37	72.10	127.77	55.55	30.47	123.17	263.80	27.10	13.10	11.00	18.80	772.73
Alamata	41.19	51.87	72.42	98.04	45.89	6.39	135.04	227.44	56.09	24.98	23.86	36.59	819.80
Waja	20.66	22.92	63.67	82.61	40.68	8.90	119.88	187.09	52.71	27.80	14.54	15.78	657.24
Kobo	19.11	13.92	39.25	71.16	50.26	18.46	164.50	210.24	58.29	43.77	19.77	22.93	731.66
Average	23.02	23.04	58.26	87.20	53.30	20.45	160.04	236.45	52.49	28.84	18.46	22.93	784.48
STDEV	13.03	14.687	14.4	25.877	13.1	11	41.075	37.037	20.96	17.19	7.49	11.19	124.739